CHARACTERIZATION AND QUANTITATION OF PROTEIN GLYCATION AND GLYCOSYLATION USING HILIC-MS

by

SONAL PRIYA

(Under the Direction of Ron Orlando)

ABSTRACT

Protein post-translational modifications (PTMs), including glycation, glycosylation, and pyroglutamation could impact protein function and stability. Liquid chromatography coupled with mass spectrometry (LC-MS) is a vital tool for PTM characterization, with hydrophilic interaction liquid chromatography (HILIC) emerging as the preferred method for characterization of hydrophilic modifications. This research focuses on improving the characterization of PTMs such as glycation and pyroglutamation by predicting the retention times of modified peptides in the HILIC-MS mode. Glycation has been linked to health conditions including diabetes, cataract and Alzheimer's disease. This modification could be introduced during the manufacturing of therapeutic monoclonal antibodies (mAbs), necessitating its accurate characterization. Thus, an analytical workflow was developed to predict and characterize glycation sites in mAbs with the aim to enhance safety and efficacy of drug products. In addition, retention prediction of peptides containing pyroglutamated N-terminus glutamic acid was performed. Pyroglutamate formation is a PTM that has been associated with several neurodegenerative disorders. Such a predictive approach is expected to serve as an

additional layer of validation in PTM characterizations, ultimately leading to faster analysis times. Further, absolute and relative quantitation of glycation modification using heavy isotope-labeled proteins containing ^{13}C and ^{15}N lysine and arginine has been developed. The proposed method was observed to have higher accuracy and precision compared to the typically established method for glycation quantitation. This quantitative approach was applied to IgGs such as Adalimumab (IgG1), Natalizumab (IgG4), and 'Frankenmab' (custom IgG2).

The proposed research also evaluates various LC-MS sample preparation techniques that are employed for N-glycosylation characterizations. The choice of LC-MS sample preparation is crucial to avoid inaccuracies in determining the absolute and relative abundances of N-glycans.

Lastly, this work provides valuable insights into the operations of shared resource laboratories (SRLs) that accommodate analytical instruments. A survey was conducted to better understand instrument usage, maintenance, associated costs, and funding sources in SRLs specializing in flow cytometry.

INDEX WORDS: Liquid Chromatography, Mass Spectrometry, Hydrophilic Interaction Liquid Chromatography, Post-Translational Modifications, Retention Prediction, Glycation, Glycosylation, Pyroglutamation, Absolute Quantitation, Relative Quantitation

CHARACTERIZATION AND QUANTITATION OF PROTEIN GLYCATION AND GLYCOSYLATION USING HILIC-MS

by

SONAL PRIYA

MS, Oklahoma State University, 2018

BS, University of Delhi, India, 2014

A Dissertation Submitted to the Graduate Faculty of The University of Georgia in Partial Fulfillment of the Requirements for the Degree

DOCTOR OF PHILOSOPHY

ATHENS, GEORGIA

2023

CHARACTERIZATION AND QUANTITATION OF PROTEIN GLYCATION AND GLYCOSYLATION USING HILIC-MS

by

SONAL PRIYA

Major Professor:	Ron Orlando
Committee:	Jon Amster
	Kelly Hines

Electronic Version Approved:

Ron Walcott
Vice Provost for Graduate Education and Dean of the Graduate School
The University of Georgia
December 2023

DEDICATION

This dissertation is dedicated to my family. To my late grandfather whom I couldn’t see due to the COVID-19 pandemic. I remember him every day and try to apply all the values he taught me. Whether it's being respectful and compassionate toward people, maintaining discipline, cultivating long-term habits, taking care of both physical and mental well-being, or staying positive in any situation, his teachings continue to guide me. I also dedicate this work to my parents. My father who instilled in me the importance of Chemistry in life from a very early age, and my mother who taught me the importance of planning, hard work, and to become a good person. Thank you both for your endless motivation and support that you gave in every way you could. To my sisters and their families, you have been there with me through all the thick and thin moments. Thank you for always being protective of me and helping me with literally anything! I also want to dedicate this work to my husband. Your availability, emotional support and help has never come in between the long-distance relation we had. Thank you for always motivating me to push through all hurdles and for being there for me in every situation.

ACKNOWLEDGEMENTS

I would like to express my deepest gratitude to my advisor, Dr. Ron Orlando for allowing me to be a part of his research group, and for his guidance throughout my Ph.D. journey. Dr. Orlando, you not only helped me understand the underlying concepts of the work, but also pushed me to reach my potential by not giving up until the solutions to problems were found. I am especially grateful for your teachings on approaching problems from multiple angles, your motivation during challenging times, and for your encouragement after both small and significant successes. I would also like to extend my heartfelt thanks to my committee members, Dr. Jon Amster and Dr. Kelly Hines, for their valuable suggestions and insights into the projects I undertook, which have been very beneficial to my research journey. Special thanks to Dr. Barry Boyes for igniting my passion for chromatography.

To my former and current lab members, I am grateful for the countless discussions and late-evening instrument troubleshooting efforts we had. I have learned from each one of you and cherished the good times we've had together. I am appreciative of the Complex Carbohydrate Research Center and the University of Georgia for providing me with the necessary resources and facilities that enabled the successful completion of my program.

Lastly, I would like to acknowledge my family and friends. Your moral support and encouragement made the long distance between us feel insignificant.

TABLE OF CONTENTS

Page

CHAPTER 1

INTRODUCTION

Characterizing protein post-translational modifications (PTMs) is of great importance in understanding their role in various biological processes. PTMs, such as glycation, glycosylation, deamidation, oxidation, and pyroglutamation among others, can significantly influence protein's function, stability, and activity.[1,2] For instance, PTMs such as glycation can be introduced during the storage and manufacturing of biotherapeutics that could impact the safety and efficacy of drug products. Liquid chromatography coupled with mass spectrometry (LC-MS) serves as a powerful tool for characterizing PTMs.[3,4] LC-MS enables the separation and identification of modified peptides by measuring their mass-to-charge (m/z) ratios, thus facilitating the detection of various PTMs with high sensitivity and accuracy. While reversed-phase (RP) chromatography is commonly used for proteomic LC-MS analysis due to its ability to separate hydrophobic peptides, hydrophilic interaction liquid chromatography (HILIC) has emerged as a superior choice for characterizing hydrophilic modifications.[5,6] HILIC excels at separating peptides that do not retain well on RP columns, making it ideal for studying hydrophilic modifications such as glycation, glycosylation, and pyroglutamation.

Firstly, this work focuses on efficiently characterizing PTMs such as glycation and pyroglutamation by predicting their retention times in the HILIC-MS mode, as described in Chapter 3. Glycation is an important PTM and is linked with various health

conditions, including diabetes, Alzheimer's disease, cataract, and Rheumatoid arthritis.[7-9] Glycation is particularly relevant for therapeutic mAbs, as it can occur during fermentation, storage, or drug infusion, impacting their overall charge, bioactivity, and stability. Characterizing glycation poses challenges as it can spread across the entire protein with low levels of glycation at individual sites, resulting in heterogeneous products of low abundances. To address these challenges, a robust analytical workflow was developed to predict and characterize glycation sites in therapeutic mAbs, aiming to ensure drug product safety and efficacy.[10] This workflow involved studying the retention behavior of *in-vitro* glycated standard peptides and proteins on HILIC and deriving a retention coefficient for glycation using dextran as an external calibrant. This retention coefficient, combined with Badgett's model[11], was applied to predict and characterize glycation in unknown mAbs, such as human IgG1 (Adalimumab), IgG4 (Natalizumab), and custom IgG2 ('Frankenmab'). The study was extended to predict the HILIC retention time of Pyroglutamation, thus aiding in its accurate characterization. This predictive approach served as an additional validation step, enhancing the speed and accuracy of PTM analyses.

Furthermore, glycation quantitation was improved by employing heavy isotope-labeled proteins and is detailed in Chapter 4. Analytical strategies to quantify glycation as reported in the literature includes quantitation of common Advanced Glycation End Products (AGEs).[12,13] However, Amadori glycated product is detected using LC-MS bottom-up approach in order to determine the glycation site on a protein.[14,15] As mentioned, quantifying glycation could be challenging due to its potential distribution across the entire protein, often resulting in low levels of glycation at specific sites. It also

hampers trypsin's activity at the C-terminus of lysine residues, resulting in missed cleavages at these sites. This is indicated by a +162 Da shift in mass spectrometry. Thus, a missed cleavage peptide along with a 162 Da mass increase served as an indicator for glycated peptides. Typically, relative quantification of glycation involves dividing the peak area of glycated missed cleavage peptides by the sum of the peak areas of glycated peptides and unmodified tryptic peptides that constitute the glycated missed cleavage peptide. However, this method assumes that the ionization efficiencies of glycated missed cleavage peptide and tryptic counterpart in the mass spectrometry are comparable. In addition, the selection of tryptic peptide for the calculation is crucial and can introduce lab-to-lab variations. The proposed approach, as described in Chapter 4 suggests using non-glycated heavy isotope-labeled variants of the target protein to determine both relative and absolute glycation levels. This strategy involved adding a known amount of protein labeled with ^{13}C and ^{15}N lysine and arginine to the target protein prior to trypsin digestion. Quantification was achieved by monitoring the peak area of an unmodified tryptic peptide containing a glycation site in relation to its heavy isotope-labeled counterpart. This method offered several advantages as it relied solely on the peak area of detectable tryptic peptides, ensured comparable ionization efficiencies, and normalized any variations in sample processing steps as the heavy isotope-labeled protein was added to the target protein sample prior to trypsin digestion. This quantitative approach was applied to IgGs such as Adalimumab (IgG1), Natalizumab (IgG4), and 'Frankenmab' (custom IgG2), which were forcibly glycated and subjected to trypsin digestion. HILIC was utilized due to the hydrophilic nature of the glycation product. It was anticipated that the light/heavy ratio of a peptide with a glycation site would decrease in the glycated

sample compared to the non-glycated control, while the ratio of a peptide lacking a glycation site would remain relatively unchanged. Thus, this approach was undertaken to aid in the improvement of accuracy and precision of glycation quantitation.

Protein glycosylation is one of the most common post-translational modifications that can impact protein folding, structure, stability, and functionality.[16,17] Chapter 5 details how efficient LC-MS sample preparation plays a crucial role in quantifying PTMs such as N-glycosylation. The protein of interest can be digested using trypsin followed by N-glycan release using PNGase F enzyme. The ionization efficiency of released N-glycans in the mass spectrometer can be enhanced by labeling them with labeling agents such as 2-aminobenzamide (2-AB), 2-aminobenzoic acid (2-AA), Procainamide among others, that not only ionizes well in the mass spectrometer but can also result in sufficient LC retention of N-glycans. Such a labeling step is accompanied by a reductive amination step to form a more stable conjugate for detection. However, variations in the reducing agent used ($NaBH_3CN$ vs 5-Ethyl-2-methyl pyridine borane) during the labeling step could result alter the absolute and relative abundances of N-glycans.[18,19] Examples have been shown for N-glycans released from bovine Fetuin as well as from more complex human serum samples. In addition, care should be taken when choosing the desalting protocol after reductive amination, such as between size-exclusion column and a polyamide column. Sample clean-up without the use of a column has also been explored. Thus, differences in LC-MS sample preparation strategies can introduce inaccuracies in absolute and relative quantitation of N-glycans, emphasizing the need for standardized protocols.

Furthermore, this work delves into the maintenance of analytical instruments in shared resource labs (SRLs), including flow cytometers and has been discussed in Chapter 6. Flow cytometry is a versatile tool used in immunology, molecular biology, cancer biology, virology, and infectious disease monitoring, and is extensively supported by SRLs.[20] These labs employ various types of flow cytometers, such as analyzers, sorters, imaging flow cytometers, and mass cytometers, each with unique maintenance and longevity challenges. An online survey was developed and distributed using www.surveymonkey.com platform that aimed to comprehend instrument usage, maintenance, replacement, and funding sources in these SRLs. More specifically, the survey queried the respondents about instrument uptime, usage, routine maintenance, associated costs, deep cleaning frequency, quality control, funding sources, and reasons for replacing their instrument. The findings, based on responses from 146 core facilities, offered insights into typical SRL operations and researchers' experiences with flow cytometer management.

CHAPTER 2

LITERATURE REVIEW

Liquid Chromatography

Liquid chromatography (LC) is an analytical technique that separates a mixture into its individual components based on the interactions of the sample with the mobile and stationary phases. [21,22] The mobile phase is typically a solvent (such as water, acetonitrile, methanol) that carries the analyte through a stationary phase. The stationary phase can either be a liquid immobilized on a solid support or a solid material itself.

Principles of Liquid Chromatography

The separation of the sample components arises from their differential partitioning between these two phases, driven by chemical or physical interactions. Broadly, chromatography can be categorized into two primary modes: partition chromatography and adsorption chromatography, each governed by distinct mechanisms. In partition chromatography, compounds within the sample partition themselves between the mobile and stationary phases based on their relative solubilities. On the other hand, adsorption chromatography relies on the adsorption of sample components onto the stationary phase, primarily due to surface interactions. Compounds may exhibit varying degrees of affinity for the stationary phase, resulting in differential retention and separation as they pass through the column.

Advancements in Liquid chromatography

The evolution of liquid chromatography from its early beginnings to the adoption of High-Performance Liquid Chromatography (HPLC)[23-25] has seen significant advancements in automation, precision, and efficiency, revolutionizing analytical chemistry practices. The process begins with the automatic injection of the sample onto a tray, followed by the continuous pumping of a solvent through the chromatographic column. As sample components traverse the column, they interact with the stationary phase, leading to differential retention and eventual elution. One distinguishing feature of HPLC is the utilization of high-pressure pumps, which enable faster separations. Moreover, the columns used in HPLC are designed for reusability and effectiveness, contributing to enhanced separations and precision. The entire process is closely monitored by a detector that captures the eluting compounds over time, generating a chromatogram, this is a graphical representation of the separation.

Chromatographic Considerations

Selecting the appropriate chromatographic method involves careful consideration of numerous factors. These include the chromatographic system, stationary phase characteristics, mobile phase composition, column size and particle type, elution method (isocratic or gradient), flow rate, and the chemical structure and composition of the analytes under investigation. The interplay of these factors is critical in achieving a successful separation for a specific mixture.[26] Ion-pairing agents may be introduced into the mobile phase to enhance the selectivity of separation.[27] Trifluoroacetic acid (TFA) is a commonly used mobile-phase modifier since it produces peptide separations that are far superior compared to other additives. However, its use in conjunction with electrospray

ionization (ESI) can result in signal suppression, leading to the preference for alternative modifiers such as formic acid and ammonium formate in LC-MS applications.

Liquid chromatography relies on the interaction between a stationary phase and a sample to separate compounds based on factors such as affinity, size, and electrostatic interactions. Typically, the stationary phase comprises of porous microscopic particles packed into a column. Among these particles, core-shell particles, also known as superficially porous particles (SPPs), are popular due to their efficiency, speed, and low back pressure.[28-30] SPPs consist of a solid, non-porous core enveloped by a porous material shell, which mimics the properties of fully porous materials used in high-performance liquid chromatography (HPLC). These particles were introduced to enhance column efficiency by shortening the diffusion path for analyte molecules, thereby improving mass transfer kinetics. Initially, SPPs were developed for analyzing large biomolecules, with the goal of achieving faster separations. The concept of shell-type particles was first conceived for macromolecule analysis in the late 1960s. Subsequently, the core diameter was reduced, and the thickness of the active layer was minimized to achieve rapid separation of peptides and proteins. In recent years, the demand for improved analytical throughput has driven manufacturers to find a balance between column efficiency and compatibility with conventional HPLC instruments. This led to the commercialization of sub-3 μm superficially porous particles, consisting of a 1.7 μm solid core covered by a 0.5 μm thick shell of porous silica. This particle structure combines the advantages of porous and non-porous particles, addressing issues including low loading capacity. Thus, these columns, packed with SPPs, enable faster and more

efficient separations for both small and large molecules, making them invaluable in pharmaceutical, biomedical, food, and environmental analyses.

Column efficiency in Liquid chromatographic separations

Following the selection of suitable stationary and mobile phases, two factors such as efficiency and resolution become crucial in chromatographic separation. Efficiency, for instance, relates to band broadening and to how similar analytes disperse within the column. LC efficiency is quantified through the height equivalent to a theoretical plate, or theoretical plate height (H).[31-34] The theoretical plate height is influenced by three key factors: how a compound channels through the porous bed, its longitudinal diffusion, and the kinetics of mass transfer between mobile and stationary phases. The theoretical plate height (H) is determined using number of plates (N) and column length (L) using Equation 1. In addition, higher number of plates (N) denotes an improved column efficiency, resulting in better analyte separation.

$$H = \frac{L}{N} \qquad \text{(Equation 1)}$$

van Deemter in 1956 established an equation[31] (Equation 2) to link the column efficiency with theoretical plate height, and to measure the equilibration of analyte between stationary phase and mobile phase.

$$H = A + \frac{B}{u} + Cu \qquad \text{(Equation 2)}$$

This equation describes how the theoretical plate height of a plate is influenced by three key factors: Eddy diffusion (A), longitudinal diffusion (B), and resistance to mass transfer (C), alongside the average mobile phase velocity (u). It is essential to minimize H in order to achieve highly efficient separation.[35] Eddy diffusion is independent of flow rate and accounts for multi-path flows in the column.[36-38] Various routes or channels

through the packing material in a column can lead to band broadening. Further, longitudinal diffusion describes solute diffusion within the mobile phase. Higher flow rates can reduce longitudinal diffusion. In addition, resistance to mass transfer signifies the movement/transfer of analyte between stationary and mobile phases. Some analytes transition between phases, increasing band width, but this can be mitigated with lower flow rates, smaller particles, or higher temperature.[39-41]

The mobile phase velocity (flow rate) plays a crucial role that can impact longitudinal diffusion and mass transfer resistance. Flow rates can vary from milliliters to nanoliters. A lower flow rate enhances sensitivity but potentially leads to longer separation times and poor peak resolution. Therefore, balancing the flow rate is critical for optimizing column efficiency while maintaining reasonable separation times and detection sensitivity.

Column efficiency plays a crucial role in assessing a column's separation capabilities, but equally important is the ability to distinguish adjacent peaks. This level of distinction is called resolution and is represented by the difference in retention times between two peaks divided by the combined widths of the chromatographic peaks (Equation 3).

$$R_s = \frac{2[(t_R)_B - (t_R)_A]}{W_B + W_A} \qquad \text{(Equation 3)}$$

In equation 3, $(t_R)_B$ refers to retention time of later eluting analyte and $(t_R)_A$ refers to retention time of earlier eluting analyte. W_A and W_B represent the peak width at half height for A and B analytes respectively. Greater resolution can be achieved when chromatographic peaks are narrow and have a high difference in retention times, thus reducing the likelihood of overlap.

Types of Liquid Chromatography

Normal Phase Chromatography: Normal-phase (NP) chromatography utilizes a polar stationary phase such as silica or alumina and an organic solvent-based mobile phase.[42,43] Weaker solvents such as hexanes and chloroform, and stronger solvents such as methanol and acetonitrile can be utilized to perform separations. Molecules containing polar groups interact with the stationary phase through dipole-dipole forces, leading to longer retention times compared to less polar compounds. NP has been found to have fewer applications compared to other separation methods in recent times. It is especially suited for separating chiral compounds, cis-trans isomers, geometric isomers, and water-sensitive substances, with elution occurring in order of increasing polarity.

Reversed Phase Chromatography: Reversed phase (RP) chromatography coupled with mass spectrometry is one of the most widely used techniques in proteomics due to its exceptional reproducibility and resolution.[44-46] RP chromatography involves polar mobile phases (water, methanol, and acetonitrile) and non-polar stationary phases. The stationary phase is typically covalently bonded long-chain hydrocarbons on silica particles that can efficiently separate nonpolar species such as hydrophobic peptides.[47] The separation principle relies on analyte hydrophobic adsorption to the stationary phase's surface and their partitioning within hydrocarbon chains.[48,49] More hydrophobic analytes elute later, altered by organic solvent addition to the mobile phase, typically acetonitrile. Acetonitrile is predominantly selected as the organic solvent for RP chromatography since it is compatible with ESI-MS, possesses a low viscosity that reduces backpressure, and exhibits minimal absorbance when employed in UV applications.[50] Buffers with salts including ammonium formate and ammonium acetate

can enhance the ionic strength for improved separation. pH modifiers such as formic acid fine-tune pH, altering analyte charge states, aiding in proteomics with complex separations and enhanced MS sensitivity.[51] The mobile phase's adaptability in RP allows easy adjustment of column selectivity. This method swiftly and effectively separates complex peptide mixtures for subsequent MS/MS analysis, facilitating high-throughput proteomic experiments.

Hydrophilic Interaction Liquid Chromatography: Hydrophilic Interaction Liquid Chromatography (HILIC) blends aspects of both RP and NP chromatography and enables the separation of polar or charged compounds.[50,52] HILIC employs stationary phases such as bare silica or silica modified with polar groups, as well as zwitterionic phases, expanding its applicability to complex analytes.[53-56] Analyte retention in HILIC involves three mechanisms: partitioning between a water-rich layer and the mobile phase, adsorption onto the hydrophilic stationary phase, and a combination of partitioning and adsorption.[57,58] The greater polarities of analytes result in longer retention due to strong interactions with the water-rich layer, including electrostatic forces, hydrogen bonding, and van der Waals interactions.[58]

HILIC employs acetonitrile as the primary organic buffer, facilitating faster mobile phase velocities and reducing longitudinal diffusion without compromising performance. This technique offers advantages in terms of lower back pressures and enhanced sensitivity in ESI-MS.[54] However, a drawback is the limited solubility of some analytes in high acetonitrile concentrations. In essence, HILIC mirrors normal phase retention patterns but utilizes water as the dominant solvent. It is ideal for analyzing highly polar compounds and has found application in proteomic studies, particularly for

the separation of polar post-translational modifications in proteins, such as glycosylation and phosphorylation. Unlike RP-LC, HILIC behaves similar to liquid-liquid partitioning due to a hydration layer forming on the polar stationary phase surfaces. This mode is especially valuable for compounds that are too polar for RP-LC but lack sufficient charge for ion-exchange chromatography.

Detectors coupled with Liquid Chromatography

Various detectors play a pivotal role in transforming analyte properties into measurable signals for accurate characterization. Detectors can be broadly categorized as destructive and non-destructive. Destructive detectors modify effluent continuously, rendering the original sample unrecoverable, as seen in mass spectrometry. On the other hand, non-destructive detectors directly measure eluent properties preserving the sample integrity. Examples of non-destructive detectors include ultraviolet (UV), fluorescence, and refractive index (RI) detectors.

The two most commonly used detectors in proteomics and glycoproteomics analysis are UV[59] and mass spectrometry[60,61] detectors. UV detectors assess chromophoric compound concentrations by monitoring the light absorption and are particularly effective when coupled with modern UV-Vis detection systems such as variable wavelength detector (VWD) or diode array detector (DAD). These detectors generate chromatograms, and the areas under the peaks are related to analyte concentrations using the Beer-Lambert law. Mass spectrometry, on the other hand, is a destructive technique. Generally, HPLC-MS excels at identifying unknown components, while DAD detectors are proficient in quantifying known components. Thus, the choice

of detector in liquid chromatography relies on the specific analytical needs and the nature of the substances being studied.

Retention Time Predictions

Retention modeling plays an important role in enhancing proteomic analyses. Initially designed for both reverse phase (RP) and normal phase (NP) chromatography, these models aimed to understand the contributions of individual amino acids to peptide retention and predict their elution times.[62-68] RP models assigned coefficients to amino acids, reflecting their hydrophobicity or hydrophilicity. Linear regression and MATLAB® were often used to derive these coefficients.

HILIC models have emerged as significant contributors to peptide retention predictions and have been developed for various stationary phases. Moreover, retention models have been developed for the analysis of proteins containing post translational modifications. These modifications, such as glycosylation, methionine oxidation, and deamidation, have been reported to have significant effects on peptide retention and elution times.[69-72] Incorporating predicted retention times into peptide analysis enhances their identification and characterization, reducing false discovery rates, and significantly improves efficiency in proteomic investigations.

Mass Spectrometry

Mass Spectrometry (MS) is a powerful analytical technique employed in the identification and characterization of molecules by measuring their mass-to-charge ratio (m/z). An analyte must carry a charge and exist in the gaseous phase for its mass spectrometric detection. A typical mass spectrometer comprises three integral components: an ion source, a mass analyzer, and a detector.[73,74] The ion source initiates

the process by converting analyte molecules into gas-phase ions. Subsequently, the mass analyzer, operating under ultra-high vacuum conditions, differentiates these ionized analytes based on their m/z values. Lastly, the detector generates electronic signals corresponding to the separated ions, ultimately yielding a mass spectrum, which graphically represents ion intensity as a function of m/z ratio. Various types of ion sources, mass analyzers, and detectors are available, each with its own distinct advantages and disadvantages, allowing for diverse experimental approaches and measurements.[75-77] To ensure precise analysis, mass spectrometry relies on low operating pressures (high vacuum) to minimize ion collisions with other molecules within the mass analyzer, since such collisions can distort the mass spectrum.

Ionization Techniques

Ionization techniques in mass spectrometry can be classified as either hard or soft, depending on the degree of fragmentation they induce. Early ionization methods such as electron ionization (EI) and chemical ionization (CI) fall into the hard ionization category. These techniques were primarily used for detecting small organic molecules[75,78] but were less suitable for proteomics, where preserving the molecular weight is crucial. The development of soft ionization techniques, such as electrospray ionization (ESI) and matrix-assisted laser desorption ionization (MALDI)[79-81], revolutionized mass spectrometry's applicability to large biomolecules. They allowed the generation of ionized species with minimal in-source fragmentation, facilitating the analysis of proteins and peptides. This development also paved the way for protein identification through database searching, where MS/MS data could be compared with theoretical masses for proteins and peptides.

ESI is the most common ionization technique used in online LC-MS due to its ability to rapidly evaporate analytes in a solvent. In ESI, a high voltage is applied to a capillary containing the analytes in a solvent, generating a plume of ions introduced into the mass spectrometer. Organic solvents mixed with water aid desolvation. Two theories, the charge residue model (CRM) and ion evaporation model (IEM), explain ion formation in ESI. CRM postulates that each charged droplet experiences solvent evaporation and Coulomb fission, eventually releasing smaller droplets, each containing one analyte ion.[82-84] IEM, on the other hand, suggests how charged droplets emit analyte ions as their charge-to-surface area ratio increases.[85,86] ESI typically produces doubly and triply charged ions, enabling the analysis of larger biomolecules at lower m/z ratios. MALDI, another soft ionization technique, employs an organic matrix that absorbs laser radiation and imparts a charge to embedded analytes. The pulsed laser causes molecules to desorb into the gas phase, generating ions for mass spectrometric detection. Proteomic identification through MALDI is straightforward due to the generation of numerous singly charged species.[87] Common matrices for MALDI in proteomics include α-cyano-4-hydroxycinnamic acid (CHCA) and 2,5-dihydroxybenzoic acid (DHB) that can produce varying levels of fragmentation.

These soft ionization techniques have revolutionized protein analysis using mass spectrometry, making it possible to analyze biomolecules without significant fragmentation. ESI and MALDI have different mechanisms for ion generation but are both invaluable tools for studying large biomolecules including proteins and peptides. ESI is widely used for online LC-MS due to its rapid evaporation capabilities, while MALDI is known for generating singly charged ions and is often coupled with time-of-

flight (TOF) instruments for precise measurements. These techniques have greatly expanded the application of mass spectrometry in various fields, particularly in proteomics and biomolecule analysis.[88]

Mass Analyzers

Mass analyzer is a critical component responsible for separating ions according to their m/z values. Various types of mass analyzers have been developed to suit different analytical needs, each offering distinct advantages and disadvantages. The choice of mass analyzer depends on the specific application.[89]

Linear quadrupole mass analyzers are widely used in mass spectrometry. They consist of four circular metal rods that apply fixed direct current (DC) and alternating radio frequency (RF) voltages.[90] These rods create an electric field wherein stable ions oscillate, while ions outside the specified m/z range collide with the rods and fail to reach the detector. A notable application of linear quadrupoles is the Triple Quadrupole (QQQ) instrument. They consist of two quadrupoles (Q1 and Q3) separated by a non-mass-resolving RF-only quadrupole acting as a collision cell for Collision-Induced Dissociation (CID).[91,92] The first quadrupole (Q1) selects precursor ions, the second (Q2) facilitates fragmentation via CID, and the third quadrupole (Q3) filters the resulting fragment ions. QQQ instruments offer four MS/MS scan modes: precursor ion scan, fragment ion scan, neutral ion scan, and selected reaction monitoring (SRM) that is also known as multiple reaction monitoring (MRM).[93] MRM uses Q1 to isolate a precursor ion and Q3 to isolate a fragment ion. This targeted approach is used to detect specific peptides and their corresponding fragments, enhancing the sensitivity and specificity in quantification. QQQ instruments offer a high duty cycle, which means they efficiently

accept ions from a continuous ion source, resulting in increased sensitivity by minimizing ion wastage. Consequently, they are commonly preferred for quantitative analysis. QQQ instruments excel in analyte selectivity and reproducibility, but they may have limited resolution. In addition, knowledge of the m/z of precursor and fragment ions are needed for such an analysis.

Quadrupole ion trap (QIT) mass analyzers come in two geometries: three-dimensional (3D) and linear (LIT).[94,95] In 3D-QIT, a ring electrode sits between two end cap electrodes, trapping ions within the space between them using DC and RF potentials. The ions can then be axially ejected for detection. On the other hand, LITs employ front and rear trapping plates to accumulate ions. QITs offer benefits such as ion accumulation, enhancing sensitivity. They employ collisional cooling with inert buffer gases, usually helium, to minimize unwanted collisions. The ability to inject ions axially or radially depends on the specific design. QITs are known for their ion storage capacity, high scan rates, and simplicity.

Linear Time-of-Flight (TOF) instruments determine ion mass by measuring the time it takes ions to traverse a known distance. Smaller ions reach the detector faster than larger ones, allowing for m/z separation.[96-98] While TOF instruments initially faced competition from other analyzers, the emergence of Matrix-Assisted Laser Desorption/Ionization (MALDI) in the 1990s renewed their popularity. TOF instruments offer rapid spectrum generation, a wide m/z range, and excellent ion transmission. Two techniques, delayed extraction and the use of a reflectron, have improved TOF instrument resolution.[99-101] Delayed extraction compensates for initial ion velocity differences, while

a reflectron corrects for varying kinetic energies. These advances have made TOF instruments invaluable for high-resolution mass spectrometry.

Fourier Transform Ion Cyclotron Resonance (FT-ICR) mass spectrometers utilize strong magnetic fields to measure the cyclotron frequencies of trapped ions. Smaller ions orbit at higher frequencies than larger ones. RF pulses excite ions, causing them to approach detector plates and generate unique image currents.[102-104] Fourier transforms then convert these currents into m/z ratios. While FT-ICR instruments offer the highest mass resolution, they require low-pressure environments and have limited dynamic ranges. The precision and resolving power they provide make them indispensable for specialized applications demanding utmost accuracy.

Orbitrap mass analyzers, introduced in 2005, share similarities with FT-ICR instruments but do not rely on magnetic fields. Instead, they utilize electrostatic attraction to confine ions in an elliptical orbit around a central electrode. Orbitraps are often paired with linear ion traps to achieve high mass accuracy for precursor ions and rapid fragmentation data generation.[105,106]

Tandem Mass Spectrometry

Tandem mass spectrometry (MS/MS) is a two-step technique used to break down selected precursor ions into fragments. This process allows for the characterization and identification of precursor ions. Prominent fragmentation techniques include collision-induced dissociation (CID) and ion-electron/ion-ion interaction methods such as electron capture dissociation (ECD) and electron transfer dissociation (ETD).[107-109] CID is a common MS/MS technique, where gas-phase ions are subjected to multiple collisions with inert gases, such as helium, argon, or nitrogen. These collisions impart internal

energy to the ions, leading to vibrational excitation and bond cleavage. The extent of fragmentation depends on the total internal energy of the excited ion, resulting in the formation of b- and y-fragment ions. In contrast, ECD and ETD utilize ion interactions with electrons or other ions to induce fragmentation, producing c and z ions. These complementary techniques are particularly valuable in proteomics for precise protein identification and structural elucidation. MS/MS detection can be performed in two ways: tandem-in-space and tandem-in-time. Tandem-in-space instruments employ two mass analyzers in series, each serving a distinct purpose, such as separation, selection, or fragmentation. Tandem-in-time instruments, on the other hand, perform both precursor ion selection and fragmentation within the same physical space, typically using QIT or FT-ICR.

Ion Detection

Ion detection is a crucial aspect of mass spectrometry (MS) systems, as it transforms a stream of mass-separated ions into a measurable signal. Among the common detectors, electron multipliers (EM) are prominent for their high sensitivity and minimal noise. These devices consist of a vacuum tube structure that undergoes a cascading process to amplify incident charges. A single electron initiates this process by striking a secondary-emissive material, releasing additional electrons. These electrons then move through an applied electric field, inducing more secondary emissions as they progress. This sequence repeats several times, resulting in a significant collection of electrons at a metal anode. There are three main types of electron multipliers: discrete dynode, continuous dynode, and microchannel plates.[110-112]

In a discrete dynode EM, electrons are sequentially attracted to individual charged plates known as dynodes. These electrons cascade down the plates within a glass or ceramic tube coated with a resistive material, emitting extra electrons upon impact. A continuous dynode system employs a horn-shaped glass funnel coated with a thin layer of semiconducting material. This principle resembles the discrete dynode, but electrons are emitted from the continuous inner surface of the horn. Additionally, microchannel plates consist of a 2-dimensional parallel array of very small continuous-dynode electron multipliers. Apart from electron multipliers, other detectors used in MS systems include Faraday cups (FC), photomultiplier conversion dynodes, and array detectors. FC detectors are cost-effective and suitable for measuring higher ion currents where EMs may face limitations. They operate by collecting ions on a conducting electrode connected to ground through a high-resistance path, generating a potential drop that can be amplified for measurement. Photomultiplier conversion dynode detectors utilize a dynode to initiate electron emission when ions initially strike it. These emitted electrons then strike a phosphor screen, releasing photons that enter a multiplier for amplification. The advantage of using photons is that the multiplier section can be maintained in a vacuum, extending its durability. Lastly, array detectors encompass a range of types, with some capable of simultaneously measuring ions with varying mass-to-charge ratios (m/z) and others being position-sensitive detectors.[112]

Characterization of Protein Post-translational modifications

Post-translational modifications (PTMs) involve alterations to proteins following their biosynthesis. Some of the common PTMs include phosphorylation, glycosylation, acetylation, methylation, and ubiquitination, among others. These modifications can exert

a significant influence over various cellular and biological processes. They enhance the functional diversity of the proteome by adding functional groups, cleaving regulatory subunits, or degrading proteins, impacting both normal cell biology and disease mechanisms. Understanding PTMs is essential for advancing cell biology and disease treatment strategies especially those involving immunoglobulins.[113-115]

Immunoglobulins

Immunoglobulins (Igs), also known as antibodies, are vital components of the adaptive immune system that recognizes and combat pathogens.[116] B cells, stimulated by specific immunogens, transform into plasma cells that produce immunoglobulins. These glycoproteins make up roughly 20% of plasma protein and contribute to humoral immune responses against a wide array of antigens. Different immunoglobulins, including IgM, IgG, IgA, IgE, and IgD play distinct roles in immune function.[117,118] The fundamental structure of antibodies involves two light chains and two heavy chains arranged in a light-heavy-heavy-light configuration. Heavy chains vary among antibody classes, comprising one Fc region for biological functions and a Fab region housing antigen-binding sites. Antibodies possess multiple functions, such as activating the complement system, opsonizing microbes for phagocytosis, preventing microbe attachment to mucosal surfaces, and neutralizing toxins and viruses.

Immunoglobulin G (IgG), a monomeric antibody with an approximate molecular weight of 146 kDa and a serum concentration of 9.0 mg/mL is the most prevalent antibody. IgG comprises of two heavy chains and two light chains, forming a quartet. IgGs contribute to numerous humoral immune functions, including neutralizing antigens, activating the complement system, enabling complement-dependent cytotoxicity (CDC),

and facilitating antibody-dependent cell-mediated cytotoxicity (ADCC).[119,120] Four IgG subclasses (IgG1, IgG2, IgG3, IgG4) exhibit structural variations in their constant regions, particularly in the hinge and upper CH2 domains, with IgG1 being the most abundance. These antibodies bear N-glycosylation at Asn-297 within the CH2 domain of the crystallizable fragment (Fc) on the heavy chains, with Fc glycans showing significant heterogeneity due to different terminal sugars. Understanding the diversity of immunoglobulins and their structures is crucial for comprehending the intricacies of the immune response and their applications in various immunoassays. IgGs can be recombinantly produced and applied as biotherapeutics.

Biotherapeutics

Biotherapeutics, a rapidly expanding segment of the pharmaceutical sector, are products that derive their active components from biological sources. Biotherapeutic drugs are produced through recombinant protein expression, frequently utilizing Chinese Hamster Ovary (CHO) cells.[121,122] These cells generate glycoproteins with human-like glycans, which is crucial for reducing immunogenicity, as humans often have antibodies against non-human glycan epitopes. A notable example is the hypersensitivity reactions observed with Cetuximab due to non-human glycans. Biotherapeutics include a diverse range of treatments, such as recombinant proteins, monoclonal antibodies (mAbs), cytokines, gene therapies, vaccines, and stem cell-based therapies. mAbs, in particular, are a fast growing category within biotherapeutics that play an important role in treating oncological, autoimmune, and inflammatory conditions. Over 100 therapeutic proteins with mAbs are approved for use in the European Union and the USA. These proteins

serve various roles, from supplementing deficient proteins to interfering with specific molecules or organisms.

While protein therapeutics have seen remarkable growth, the field requires new methodological advancements to address complexities such as resistance to therapy, target accessibility, biological system intricacies, and individual variations. Nonetheless, they continue to hold immense promise in revolutionizing healthcare and treating a wide array of diseases. Moreover, biotherapeutics have distinct requirements for non-clinical pharmacology and toxicology testing, as they originate from biological sources.[121] Challenges exist in predicting potential adverse reactions, especially concerning specific patient populations. To address these challenges, new methodologies and bioinformatics tools are being developed to better assess and monitor potential adverse drug reactions.

Post-translational modifications in Biotherapeutics

The growing biopharmaceutical market presents new challenges for ensuring product quality and safety, primarily due to the variability arising from PTMs.[123] Proteins, constituting the majority of biological drugs, commonly undergo PTMs such as phosphorylation, glycosylation, acetylation, methylation, ubiquitination, glycation, oxidation, deamidation, glycation and pyroglutamation. PTMs can occur at various protein sites, affecting their biological activity, half-life, and immunogenicity. Characterizing PTM patterns is a complex, time-consuming aspect of biopharmaceutical development and production. For instance, Glycation PTM can potentially affect bioactivity and molecular stability, requiring thorough characterization in therapeutic proteins such as mAbs. Glycated proteins may further degrade into advanced glycation end (AGE) products, emphasizing the need for comprehensive investigation of this

modification during manufacturing, storage, and *in vivo* circulation.[124] Moreover, glycosylation PTM plays a pivotal role in determining the pharmacological properties of biotherapeutics, influencing their stability, potency, solubility, bioavailability, pharmacokinetics, and immunogenicity. Therefore, great attention is focused on optimizing glycosylation properties in biotherapeutic development.[125] Further, Pyroglutamate formation, can occur at the polypeptide chain's N terminus. Both glutamine and glutamate at the N termini of recombinant monoclonal antibodies can spontaneously cyclize to pyroglutamate (pE) *in vitro*, with glutamate conversion to pyroglutamate occurring under nearly physiological conditions.[126] Thus, it is essential to characterize these PTMs to ensure the safety and efficacy of therapeutic drug products.

Glycation

The biopharmaceutical sector has witnessed a significant growth, with the global market estimated at $333.09 billion in 2022 and an expected annual growth rate of 12.5% between 2022 and 2030. However, the industry faces the challenge of guaranteeing the quality, efficacy, and safety of its products.[124] Since most biological drugs consist of proteins, they are susceptible to various PTMs, such as glycation, oxidation, deamidation, and glycosylation. Glycation, an important PTM, is linked with various health conditions, including diabetes, Alzheimer's disease, cataracts, and Rheumatoid arthritis.[127,128] This process involves the interaction between a reducing sugar and a protein's primary amine, either at its N-terminus or on a lysine sidechain. It is crucial to characterize glycation to ensure the safety and efficacy of therapeutic drug products, since this modification can occur during fermentation, storage, or drug infusion steps, impacting the overall charge, bioactivity, and stability of mAbs. Glycated mAbs are vulnerable to degradation, leading

to the formation of AGEs, which can crosslink with tissue macromolecules and interact with the receptor for AGEs (RAGE). This interaction may contribute to pathological responses in conditions such as aging, diabetes, and arthritis.

Characterizing glycation poses challenges due to the difficulty in observing detectable signals for potential glycation sites, and it can spread across the entire protein, resulting in heterogeneous products of low abundances. Various techniques are employed for glycation characterization, including Boronate Affinity Chromatography (BAC) and charge-based methods such as capillary isoelectric focusing (cIEF) and ion exchange chromatography (IEC).[124] Liquid Chromatography-Mass Spectrometry (LC-MS) is widely used, either in top-down mass spectrometry or bottom-up peptide mapping, to determine glycation levels and locations. HILIC chromatography is effective in characterizing hydrophilic modifications including glycation.[69,71]

Several techniques are available for detecting and quantifying glycation, including ELISA, HPLC-FLD, LC-MS/MS, and GC-MS detection of AGEs.[129,130] Quantitation approaches that target glycated peptides (Amadori product) often rely on the peak area of glycated peptides, assuming similar ionization efficiency to tryptic peptides.[131] These methods typically require detectable levels of glycated peptides and may involve enrichment steps before LC-MS analysis. An alternative approach involves using a heavy isotope-labeled variant of the target protein to determine glycation levels accurately, offering advantages such as accurate and precise quantitation.

Glycosylation

Among PTMs, glycosylation is one of the most prevalent, affecting approximately 50% to 70% of human proteins. Glycosylation, either through N- or O-linkages, is a

tightly regulated mechanism in cells that profoundly influences protein structure, function, and stability. In N-linked glycoproteins, a glycan is covalently attached to an Asparagine (Asn) residue via a N-glycosidic bond, typically within the Asn-X-Ser/Thr motif, where "X" represents any amino acid except Proline (Pro). Three types of N-glycans—Oligomannose, Complex, and Hybrid—have specific structural variations, with potential modifications such as Galactose (Gal), N-Acetylneuraminic acid (Neu5Ac), or N-Glycolylneuraminic acid (Neu5Gc). Glycoproteins play a vital role in cellular functions, and their analysis and characterization rely heavily on LC-MS methods.[132]

LC-MS is the preferred analytical tool to comprehensively characterize glycoproteins. The "bottom-up" approach is commonly favored for glycoproteomics, allowing efficient separation, simpler spectral interpretation, and identification of modification sites.[133] The process includes denaturation, reduction, alkylation, proteolytic digestion with enzymes such as Trypsin, and subsequent analysis of glycopeptides. Alternatively, "glycomics" focuses on released glycans and is particularly useful for structural analysis. The N-glycans can be released from the digested protein using enzymes such as PNGaseF, tagged with a labeling agent such as 2-AB, 2-AA, Procainamide among others to enhance its ionization in the mass spectrometry.[134,135] The labeling method is followed by a reductive amination step to form a more stable conjugate for detection. This can be carried out using reducing agents such as $NaBH_3CN$, or a less toxic 5-ethyl-2-methylpyridine borane (EMP) reducing agent. The sample is typically desalted and using size-exclusion column, polyamide column or can be cleaned-up without the use of a column for LC-MS analyses. Tandem mass spectrometry (MS/MS) plays a crucial role in glycosylation analysis by providing structural

information, including glycosidic cleavage ions and oxonium ions, thus aiding in the identification. Liquid chromatography separation, particularly HILIC, helps resolve glycoforms, contributing to N-glycan characterization.[69-72]

Pyroglutamation

Pyroglutamate modification is a post-translational modification that converts N-terminal glutamine or glutamate into a cyclic ring structure known as pyroglutamate (pyroGlu) or pyrrolidone carboxylate.[136-138] This modification has been identified in various species, including plants, animals, and bacteria, and is catalyzed by enzymes such as glutaminyl cyclase or isoglutaminyl cyclase. Researchers commonly study pyroglutamate modification to explore the functions of numerous peptide hormones, such as gastrin, neurotensin, and thyrotropin-releasing hormone (TRH). Notably, pyroglutamic acid has been detected at the N-termini of proteins such as collagen, fibrinogen, antibody light and heavy chains, and kinins. Pyroglutamate formation can significantly impact a protein's structure, stability, and biological activity.[126] It has been observed to safeguard proteins including fibrin, fibrinogen, and collagen-like proteins from degradation by aminopeptidases. Moreover, this modification has implications for neurodegenerative disorders such as Alzheimer's disease, familial British dementia, and familial Danish dementia. In these disorders, N-terminally truncated and pyroglutamate-modified amyloid-β peptides are prone to accelerated aggregation due to increased hydrophobicity.

Given the functional importance of pyroglutamate modification and its occurrence during the manufacturing and storage of monoclonal antibodies (mAbs), it is crucial to characterize pyroglutamated peptides and proteins. Utilizing techniques such as LC-MS can help in this characterization process. The pyroglutamate formation from glutamic

acid results in 18 Da loss owing to the elimination of water molecules. In addition, pyroglutamate formation when N-terminus amino acid is glutamine results in a loss of 17 Da owing to the release of NH_3 molecule.[126,136-138] This change in the m/z of the modified peptide can be characterized using bottom-up approach in LC-MS. The presence of both pyroglutamated and unmodified peptides as pairs can serve as additional confirmation for the presence of specific peptides. The thorough characterization of pyroglutamation also proves valuable when quantifying unmodified peptides.

CHAPTER 3

PREDICTION AND CHARACTERIZATION OF GLYCATED AND PYROGLUTAMATED PEPTIDES AND PROTEINS USING HILIC-MS[1]

[1] Priya, S., Kowalski, E. L., Popov, M. and Orlando, R. To be submitted to *The Journal of Biomolecular Techniques*.

Abstract

Glycation is an important post-translational modification (PTM) that has been linked to diabetes, cataract, Alzheimer's, and Rheumatoid arthritis. This reaction occurs between a reducing sugar and a primary amine at the N-terminus of a protein or at a lysine sidechain. Ultimately this interaction can lead to advanced glycation end products (AGEs) that are associated with several disease complications. Glycation could occur during manufacturing and storage of therapeutic proteins, including monoclonal antibodies (mAbs), necessitating the characterization of this modification to ensure safety and efficacy of therapeutic drug products. Hydrophilic Interaction Liquid Chromatography (HILIC) has been previously employed to characterize hydrophilic modifications. It can also be utilized to study glycation PTM since the hydrophilic nature of the glycation product could lead to a characteristic shift in HILIC retention. This work focuses on deriving a retention coefficient that describes the extent of hydrophilicity of glycation modification on HILIC using *in-vitro* glycated peptide and protein samples. The HILIC retention coefficient can be utilized to predict the retention time of tryptic peptides with glycation modification in complex unknown protein samples including immunoglobulins (IgGs). The analysis was further extended to characterize peptides generated from Endoproteinase Glu-C. In addition, retention prediction of peptides containing pyroglutamated N-terminus glutamic acid was performed. Pyroglutamation PTM has been linked to several neurodegenerative disorders that necessitate accurate characterization.

Introduction

The demand for biopharmaceuticals has shown a significant growth over the years with a global market size of $333.09 billion in 2022 and an expected growth of 12.5% (CAGR) between 2022 and 2030.[139] One of the key challenges that drug developers and manufacturers need to combat is assuring the drug product's quality, efficacy, and safety. Most biological drugs are proteins that can undergo some form of post-translational modification (PTM), which can affect their biological activity, immunogenicity, and half-life.[140,141] Common protein modifications include glycosylation, oxidation, deamidation and glycation among others. Characterizing these modifications could be a complicated and time-consuming part of biotechnology industry.

Glycation is an important PTM that has been linked to diabetes, Alzheimer's, Cataract and Rheumatoid arthritis.[127,128] This process involves reaction between a reducing sugar such as glucose, fructose, or galactose and the alpha amine terminal of a protein or epsilon amine group on a lysine side chain.[142] An unstable Schiff's base intermediate is produced that can potentially undergo a spontaneous multistep Amadori rearrangement giving rise to a more stable, covalently bonded ketoamine product (Figure 3.1). Glycated proteins when exposed to elevated oxidation conditions over prolonged period can undergo further degradation resulting in Advanced Glycation End products (AGEs). AGEs could be responsible for various pathological responses observed in aging, diabetes, and arthritis as a result of intracellular accumulation, crosslinking with tissue macromolecules, and interaction with specific receptor for AGEs called RAGE.[143-145]

Glycation is a potential Critical Quality Attribute (CQA) in therapeutic monoclonal antibodies (mAbs). It could be introduced during fermentation step, where glucose acts as an energy source for mAb producing cells.[146] Glycation could also be introduced during the storage of therapeutic mAbs due to the presence of carbohydrates in the formulation.[147] Although non-reducing disaccharides such as sucrose are typically used in the formulation, sucrose hydrolysis could produce reducing sugars under acidic pH and elevated temperatures thereby causing glycation. In addition, glucose is an ingredient of commonly used solutions for drug infusion. Glycation can alter the overall charge on therapeutic proteins thus hindering the biological functional site and reducing the bioactivity of therapeutic proteins.[148] Antibody aggregation is also an important CQA that is associated with AGE formation and cross-linking.[147] AGE-damaged antibody could also trigger an immune response by forming anti-IgG autoantibodies in Rheumatoid Arthritis patients. It is expected that glycated proteins are targeted for cellular proteolysis and have a decreased half-life.[149]

Some of the challenges associated with glycation characterization include the lack of a specific sequence that signals a potential glycation site as the reaction is non-enzymatic.[150] Furthermore, if a protein does not contain a highly reactive site for this modification, glycation could spread across the entire protein with low levels of glycation on all the susceptible glycation sites forming heterogeneous products of low abundances.[151] Therefore, it is essential to perform comprehensive studies to characterize glycated products to ensure safety and efficacy of therapeutic drugs.

One of the current strategies that is used for glycation characterization includes Boronate Affinity Chromatography (BAC)[146,152] that requires native running conditions

and minimum sample preparation. However, non-specific binding could arise as the glycation species could also interact with the BAC surface. In addition, the quantitation is an estimate as it is challenging to differentiate between proteins with a single glycation or multiple glycations.[10] Another strategy to identify glycated species is based on charge of the molecule as glycation neutralizes the positive charge at the glycation site. Therefore, certain charge-based methods such as capillary isoelectric focusing (cIEF)[10], imaged capillary isoelectric focusing (icIEF) and ion exchange chromatography (IEC) can be employed.[146] However, IEC may not have sufficient resolution to separate the glycated variants due to combined charge effects arising from multiple sites of low-level glycation spread across the molecule. In addition, several charged sites corresponding to different PTMs could further complicate the analysis when it comes to complex protein samples such as antibodies.

Liquid Chromatography-Mass Spectrometry (LC-MS) has been widely utilized for efficient characterization of PTMs.[10] Top-down mass spectrometry of intact antibody or enzymatically cleaved monoclonal antibody fragments could be used to determine the glycation level with every glycation site showing a +162 Da mass shift. Bottom-up peptide mapping is widely used to locate the glycation site.[148,150] Glycation has been reported to inhibit the action of trypsin at the C-terminus of lysine residue. Thus, a missed tryptic cleavage at the lysine residue with a +162 Da shift in MS indicates a glycated peptide.[10,153] Further, HILIC separation mode is an effective strategy to characterize hydrophilic modifications such as deamidation, methionine oxidation, and glycosylation.[153,154,69] Glycation involves the addition of a hydrophilic glucose molecule that may lead to an increase in HILIC retention. Glycation PTM also neutralizes the

positive charge on primary amine that could decrease the retention time. It was hypothesized that a combined effect from these two circumstances could result in a characteristic shift under HILIC mode.

This study was undertaken to develop a robust analytical workflow to predict and characterize Glycation sites in therapeutic mAbs with the aim to ensure safety and efficacy of drug products. Herein, the retention behavior of several *in-vitro* glycated[155] standard peptides and proteins on HILIC were studied and a retention coefficient for this modification was derived using dextran as an external calibrant. This retention coefficient in combination with the Badgett's model[69] that has been previously described for tryptic peptide prediction was used to predict and characterize glycation in unknown mAbs such as human IgG1 (Adalimumab), IgG4 (Natalizumab) and custom IgG2 ('Frankenmab').

Furthermore, retention prediction was performed on tryptic peptides with pyroglutamate modification when the N-terminus contained a glutamic acid residue. Pyroglutamate modification is a post-translational conversion of N-terminal glutamine or glutamate to form a five-membered cyclic ring structure known as pyroglutamate (pyroGlu), or pyrrolidone carboxylate.[136-138] This modification has been reported in species such as plants, animals, bacteria, and is said to be catalyzed by glutaminyl cyclase or isoglutaminyl cyclase. It is commonly studied to understand the functionality of several peptide hormones such as gastrin, neurotensin and thyrotropin releasing hormone (TRH). Pyroglutamic acid has also been identified at the N-terminus of collagen, fibrinogen, light and heavy chains of antibodies and kinines. With a potential to influence the structure, stability and biological activity of a protein, pGlu formation has been observed to protect fibrin, fibrinogen, collagen-like proteins from aminopeptidase

degradation. This modification is also linked to neurodegenerative disorders including Alzheimer's disease, familial British Dementia and familial Danish dementia as N-terminally truncated and pyroglutamate modified amyloid-β peptides could undergo accelerated aggregation owing to an increase in hydrophobicity. Given the functional relevance of this post-translational modification and its occurrence during manufacturing and storage of mAbs, it becomes particularly important to characterize the pyroglutamated peptides/proteins using methods such as LC/MS technique. Observance of both pyroglutamated peptide and unmodified peptide in pairs can serve as an additional validation for the presence of a specific peptide. Characterizing pyroglutamation could also be beneficial when performing unmodified peptide quantitation.

Materials And Methods

Protein digestion

Protein samples including bovine insulin and bovine Cytochrome C (both purchased from Sigma Aldrich, St. Louis, MO, USA), human IgG1 (Adalimumab), custom IgG2 ('Frankenmab') and IgG4 (Natalizumab) from GlycoScientific (Athens, GA, USA) were buffer exchanged with 50 mM ammonium bicarbonate (pH 7.8) to have a final concentration of 1 mg/mL. They were then reduced using 200 mM Dithiothreitol (DTT) and alkylated using 1 M iodoacetamide, both purchased from Sigma Aldrich (St. Louis, MO, USA), to have a final concentration of 5 mM DTT and 8 mM iodoacetamide. Further, sequencing grade trypsin from Promega (Madison, WI, USA) was added at 20:1 ratio (w/w, protein/trypsin) and incubated at 37°C overnight. The digested protein samples were then dried on SpeedVac and resuspended in 80% ACN (1 mg/mL) and 20%

H_2O before LCMS analyses. Endoproteinase Glu-C (Staphylococcus aureus strain V8 from Thomas Scientific, Swedesboro, NJ, USA) digestion was carried on human IgG1 by performing reduction and alkylation as above and adding Glu-C to a final protein:proteinase ratio of 20:1 (w/w). IgG1 was then incubated at 37^{o}C in either PBS or ammonium bicarbonate overnight.

in-vitro Glycation

A series of standard peptides such as human [Glu1]-Fibrinopeptide B (GluFib), Leucine Enkephalin, Bradykinin and Substance P (Frag 2-11) were purchased from Sigma Aldrich (St. Louis, MO, USA). The standard peptides along with digested bovine Cytochrome C, bovine Insulin, human IgG1, custom IgG2 and IgG4 were glycated *in-vitro*. GluFib, Leucine Enkephalin, Bradykinin, Substance P, Insulin and Cytochrome C were glycated using 2:1 D-Glucose: peptide/protein molar ratio at pH=2.4 (65^{o}C, 1d). D-Glucose: protein molar ratio of 1000: 1 was used for IgG samples. The samples were then dried and resuspended in 80% ACN (1 mg/mL) for LCMS analyses.

Procainamide labeled Dextran (Mr 6,000) from Sigma Aldrich (St. Louis, MO, USA) was used as a retention calibrant and Procainamide labeled maltopentaose from Supelco Analytical (Bellefonte, PA, USA) was used as an internal standard. For 200 µg each of Dextran and maltopentaose was added 60 µL of 0.4 M Procainamide.HCl (Sigma Aldrich), 0.8 M sodium cyanoborohydride (Sigma Aldrich), mixed in DMSO:acetic acid;7:3 (v/v) and incubated at 65°C overnight. The samples were dried using SpeedVac, resuspended in 5% Acetic acid (240 µL) and cleaned on a PD MiniTrap G10 desalting column (Cytiva, Marlborough, MA) using the manufacturer's protocol. The samples were then dried and resuspended in 80% ACN (1 mg/mL).

in-vitro Pyroglutamate formation

In order to achieve efficient comparison in retention times between a significant number of pyroglutamated peptides and their un-modified variants, forced *in-vitro* pyroglutamation was performed. The digested peptide samples were dissolved in milli-Q water (1 mg/mL) followed by addition of acetic acid (pH = 2.4) and incubated at 37^{o}C for 4 days. The samples were then dried using Speed vac and re-suspended in 80% ACN for HILIC-MS analysis. Standard peptide such as Human [Glu1]-Fibrinopeptide B was suspended in 80% ACN (1 mg/mL) and was directly subjected to LC-MS.

LC-MS settings and instrumentation

Data were acquired using an Agilent1100 series (Santa Clara, CA, USA) coupled to Waters SYNAPT-G2 QTOF (Milford, MA, USA) system with ESI source. Peptides were separated using a 2.1-mm × 150-mm HALO Penta-HILIC column packed with 2.7-μm diameter superficially porous particles that have a 90-Å pore diameter (Advanced Materials Technology, Wilmington, DE, USA) at 60 °C column temperature. The mobile phases used to perform separation were 50 mM ammonium formate in water with 0.1% Formic acid (Solvent A), and 0.1% Formic acid in Acetonitrile (Solvent B). A linear gradient of 80% to 40% Solvent B over 40 minutes (1%B per minute) at 0.2 mL/min flow rate was used for separation. DDA Survey type experiments were run to characterize glycation in the peptide and protein samples. Mass spectral analyses were carried out using Waters MassLynx, Protein Lynx Global Server (PLGS) and Skyline software. Peptide retention times in minutes were converted to glucose units based on dextran samples that were run immediately before and after the protein/peptide sample of interest.

Results And Discussion

Resolving glycated peptides from unmodified peptides

The study began with *in-vitro* glycation[155] of several standard peptides that possess a single primary amine located either at the N-terminus or at a lysine residue. Peptides such as human [Glu1]-Fibrinopeptide B (GluFib), Leucine Enkephalin, Bradykinin and Substance P (Frag 2-11) were chosen. Substance P (Frag 2-11) was used to study lysine glycation as it contains Proline at the N-terminus with no primary amine available for glycation at that site. The *in-vitro* glycated samples were run on a Penta-HILIC column to understand the retention behavior of the glycated variants. Badgett's retention model[69] was first used to confirm the peaks corresponding to the unmodified peptides. For instance, the experimental retention time of unmodified Bradykinin (RPPGFSPFR) was observed to be 9.40 min (Figure 3.2), which was close to the retention time predicted by Badgett's model (9.31 min). The experimental retention time of all the unmodified peptides correlated well with their predicted retention time, which was calculated by Badgett's model. Moreover, a glycated peptide with +162 Da m/z was observed for each standard peptide. For example, glycated Bradykinin (**R**PPGFSPFR) eluted at 10.08 min demonstrating a net increase in HILIC retention (+0.68 min) upon glycation. Thus, a characteristic chromatographic shift was observed for the glycated variant in the HILIC mode when compared to its unmodified counterpart. The retention shift ranged from +0.21 min for Leucine Enkephalin to +1.19 min for Substance P (Table 3.1). Glycation modification introduces a hydrophilic glucose molecule on the protein that can increase the retention on a HILIC column, but at the same time, the positive charge at the primary amine is neutralized causing a decrease in retention. A combined

effect from both of these factors had resulted in a net increase in retention time upon glycation.

Proteins containing more than one glycation site were analyzed next, including bovine Insulin and bovine Cytochrome C. LC-MS analysis after S-S cleavage in Insulin revealed an increase in retention time for N-terminus glycated Chain A (+0.77 min) and Chain B (+0.73 min) peptides when compared to their unmodified counterparts (Table 3.1). In addition, *in-vitro* glycation was performed on bovine Cytochrome C followed by trypsin digestion. Cytochrome C has 18 lysine residues that could undergo glycation. 11 peptides glycated at the lysine residues were identified using MS1 spectra. Glycation on the lysine sidechain generated a missed cleavage peptide with an additional 162 Da m/z. Trypsin activity was seen to be inhibited by glycation on a lysine residue. Trypsin possesses a negative pocket and has specificity for a long, slender tryptic peptide with positive charge on it such as on a lysine residue. However, a lysine-glycated peptide that has a sugar molecule neither contains the positive charge at primary amine nor has the appropriate shape to fit into the trypsin pocket resulting in a potential loss of enzymatic activity. Therefore, a missed tryptic cleavage peptide in conjugation with a +162 Da m/z was used as an indicator for glycation. The retention shift in the case of lysine glycation was calculated from the unmodified missed cleavage peptide. The experimental retention times for the unmodified variants were consistent with those predicted by Badgett's model. Figure 3.3 demonstrates that the unmodified EDLIAYLKK peptide in Cytochrome C with 1 missed cleavage eluted at 15.68 min which was close to the retention time calculated by Badgett's model (15.55 min). The glycated missed cleavage peptide EDLIAYL**K**K demonstrated an overall increase in HILIC retention (+0.31 min)

upon glycation. Retention time shifts for glycated peptides ranged from +0.22 min to +1.15 min (Table 3.1). Overall, it was observed that there was a slight increase in retention time upon glycation when the glycation occurred at either the N-terminus of a peptide/protein or at the lysine residues.

Derivation of HILIC retention coefficient:

The retention shifts have been expressed in minutes thus far, but in order to use this prediction model on any LC-MS system with different LC conditions, a Procainamide labeled Dextran was used as a retention calibrant. Dextran is a glucose polymer that elutes in the order of increasing monosaccharide linkage and can provide a useful reference for the retention times of peptides that are in minutes. Procainamide labeled dextran samples were run before and after the glycated protein/peptide sample, the retention times were averaged and used to convert the retention time of peptides in minutes to Glucose Units (GU) based on the logarithmic fit for the dextran samples.[69] The retention time difference (in minutes) between a glycated and non-glycated peptide was therefore converted to GU and was used to calculate HILIC retention coefficient for this modification in GU. Such a strategy allows the model to be used on any LC-MS system as long as the dextran standard ladder is run along with the protein sample of interest with identical separation conditions. The HILIC retention coefficient for glycation PTM from standard peptides and proteins was calculated to be +0.35 GU with a standard deviation of 0.12 GU (Table 3.1).

Prediction of glycation in unknown test samples:

The HILIC retention model for glycation PTM was then put to test by predicting and characterizing glycation in more complex samples such as IgGs including

Adalimumab (human IgG1), Natalizumab (IgG4 expressed in CHO cell) and 'Frankenmab' (custom IgG2). These IgGs were received from GlycoScientific, Athens, GA.

Adalimumab glycation was achieved by incubating the protein at 65^{o}C for 1d followed by reduction, alkylation, and overnight trypsin digestion. Glycation could undergo at the N-terminus of light and heavy chains as well as on the lysine residues. The predicted retention time for the glycated peptide was calculated by adding 0.35 GU (coefficient derived for glycation) to Badgett's predicted retention time for unmodified peptide (in GU). For instance, the predicted retention time of VYACEVTHQGLSSPVTKSFNR missed cleavage peptide as per Badgett's model was 7.50 GU, which corresponded to 20.08 min (Figure 3.4). The experimental retention time for this peptide was 20.21 min (7.58 GU) that was close to the predicted value. The retention time of its glycated variant VYACEVTHQGLSSPVT**K**SFNR was then predicted by adding 0.35 GU to 7.50 GU that gave 7.85 GU or 20.74 min. A chromatographic peak at 20.62 min (7.84 GU) was observed that was close to the predicted retention time. It is worth mentioning that the peak intensity of the unmodified missed cleavage peptide was low that could be attributed to the trypsin being able to efficiently cleave at the C-terminus of every lysine and arginine residue. The unmodified missed cleavage peptides were in fact not detected in all the cases, highlighting the importance of calculating predicted retention time for glycation by adding 0.35 GU to Badgett's predicted retention time (in GU), which was developed for unmodified variants. For example, the unmodified peptide ALPAPIEKTISK (missed 1) was not present in detectable amount (Figure 3.5 panel A). Even so, the predicted retention time

of glycated ALPAPIE**K**TISK (missed 1) could be calculated by adding 0.35 GU to Badgett's predicted retention time for unmodified peptide i.e., 5.74 GU (Table 3.2) resulting in 6.09 GU, or 17.75 min. A peak at 18.41 min was observed in the extracted ion chromatogram (XIC) corresponding to the m/z of singly charged ALPAPIE**K**TISK peptide (Figure 3.5 panel B). Thus, the experimental retention time for glycated variants were seen to be close to the predicted retention time. The predicted and experimental retention times of all detected unmodified and glycated peptides in minutes as well as in GU are reported in Table 3.2. Overall, the average retention shift in Adalimumab tryptic peptides upon glycation was observed to be +0.50 GU that was within a close range of the calculated coefficient of +0.35 GU.

All the glycated peptides were confirmed using the retention model and MS1 spectra. Low levels of glycation at multiple sites along with poor ionization efficiency of a bulkier glycated peptide that is devoid of a positive charge resulted in a weak peak intensity when compared to tryptic peptides in the sample. This made the analysis by MS2 very challenging as the chances that the ion corresponding to the glycated variant would be picked up for MS2 was very low even with Survey Top 4 or Top 5 experiments. It may not be abundant enough to fragment well even if it was picked up for MS2.

The second unknown sample on which the model was tested was Natalizumab, an IgG4 mAb expressed in CHO cell. The analysis proceeded in a similar fashion i.e., predicting the retention time of a glycated peptide by adding 0.35 GU to Badgett's retention time for unmodified peptide and confirming the chromatographic peak in the XIC using MS1 spectra. Figure 3.6 panel A shows an example of glycation on peptide VYACEVTHQGLSSPVT**K**SFNR (missed 1) in IgG4. The predicted retention time of

the glycated peptide was calculated to be 8.83 GU (19.99 min) and the XIC contained a chromatographic peak at 20.26 min, which was close to the predicted value. The retention shifts upon glycation for all the peptides observed in IgG4 are shown in Table 3.3. The average retention shift due to glycation in IgG4 was observed to be +0.53 GU. Finally, the third unknown IgG sample on which this model was tested was a custom made IgG2 mAb ('Frankenmab'). Glycation characterization was performed as before. Figure 3.6 panel B depicts the XIC of a glycated peptide AP**K**LLIYAASTLQSGVPSR in IgG2. The experimental retention time was 17.84 min that was close to the predicted retention time of 17.26 min. The retention shifts upon glycation for all the peptides observed and analyzed in IgG2 are shown in Table 3.4. The average retention shift due to glycation in IgG2 was observed to be +0.52 GU.

Initially, a retention coefficient of +0.35 GU was proposed for predicting glycation-induced shifts in HILIC. However, the analysis of the real-world peptides from IgG proteins indicated that the average shift in HILIC retention due to glycation PTM was +0.52 GU. We propose that 0.52 GU can be added to Badgett's retention model to predict the retention time of glycated peptides with better accuracy.

We then expanded glycation characterizations to analyze peptides generated by an enzyme different from trypsin. Endoproteinase Glu-C digestion was performed on human IgG1 after *in-vitro* glycation. Since the Badgett's model has been described for tryptic peptides, the predicted retention time for a glycated peptide was calculated by adding 0.52 GU to the experimental retention time of its non-glycated variant (in GU). The unmodified peptides in this case were present in detectable amounts since Glu-C cleaves at the C-terminus of either aspartic or glutamic acid residues with no interference from

glycation at lysine residue. Peptide IKRTVAAPSVFIFPPSDE was one of the Glu-C generated peptides observed in human IgG1 (Figure 3.7). The unmodified variant eluted at 14.06 min (4.20 GU). The predicted retention time for glycated peptide was calculated by adding 0.52 GU to 4.20 GU to give 4.72 GU, or 15.21 min. The chromatographic peak for the glycated I**K**RTVAAPSVFIFPPSDE peptide (at 15.30 min) was noted to be very close to the predicted retention time of 15.21 min (Table 3.5). This observation indicated that the proposed model could predict retention times not only for glycated tryptic peptides but also for glycated Glu-C peptides.

Prediction of pyroglutamated tryptic peptides

Standard peptides such as human GluFib as well as tryptic peptides in bovine Transferrin and Adalimumab (human IgG1) after forced pyroglutamation were analyzed next. Pyroglutamate modification on N-terminal glutamic acid (pyroGlu) results in a loss of a primary amine to generate a cyclized variant (Figure 3.8). The conversion occurs with the elimination of a water molecule that corresponds to a mass shift of -18 Da. Separation between modified and unmodified peptide was achieved under HILIC mode. It was observed that the pyroGlu variant of human GluFib (EGVNDNEEGFFSAR) eluted 3.57 min (or -2.21 GU) earlier than the unmodified peptide (Figure 3.9). A similar trend was observed in the case of bovine transferrin and humira heavy chain peptides that contained glutamic acid at their N-terminus. On an average, the pyroGlu variant of ELPDPQESIQR, ESKPPDSSK and ENFEVLCK peptides in bovine transferrin eluted earlier by 4.34 min (-2.61 GU), 4.74 min (-1.67 GU) and 5.15 min (-2.03 GU) respectively. Furthermore, EVQLVESGGGLVQPGR and EPQVYTLPPSR peptides in Adalimumab heavy chain again had a lower retention on Penta-HILIC column than their

native variants by 4.83 min (-2.09) and 5.01 min (-1.99 GU) respectively. The average shift in retention (in GU) on account of pyroGlu modification was calculated to be -2.10 GU (Table 3.6). The decreased retention time is likely due to decreased peptide hydrophilicity and a higher peptide isoelectric point,[138] since the positive charge at the primary amine was neutralized upon cyclization.

The mAbs used in this study are pure protein samples but we expect that the proposed model would benefit researchers aiming to characterize complex protein mixtures. Retention time prediction would allow one to narrow down the retention window in the XIC where multiple peaks could appear corresponding to the same m/z, thus leading in faster analyses. Such a prediction can also provide an additional level of confidence when characterizing glycated and pyroglutamated peptides.

Conclusions

The glycated peptides were shown to be resolvable from their unmodified variants by HILIC chromatography. Glycation modification introduces a hydrophilic glucose moiety on the protein that can cause an increase in HILIC retention. On the other hand, the neutralization of the positive charge on the primary amine could result in decrease in retention. An interplay of these two factors resulted in a slight overall increase in HILIC retention. Several standard peptides and proteins were utilized to derive a retention coefficient for glycation using Dextran ladder as a calibrant. This coefficient was then incorporated into the Badgett's peptide retention prediction model and was used to predict and characterize glycation in unknown complex mAb samples such as Adalimumab (human IgG1), Natalizumab (IgG4) and 'Frankenmab' (custom IgG2). In all these cases, the experimental retention time of glycated peptides was seen to be

consistent with the predicted retention time. It was discerned that on an average, a glycated peptide eluted later than its unmodified variant by +0.52 GU. We propose that this value when added to Badgett's tryptic peptide retention model can predict the retention time of glycated tryptic peptides. Additionally, the proposed model was able to accurately predict glycated peptides generated by Glu-C enzymatic digestion of human IgG1. The HILIC coefficient (0.52 GU) must be added to the experimental retention time (in GU) of unmodified variant when characterizing Glu-C generated peptides. Pyroglutamation PTM was also studied wherein it was observed that the average retention shift upon this modification was -2.10 GU in the HILIC mode as the pyroglutamated variant was less hydrophilic than the unmodified variant.

We believe that this model will aid in the analysis of complex protein mixtures by adding another layer of confidence in peak identifications as well as by cutting down the analysis time. We expect that this strategy would assist in ensuring safety and efficacy of therapeutic drug products that could be prone to glycation and pyroglutamation modifications.

Acknowledgements

The authors thank Dr. Barry Boyes (Advanced Materials Technology, Wilmington, DE) for providing Penta-HILIC columns for LC-MS analyses.

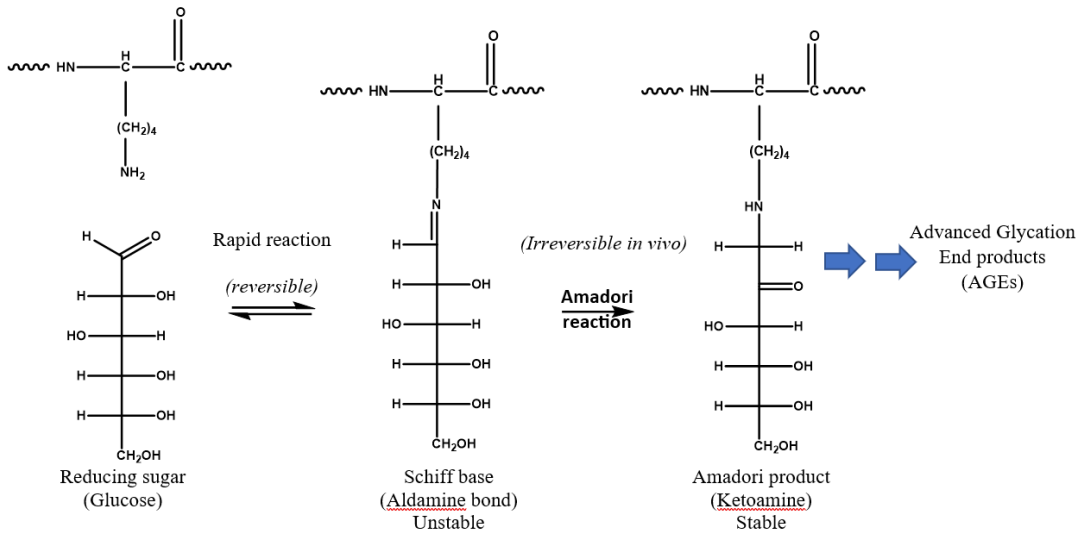

Figure 3.1: Scheme for glycation reaction on a lysine residue. The reducing end of sugar can undergo Schiff's base reaction with the primary amine of lysine residue to produce a ketoamine Amadori product. The Amadori product in the presence of reactive intermediaries can ultimately result in advanced glycation end products (AGEs).

(A)

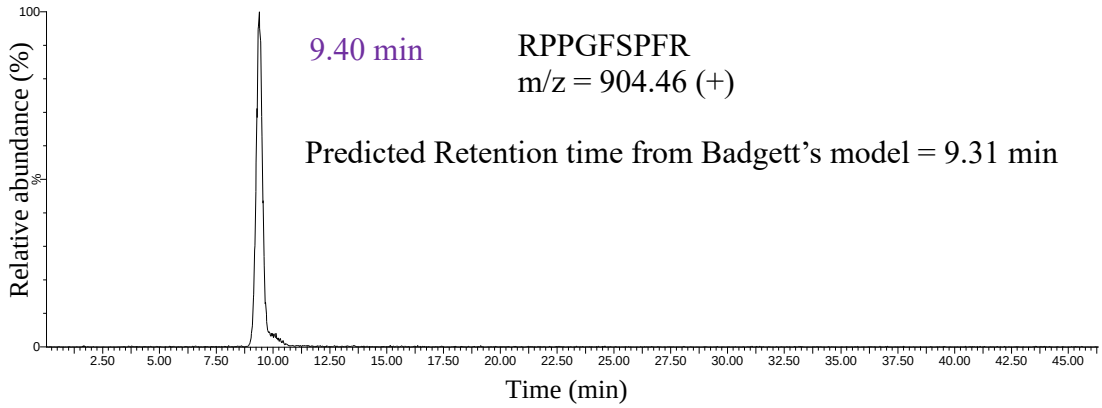

(B)

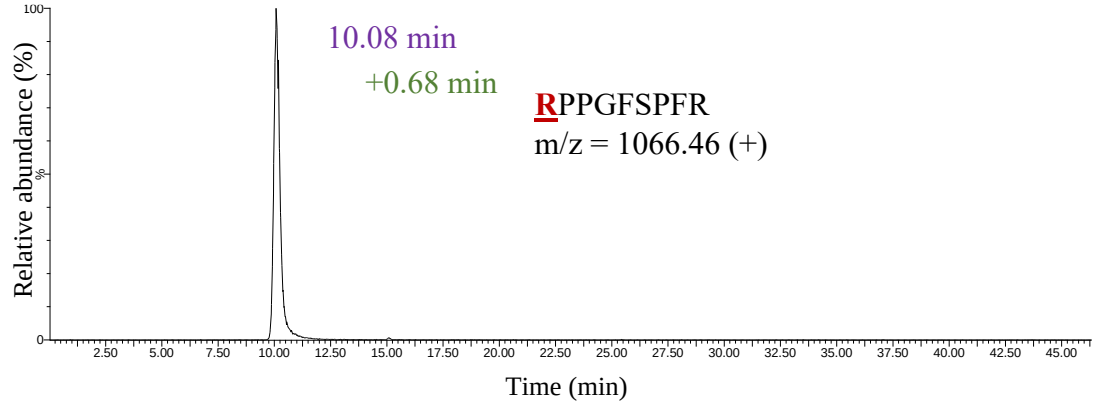

Figure 3.2: Extracted ion chromatogram (XIC) for **(A)** unmodified Bradykinin RPPGFSPFR and **(B)** glycated Bradykinin **R**PPGFSPFR demonstrating a net increase in HILIC retention (+0.68 min) upon glycation. The experimental retention time of the unmodified peptide (9.40 min) was observed to be close to the retention time predicted by Badgett's model (9.31 min).

(A)

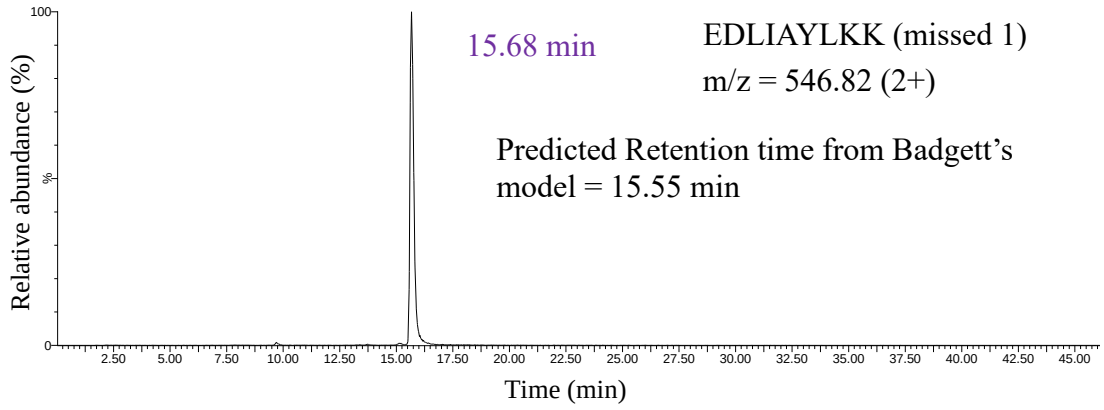

(B)

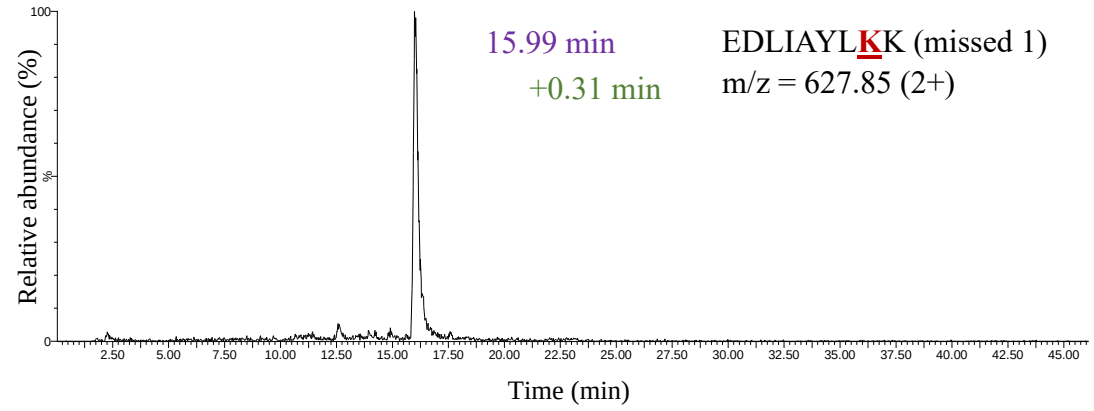

Figure 3.3: XIC for **(A)** unmodified missed cleavage peptide EDLIAYLKK and **(B)** glycated missed cleavage peptide EDLIAYL**K**K in bovine Cytochrome C demonstrating an overall increase in HILIC retention (+0.31 min) upon glycation. The experimental retention time of the unmodified peptide (15.68 min) was observed to be close to the retention time predicted by Badgett's model (15.55 min).

(A)

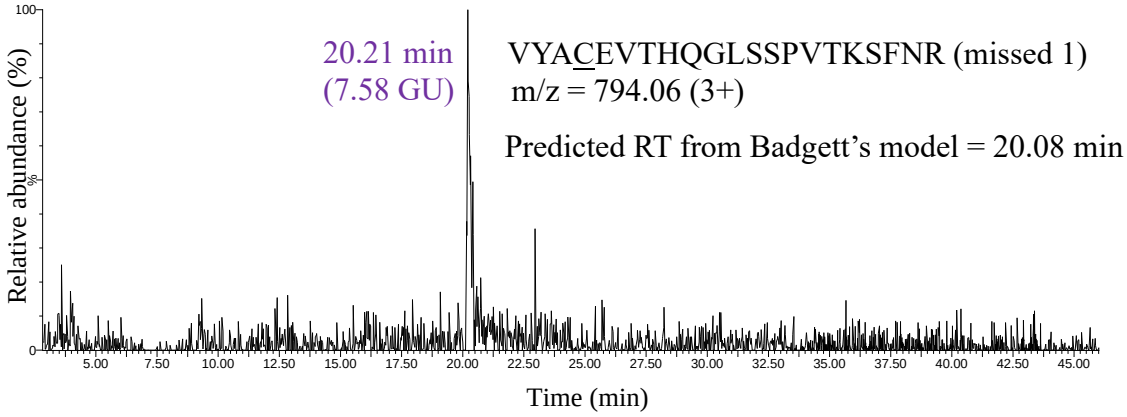

(B)

Predicted RT for glycated variant = 7.50 GU + 0.35 GU = 7.85 GU (**20.74 min**)

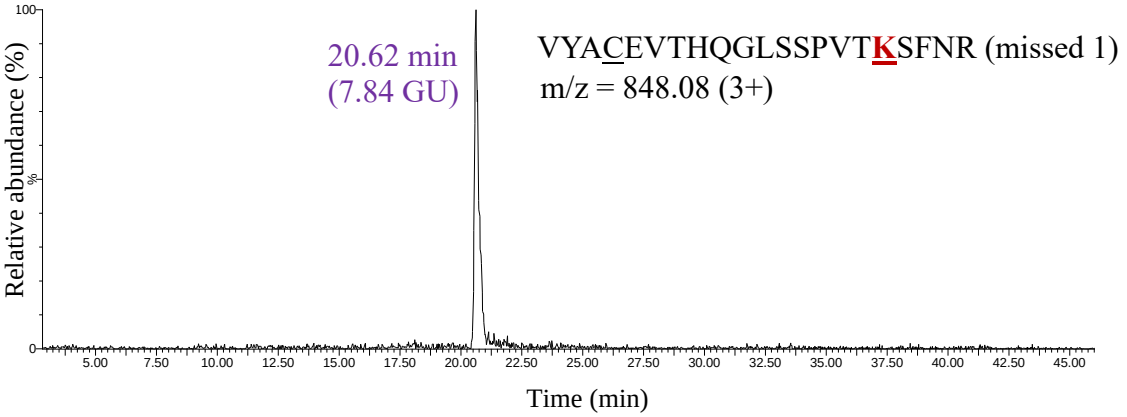

Figure 3.4: XIC for **(A)** unmodified missed cleavage peptide VYACEVTHQGLSSPVTKSFNR and **(B)** glycated missed cleavage peptide VYACEVTHQGLSSPVTKSFNR in human IgG1 (Adalimumab). The experimental retention time for the unmodified peptide (20.21 min) was observed to be close to the retention time predicted by Badgett's model (20.08 min). The experimental retention time of the glycated variant (20.62 min) was close to the predicted retention time (20.74 min), which was calculated using the HILIC retention coefficient for glycation.

(A)

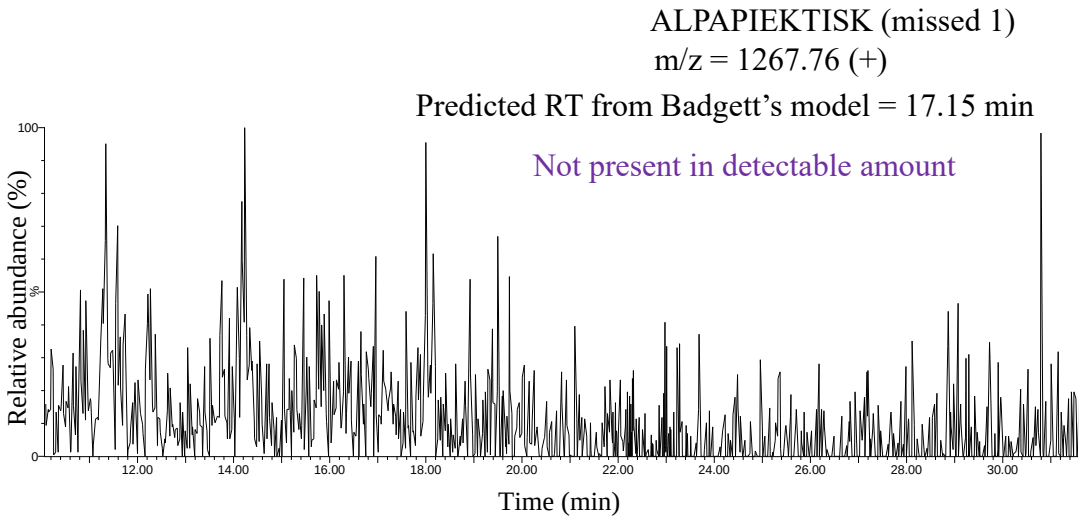

(B)

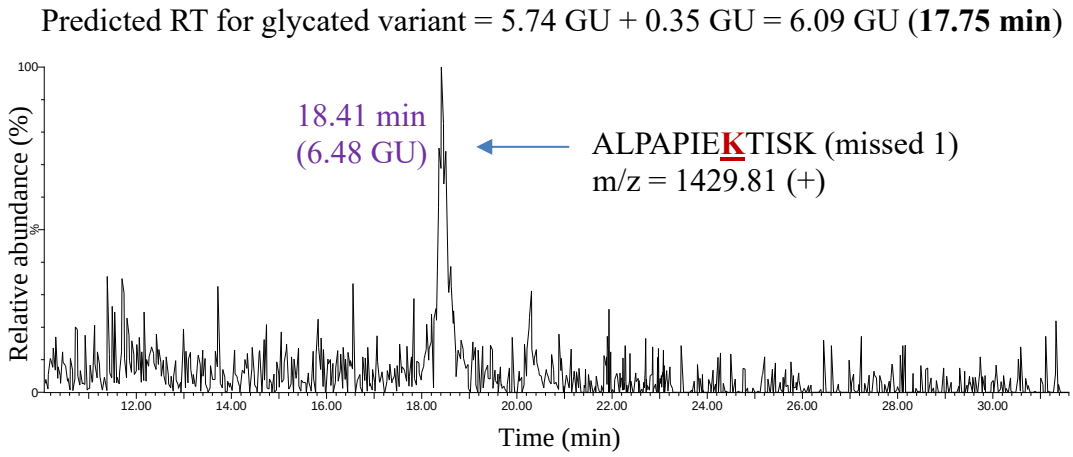

Figure 3.5: XIC for **(A)** unmodified missed cleavage peptide ALPAPIEKTISK and **(B)** glycated missed cleavage peptide ALPAPIE**K**TISK in human IgG1 (Adalimumab). The predicted retention time of the unmodified peptide calculated using Badgett's model was 17.15 min, but the unmodified peptide was not present in detectable amount. The experimental retention time of the glycated variant (18.41 min) was within a close range to the predicted retention time of 17.75 min, which was calculated using the HILIC retention coefficient for glycation.

(A)

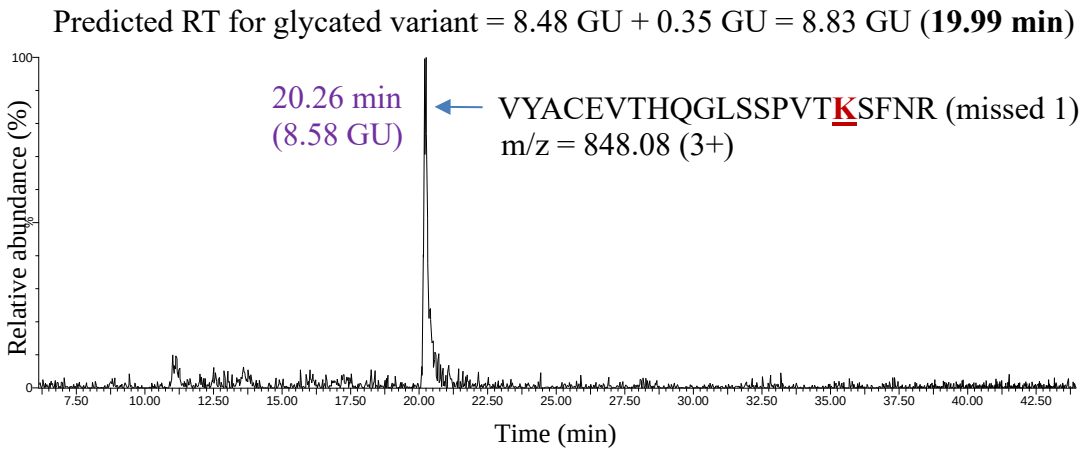

(B)

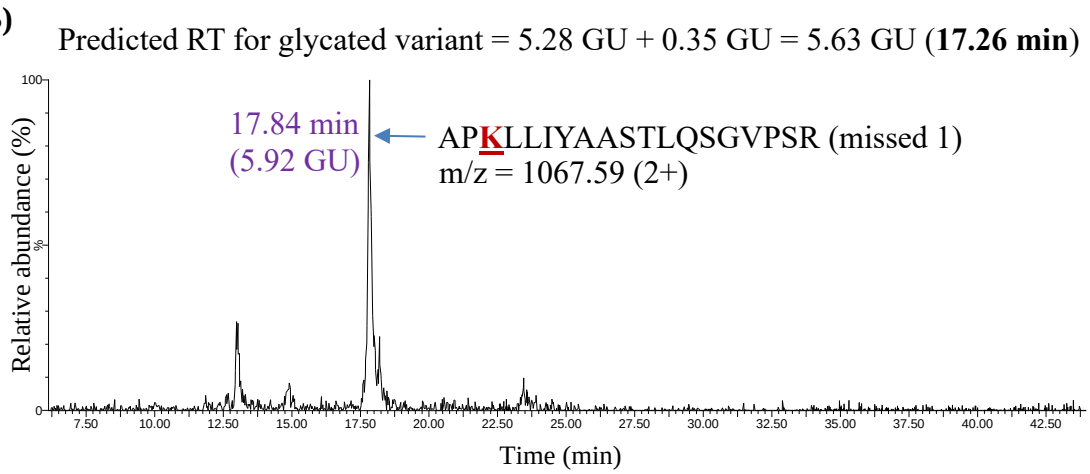

Figure 3.6: XIC for **(A)** glycated missed cleavage peptide VYACEVTHQGLSSPVTKSFNR in IgG4 (Natalizumab). The experimental retention time of the glycated variant (20.26 min) was within a close range to the predicted retention time of 19.99 min, which was calculated using the HILIC retention coefficient for glycation. **(B)** depicts the XIC for glycated missed cleavage peptide APKLLIYAASTLQSGVPSR in IgG2 ('Frankenmab'). The experimental retention time of the glycated variant (17.84 min) was within a close range to the predicted retention time of 17.26 min, which was calculated using the HILIC retention coefficient for glycation.

(A)

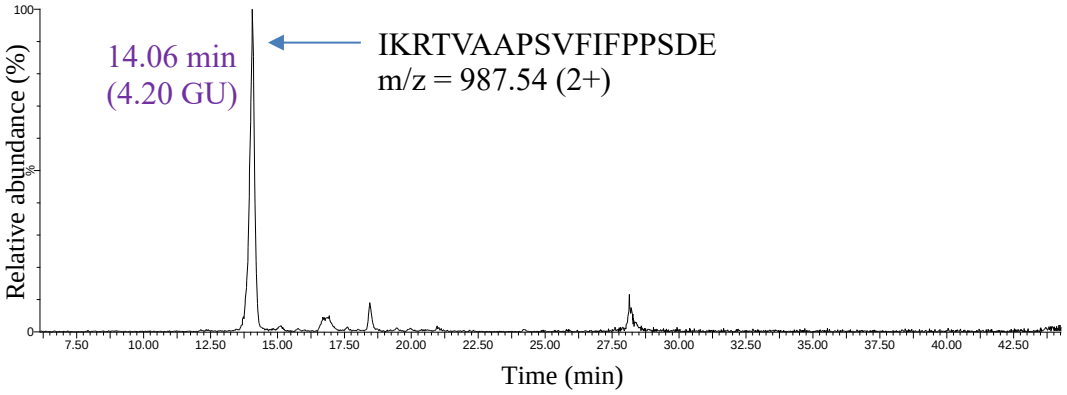

(B) Predicted RT for glycated variant = 4.20 GU + 0.52 GU = 4.72 GU (**15.21 min**)

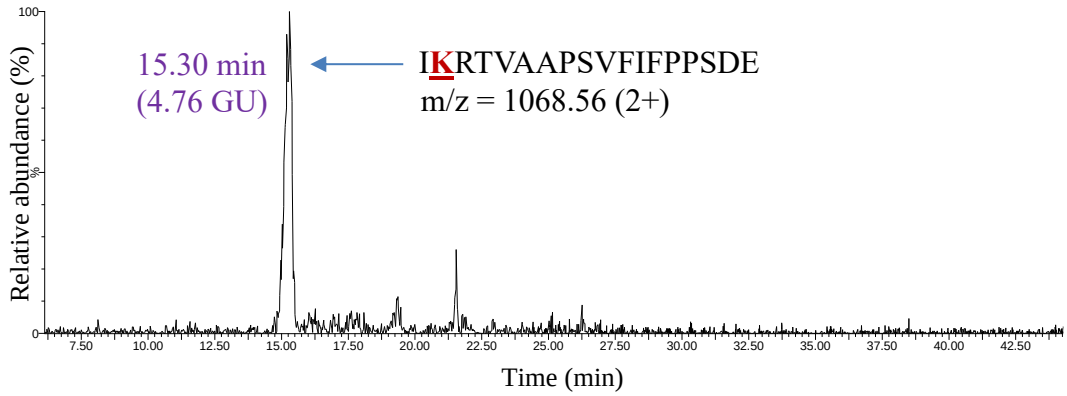

Figure 3.7: XIC for **(A)** unmodified Glu-C peptide IKRTVAAPSVFIFPPSDE and **(B)** glycated peptide IKRTVAAPSVFIFPPSDE in human IgG1 (Adalimumab). The experimental retention time of the glycated variant (15.30 min) was within a close range to the predicted retention time of 15.21 min, which was calculated using the HILIC retention coefficient for glycation.

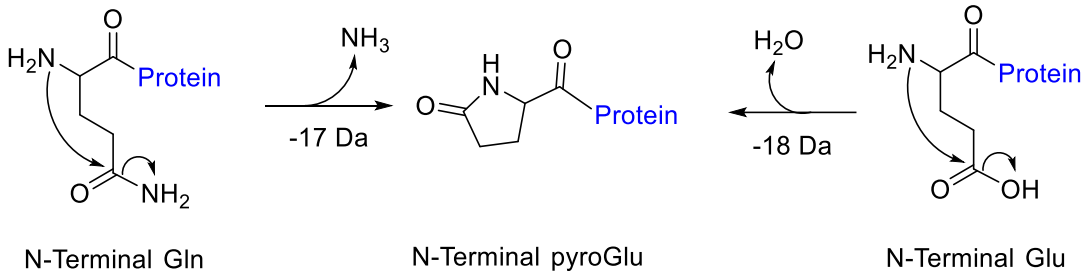

Figure 3.8: Mechanism for pyroglutamate formation (pyroGlu) when the N-terminus amino acid is glutamine (Gln) or glutamic acid (Glu). Cyclization to form pyroGlu from glutamine results in a 17 Da mass decrease owing to the loss of $-NH_3$, whereas pyroGlu formation from N-terminus glutamic acid proceeds through a loss of $-H_2O$ molecule resulting in 18 Da mass decrease.

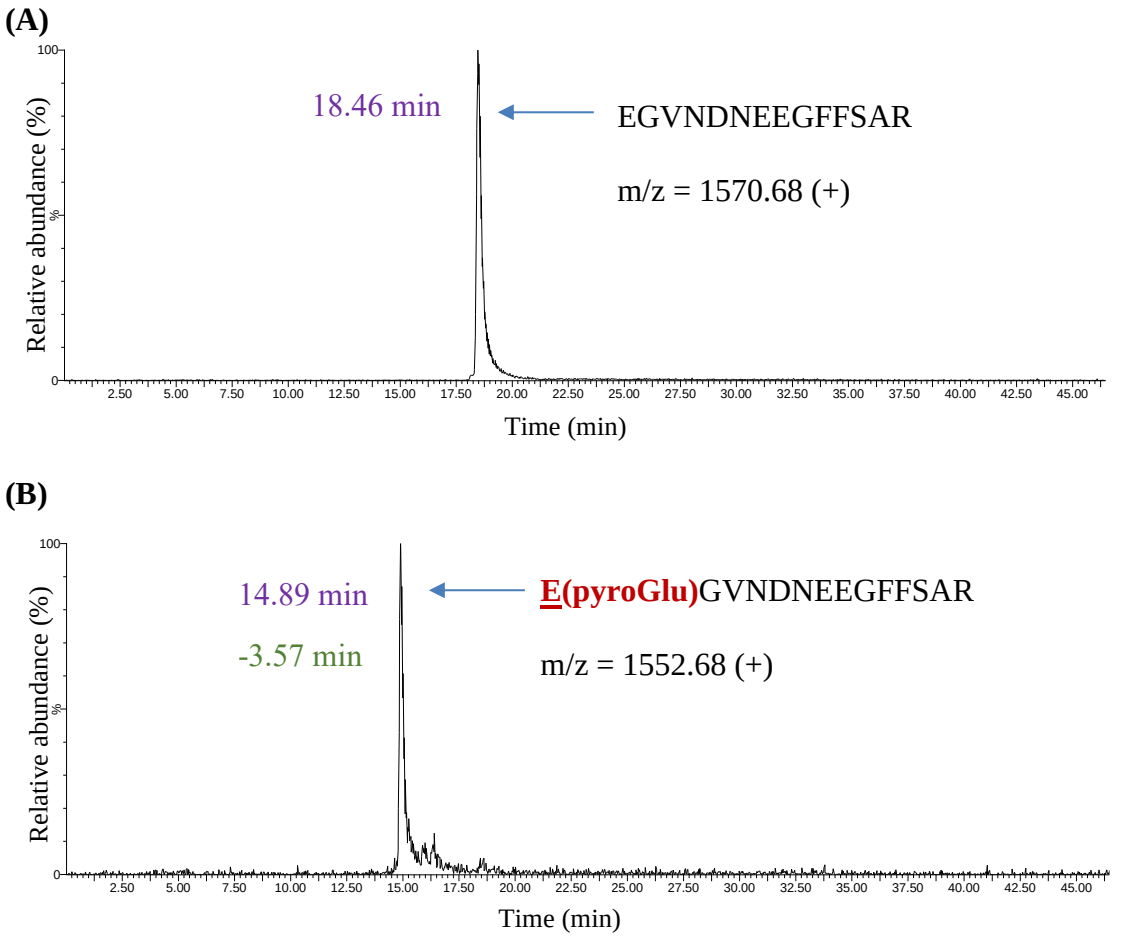

Figure 3.9: XICs for (**A**) unmodified human GluFib peptide EGVNDNEEGFFSAR as well as (**B**) the pyroglutamated (pyroGlu) variant **E(pyroGlu)**GVNDNEEGFFSAR. The retention time of unmodified GluFib was observed to be 18.46 min. The pyroGlu variant being less hydrophilic than the unmodified variant eluted earlier with a retention time of 14.89 min, showing a 3.57 min decrease in HILIC retention upon pyroglutamation.

Table 3.1

Calculation of HILIC retention coefficient for glycation PTM using standard peptides and proteins. The average coefficient for glycation was calculated to be +0.35 GU with a standard deviation of 0.12 GU.

Protein/ Peptide	Sequence	Retention shift upon glycation (min)	Retention shift upon glycation (GU)
Cytochrome C (bovine)	TGQAPGFSYTDAN**K**NK	0.22	0.14
	H**K**TGPNLHGLFGR	0.28	0.18
	EDLIAYL**K**K	0.31	0.19
	KTGQAPGFSYTDANK	0.59	0.31
	KIFVQK	0.71	0.40
	MIFAGI**K**K	0.72	0.41
	GITWGEETLMEYLENP**K**K	0.78	0.46
	KYIPGTK	0.79	0.46
	YIPGT**K**MIFAGIK	1.15	0.53
	YIPGT**K**MIFAGIK	1.04	0.51
	MIFAGI**K**K	0.45	0.24
Insulin (bovine)	**G**IVEQCCASVCSLYQLENYCN	0.77	0.49
	FVNQHLCGSHLVEALYLVCGERGFFYTPKA	0.73	0.45
GluFib	**E**GVNDNEEGFFSAR	0.46	0.24
Bradykinin	**R**PPGFSPFR	0.68	0.35
Leucine Enkephalin	**Y**GGFL	0.21	0.12
Substance P (Frag 2-11)	P**K**PQQFFGLM	1.19	0.54

Average coefficient for glycation	**0.35 GU**
Standard deviation of glycation	0.12 GU

Table 3.2

Prediction and characterization of glycation in human IgG1 sample (Adalimumab). The experimental retention time of glycated peptides was close to the predicted value. Average retention shift upon glycation was observed to be +0.50 GU. The experimental retention times of the unmodified peptides (in minutes and in GU) are also listed for when they were detected.

IgG1 Peptide sequence	Predicted RT (GU)	Predicted RT (min)	Experimental RT (min)	Experimental RT (GU)	Retention shift upon glycation (min)	Retention shift upon glycation (GU)
ALPAPIEKTISK	5.74	17.15				
ALPAPIE**K**TISK	6.09	17.75	18.41	6.48	1.26	0.74
LTVDKSR	5.87	17.37	18.85	6.74		
LTVD**K**SR	6.22	17.97	19.52	7.15	1.15	0.27
EVQLVESGGGLVQPGR	5.09	15.95	16.68	5.48		
EVQLVESGGGLVQPGR	5.44	16.61	17.47	5.93	1.52	0.64
VVSVLTVLHQDWLNGKEYK	5.91	17.44				
VVSVLTVLHQDWLNG**K**EYK	6.26	18.04	17.64	6.02	0.20	0.11
VSNKALPAPIEK	6.31	18.13				
VSN**K**ALPAPIEK	6.66	18.71	20.31	7.64	1.18	0.83
DELTKNQVSLTCLVK	6.94	19.17				
DELT**K**NQVSLTCLVK	7.29	19.74	19.67	7.24	0.50	0.30
APKLLIYAASTLQSGVPSR	4.78	15.33	16.63	5.45		
AP**K**LLIYAASTLQSGVPSR	5.13	16.02	16.42	5.38	1.09	0.60
APYTFGQGTKVEIK	6.35	18.20	18.51	6.54		
APYTFGQGT**K**VEIK	6.70	18.77	18.92	6.79	0.72	0.43
VYACEVTHQGLSSPVTKSFNR	7.50	20.08	20.21	7.58		
VYACEVTHQGLSSPVT**K**SFNR	7.85	20.74	20.62	7.84	0.54	0.34
DIQMTQSPSSLSASVGDR	6.83	18.99				
DIQMTQSPSSLSASVGDR	7.18	19.57	20.22	7.58	1.23	0.75
ADYEKHK	8.59	21.73				
ADYE**K**HK	8.94	22.16	22.44	9.12	0.71	0.53

Table 3.3

Prediction and characterization of glycation in IgG4 sample (Natalizumab). The experimental retention time of glycated peptides was close to the predicted value. Average retention shift upon glycation was observed to be +0.53 GU. The experimental retention times of the unmodified peptides (in minutes and in GU) are also listed for when they were detected.

IgG4 Peptide sequence	Predicted RT (GU)	Predicted RT (min)	Experimental RT (min)	Experimental RT (GU)	Retention shift upon glycation (min)	Retention shift upon glycation (GU)
VSCKASGFNIK	5.86	17.40	16.19	5.16		
VSC**K**ASGFNIK	6.21	17.93	17.67	6.03	0.27	0.17
ASGFNIKDTYIHWVR	5.47	16.75	17.89	6.18		
ASGFNI**K**DTYIHWVR	5.82	17.33	17.99	6.25	1.24	0.78
VSNKGLPSSIEK	6.75	18.67	19.74	7.82		
VSN**K**GLPSSIEK	7.10	19.08	20.01	8.40	1.34	0.86
GLPSSIEKTISK	6.15	17.85	18.46	6.59		
GLPSSIE**K**TISK	6.50	18.34	19.07	7.09	1.22	0.94
EPQVYTLPPSQEEMTKNQVSL TCLVK	8.99	19.92				
EPQVYTLPPSQEEMT**K**NQVSL TCLVK	9.34	19.62	20.32	9.59	0.40	0.60
LTVDKSR	5.79	17.29				
LTVD**K**SR	6.14	17.83	18.16	6.37	0.87	0.58
DIQMTQSPSSLSASVGDR	6.83	18.77				
DIQMTQSPSSLSASVGDR	7.18	19.17	19.59	7.34	0.82	0.51
TSQDINKYMAWYQQTPGK	7.92	19.81				
TSQDIN**K**YMAWYQQTPGK	8.27	19.96	20.16	8.30	0.35	0.38
YMAWYQQTPGKAPR	5.69	17.13	17.22	5.75		
YMAWYQQTPG**K**APR	6.04	17.68	17.79	6.11	0.66	0.42
TVAAPSVFIFPPSDEQLKSGTA SVVCLLNNFYPR	4.92	14.78	15.46	4.78		
TVAAPSVFIFPPSDEQL**K**SGTA SVVCLLNNFYPR	5.27	16.44	15.57	4.84	0.79	0.16
EAKVQWK	5.92	17.50				
EA**K**VQWK	6.27	18.02	18.70	6.77	1.20	0.85
VYACEVTHQGLSSPVTKSFNR	8.48	20.02				
VYACEVTHQGLSSPVT**K**SFNR	8.83	19.99	20.26	8.58	0.24	0.10

Table 3.4

Prediction and characterization of glycation in IgG2 sample (‘Frankenmab’). The experimental retention time of glycated peptides was close to the predicted value. Average retention shift upon glycation was observed to be +0.52 GU. The experimental retention times of the unmodified peptides (in minutes and in GU) are also listed for when they were detected.

IgG2 Peptide sequence	Predicted RT (GU)	Predicted RT (min)	Experimental RT (min)	Experimental RT (GU)	Retention shift upon glycation (min)	Retention shift upon glycation (GU)
EVQLVESGGGLVQPGR	5.09	16.14	17.11	5.56		
EVQLVESGGGLVQPGR	5.44	16.87	17.79	5.89	1.65	0.80
VSNKGLPAPIEK	6.38	18.75	19.08	6.55		
VSN**K**GLPAPIEK	6.73	19.43	20.11	7.08	1.36	0.71
GLPAPIEKTISK	5.77	17.54	18.15	6.08		
GLPAPIE**K**TISK	6.12	18.24	19.52	6.98	1.98	1.21
EEMTKNQVSLTCLVK	7.32	19.59	19.81	6.92		
EEMT**K**NQVSLTCLVK	7.67	21.29	20.58	7.61	0.99	0.29
LTVDKSR	5.79	17.58	18.41	6.06		
LTVD**K**SR	6.14	18.27	18.93	6.34	1.35	0.55
NYLAWYQQKPGKAPK	7.92	21.20	21.15	7.60		
NYLAWYQQKPG**K**APK	8.27	21.53	21.40	8.02	0.20	0.11
APKLLIYAASTLQSGVPSR	5.28	16.54				
AP**K**LLIYAASTLQSGVPSR	5.63	17.26	17.84	5.92	1.30	0.64
APYTFGQGTKVEIK	6.35	18.19	17.27	5.64		
APYTFGQGT**K**VEIK	6.70	19.37	18.62	6.48	0.43	0.13
TVAAPSVFIFPPSDEQLKSGTA SVVCLLNNFYPR	4.94	15.81	15.68	4.88		
TVAAPSVFIFPPSDEQL**K**SGTA SVVCLLNNFYPR	5.29	16.56	16.30	5.17	0.49	0.23
EAKVQWK	5.92	17.84				
EA**K**VQWK	6.27	18.53	18.91	6.46	1.07	0.54

Table 3.5

Glycation characterization performed on Glu-C generated peptides in human IgG1 (Adalimumab). The experimental retention time of glycated peptides was observed to be close to the predicted retention time.

IgG1 Glu-C Peptide sequence	Predicted RT (GU)	Predicted RT (min)	Experimental RT (min)	Experimental RT (GU)
IKRTVAAPSVFIFPPSDE			14.06	4.20
I**K**RTVAAPSVFIFPPSDE	4.72	15.21	15.30	4.76
VKFNWYVDGVE			12.14	3.43
V**K**FNWYVDGVE	3.95	13.48	13.74	4.06
KSRWQQGNVFS**C**SVMHE			21.79	8.64
KSRWQQGNVFS**C**SVMHE	9.16	22.38	22.52	9.32
ALHNHYTQKSLSLSPG			19.89	7.38
ALHNHYTQ**K**SLSLSPG	7.90	20.72	20.97	7.89

Table 3.6

Difference in retention time of unmodified peptides and their pyroglutamated (pyroGlu) variants for human [Glu1]-Fibrinopeptide B, bovine Transferrin and Adalimumab (human IgG1) tryptic peptides are shown from 3 replicates. The average retention time shift (in GU) between unmodified and modified variants was calculated to be -2.10 GU with a standard deviation of 0.31 GU.

Peptide sequence	Retention time of pyroGlu modified peptides (in GU)	Retention time of unmodified peptides (in GU)	Retention difference (in GU)
EGVNDNEEGFFSAR	4.71	6.92	-2.23
ELPDPQESIQR	4.40	7.01	-2.61
ESKPPDSSK	2.24	3.91	-1.67
ENFEVLCK	2.81	4.85	-2.03
EVQLVESGGGLVQPGR	3.26	5.35	-2.09
EPQVYTLPPSR	2.88	4.87	-1.99

CHAPTER 4

UTILIZING HEAVY ISOTOPE-LABELED PROTEINS FOR THE ABSOLUTE AND RELATIVE QUANTITATION OF GLYCATION[2]

[2] Priya, S., Popov, M. and Orlando, R. To be submitted to *The Journal of Biomolecular Techniques*.

Abstract

Post-translational modifications (PTMs) such as glycation can be introduced during manufacturing and storage of therapeutic proteins including monoclonal antibodies (mAbs). Glycation modification may alter the safety and efficacy of therapeutic drugs thus necessitating their accurate quantification. Relative quantitation is typically performed by comparing the peak area of the glycated peptide with that of its unmodified counterparts. Accuracy of this method depends on the unmodified and modified peptides having similar ionization efficiencies as well as the selection of native peptide chosen to perform quantitation. We propose the use of non-glycated heavy isotope-labeled proteins for glycation quantitation. The heavy isotope-labeled proteins can provide both the relative and absolute level of glycation by comparing the peak area of the unmodified tryptic peptides to that of the heavy isotope-labeled variants. To develop this approach, glycation was intentionally induced in an immunoglobulin (IgG) to have detectable glycation. A heavy isotope-labeled variant of the IgG (containing ^{13}C and ^{15}N lysine and arginine residues) was added to serve as an internal standard. Further, this mixture was subjected to trypsin digestion and a bottom-up approach using Hydrophilic Interaction Liquid Chromatography (HILIC)-MS was performed. The light/heavy ratio of tryptic peptides with and without a glycation site in the forced glycation sample was monitored. Any decrease in the light/heavy ratio of peptides containing a glycation site relative to the expected ratio was attributed to the production of glycated variants. Glycation quantitation in IgGs such as Adalimumab (IgG1), Natalizumab (IgG4) and 'Frankenmab' (IgG2) were performed. We expect this approach will be applicable to other PTMs.

Introduction

Glycation is an important post-translational modification (PTM) that has been linked to diabetes, Alzheimer's, cataract, and rheumatoid arthritis.[127,128] It involves reaction between a reducing sugar (glucose, galactose, fructose) and the α-amine terminal of a protein or ε-amine group on a lysine side chain.[142,156-158] An unstable Schiff's base intermediate is produced in this reaction that further rearranges into a more stable ketoamine product (Amadori product). Glycated proteins in the presence of reactive intermediaries over time can degrade into Advanced Glycation End products (AGEs) that have been associated with various pathological conditions including Alzheimer's disease.[143-145] Glycation is considered as one of the critical quality attributes (CQA) for biotherapeutics as it can impact the efficacy, stability as well as half-life of biotherapeutic drug products.[146-149] There is a growing need to develop sensitive methods for detecting glycation PTM, as regulatory filings demand detailed characterizations of the structural and chemical heterogeneity of recombinant antibodies.[159]

A number of approaches to detect and quantify glycation have been reported in the literature. These methods include quantifying common AGEs such as carboxymethyl-lysine (CML), carboxyethyl-lysine (CEL), pyralline (Pyr), pentosidine (Pento-s) and arg-pyrimidine (Arg-p) using enzyme-linked immunosorbent assay (ELISA)[160,161,129], HPLC-FLD, LC-MS/MS, and GC-MS methods.[130,149,162] Further, LC/MS detection of more stable Amadori product is performed in order to determine information about the glycation site on a protein.[10] However, characterizing glycation can be challenging because it could be distributed across the entire protein often resulting in low levels of glycation at individual sites.[163] Furthermore, glycation is known to hinder trypsin's

activity at the C-terminus of a lysine residue. [10,153] Glycated peptide that is bound to a sugar molecule neither contains the positive charge at primary amine nor has the appropriate shape to fit into the negatively charged trypsin pocket causing a loss of enzymatic activity. Thus, a missed tryptic cleavage at the lysine residue with a +162 Da shift in MS is considered to be an indicator of a glycated peptide. Relative quantitation for glycation PTM is typically performed by dividing the peak area of glycated missed cleavage peptide by the sum of the peak areas of glycated peptide and tryptic unmodified peptide constituting the glycated missed cleavage peptide.[131,163] An alternative method for quantifying glycation at a particular site is by comparing the peak area of a tryptic peptide containing glycation site to a peptide within the same protein that is insensitive to glycation.[164] Quantitation has also been attempted by first performing *in vitro* glycation of a protein with [$^{13}C_6$]-glucose and then determining the ratio between the peak areas corresponding to the peptides labeled with [$^{12}C_6$]-glucose and those labeled with [$^{13}C_6$]-glucose.[165] The peptides glycated with [$^{12}C_6$]-glucose in this study were indicative of their concentration in the biological sample. Other quantitation strategies include introducing stable isotopes to glycated peptides by sodium borodeuteride reduction[166] and spiking the samples with isotope-labeled peptides.[167]

Quantitation approaches that rely on peak area of glycated peptides[131] assume that the ionization efficiency of longer glycated missed cleavage peptide, where the positive charge at the primary amine is neutralized due to glycation, is comparable to that of tryptic peptides. The selection of the tryptic peptide constituting the glycated missed cleavage peptide is also critical as it could affect the accuracy of this method. Additionally, these approaches necessitate detectable levels of glycated peptides for

precise quantitation and often require an enrichment step such as Boronate affinity chromatography[146,167] prior to LC-MS analysis. Herein, we propose the use of non-glycated heavy isotope-labeled variant of the target protein to determine both the relative and absolute levels of glycation. A known amount of ^{13}C and ^{15}N lysine and arginine labeled protein could be added to the target protein prior to trypsin digestion (Figure 4.1). Quantitation can then be performed by monitoring the peak area of an unmodified tryptic peptide containing a glycation site relative to the peak area of its heavy isotope-labeled variant. This method offers several advantages. The characterization relies solely on the peak area of tryptic peptides as opposed to peak area of potentially lower abundant glycated missed cleavage peptides with poor ionization efficiencies. The heavy isotope-labeled variant of the target protein has comparable physical and chemical properties to the protein of interest enabling accurate quantitation. The ionization efficiency of heavy isotope-labeled peptides in mass spectrometry is similar to that of the corresponding light peptides in the protein of interest. Additionally, they exhibit similar retention times on an LC column, such as on Hydrophilic Interaction Liquid Chromatography (HILIC) column.[5] Further, any variations in the sample processing steps such as during enzymatic digestion can be accounted for since the heavy isotope-labeled internal standard is added prior to trypsin digestion, resulting in more reliable results.

To develop this method, IgGs such as Adalimumab (IgG1), Natalizumab (IgG4) and 'Frankenmab' (custom IgG2) were first forcibly glycated to achieve detectable glycation. Subsequently, their heavy isotope-labeled variants containing ^{13}C and ^{15}N lysine and arginine amino acids were added followed by trypsin digestion. A control IgG sample without glucose was processed in a similar fashion. HILIC chromatography that

has been previously employed to study hydrophilic modifications[69,154,164] was used in this study owing to the hydrophilic nature of the glycation product. It was hypothesized that the light/heavy ratio of a peptide containing a glycation site may decrease in the glycated sample compared to the non-glycated control due to the formation of its glycated variant (Peptide 1 in Figure 4.1 panel B). Conversely, it was anticipated that the light/heavy ratio of a peptide lacking a glycation site (Peptide 2 in Figure 4.1 panel B) would not change significantly when comparing the glycated sample to the non-glycated control.

Materials And Methods

in-vitro Glycation

IgGs such as Adalimumab (human IgG1), Natalizumab (IgG4 expressed in CHO cell) and 'Frankenmab' (custom IgG2) were obtained from GlycoScientific (Athens, GA, USA). *in-vitro* glycation of these IgGs were performed by incubating the protein with 1000:1 D-Glucose: protein molar ratio in the presence of acetic acid (pH=2.4), overnight at 65^{o}C. IgGs with no D-Glucose were also subjected to above-mentioned conditions to serve as a non-glycation control. D-Glucose was removed from the reaction mixture by performing buffer exchange using Amicon Ultra-0.5 Centrifugal Filters (Merck Millipore Ltd., Burlington, MA).

Addition of heavy isotope-labeled internal standard

Heavy isotope-labeled Adalimumab (IgG1), 'Frankenmab' (IgG2) and Natalizumab (IgG4) were obtained from GlycoScientific (Athens, GA, USA). These heavy isotope-labeled variants were added to the glycated protein samples as well as to the non-glycation control samples in a 1:1 molar ratio. For instance, heavy isotope-

labeled IgG1 was added to IgG1 glycated sample as well as to IgG1 non-glycated control in a 1:1 molar ratio.

Trypsin digestion

After adding the heavy isotope-labeled internal standard, the protein mixtures were buffer exchanged with 50 mM ammonium bicarbonate (pH 7.8) to have a final concentration of 1 mg/mL. They were then reduced using 200 mM Dithiothreitol (DTT) and alkylated using 1 M iodoacetamide, both purchased from Sigma Aldrich (St. Louis, MO, USA), to have a final concentration of 5 mM DTT and 8 mM iodoacetamide. Further, sequencing grade trypsin purchased from Promega (Madison, WI, USA) was added at 20:1 ratio (w/w, protein/trypsin) and incubated overnight at 37°C. The digested protein samples were then dried on SpeedVac and resuspended in 80% ACN (1 mg/mL) and 20% H_2O before LCMS analyses.

LC/MS settings and instrumentation

Data were acquired on an Agilent1100 series (Santa Clara, CA, USA) coupled to Waters SYNAPT-G2 QTOF (Milford, MA, USA) system with ESI source. Peptides were separated using a 2.1-mm × 150-mm HALO Penta-HILIC column packed with 2.7-μm diameter superficially porous particles that have a 90-Å pore diameter (Advanced Materials Technology, Wilmington, DE, USA) at 60°C column temperature. The mobile phases used to perform separation were 50 mM ammonium formate in water with 0.1% Formic acid (Solvent A), and 0.1% Formic acid in Acetonitrile (Solvent B). A linear gradient of 80% to 40% Solvent B over 40 minutes (1%B per minute) at 0.2 mL/min flow rate was used for separation. DDA Survey type experiments were run to characterize

glycation. Mass spectral analyses were carried out using Waters MassLynx, Protein Lynx Global Server (PLGS) and Skyline software.

Results And Discussion

Quantitation using published method:

Glycation quantitation was first performed by calculating the ratio of the peak area of a glycated missed cleavage peptide to the total peak area of both the glycated peptide and the tryptic peptide it comprises, as described in the literature (Equation 1).[131]

% Relative glycation =

$$\frac{[\text{Glycated peptide}]}{[\text{Glycated peptide}]+[\text{Unmodified tryptic peptide constituting glycated peptide}]} \; x\; 100 \quad \text{(Equation 1)}$$

Protein with substantial glycation was required to perform quantitation. Therefore, the study began with *in-vitro* glycation of an IgG such as Adalimumab (human IgG1). The glycated sample was then enzymatically digested using trypsin followed by LC-MS analysis using Penta-HILIC column and a QTOF mass analyzer. Since glycation can inhibit the activity of trypsin[10,153], a missed tryptic cleavage in conjugation with a 162 Da mass increase was used as an indicator for glycation. The glycated missed cleavage peptides were confirmed using HILIC retention coefficient developed for glycation PTM.

For instance, one of the glycated peptides observed in Adalimumab (human IgG1) was AP**K**LLIYAASTLQSGVPSR. Quantitation could be performed at this site by using Equation 1, i.e., dividing the peak area of the glycated peptide AP**K**LLIYAASTLQSGVPSR by the sum of the peak areas of the glycated peptide and its unmodified tryptic counterpart. The two tryptic peptides that constitute this glycated missed cleavage peptide are APK and LLIYAASTLQSGVPSR. The unmodified tryptic peptide to be used for calculation, as per the published method, could either be the longer

of the two tryptic peptides that make up the glycated missed cleavage variant or the tryptic peptide that included the glycation site. LLIYAASTLQSGVPSR is the longer of the two peptides in this case, while APK is the tryptic peptide containing the glycation site. Thus, quantitation was performed using both ways and any inaccuracies were examined (Figure 4.2). It was observed that the percent relative glycation was calculated to be 6.9% when the longer LLIYAASTLQSGVPSR tryptic peptide was used. On the other hand, percent relative glycation was seen to be 34.4% on using APK tryptic peptide, that contained the glycation site. These results indicated that the accuracy of this method relied on the choice of the tryptic peptide used in the calculations. Another challenge associated with this approach was that the ionization efficiency of the glycated peptides was assumed to be comparable with that of the tryptic peptides. However, a bulkier glycated missed cleavage peptide with a glucose molecule attached and a neutralized positive charge at the glycation site may exhibit lower ionization efficiency compared to a tryptic peptide. There could also be instances when a glycated peptide may coelute with another tryptic peptide making peak area integration challenging.

Glycation quantitation using heavy isotope-labeled protein:

It was hypothesized that a non-glycated heavy isotope-labeled variant of target protein containing ^{13}C and ^{15}N labeled lysine and arginine could be utilized to perform glycation quantitation. The heavy labeled lysine was +8 Da than unlabeled lysine, and heavy labeled arginine was +10 Da compared to unlabeled arginine (Figure 4.1 panel A). Heavy isotope-labeled proteins with glycation modification are not commercially available, therefore, non-glycated heavy isotope-labeled proteins could be utilized. It was anticipated that the abundance of unmodified peptides lacking a glycation site, i.e., those

without a lysine residue and not being N-terminus peptides, would be similar to the abundance of its heavy isotope-labeled variant. On the other hand, the light/heavy ratio of peptides that contain a glycation site or that is next to a glycation site may decrease after *in-vitro* glycation. This decrease in ratio could be extrapolated to find the absolute and relative glycation in a protein.

Glycation quantitation was performed on Adalimumab (human IgG1) to test this hypothesis. Firstly, IgG1 was glycated to obtain observable glycation, and then buffer exchanged to remove excess glucose. Next, heavy isotope-labeled IgG1 was added in a 1:1 molar ratio with unlabeled IgG1. This mixture was subjected to trypsin digestion. Parallelly, a control IgG1 sample underwent an *in-vitro* glycation process without glucose. An equal amount of heavy isotope-labeled IgG1 (in a 1:1 ratio with control IgG1) was added prior to trypsin digestion. Control IgG1 sample was used to study potential alterations that might occur in tryptic peptides in the absence of glucose.

Firstly, light/heavy ratios of tryptic peptides lacking a glycation site in the glycation sample were compared with their light/heavy ratios in the non-glycation control (Figure 4.3 panel A). Several criteria were established for the selection of these peptides such as 1) the tryptic peptide should not contain a glycation site (lysine residue) or be adjacent to one, 2) it should not be a N-terminus peptide that is susceptible to glycation, 3) peptide intensity needs to be above 1000 counts for accurate integration, 4) peptide should not co-elute with another species that may hamper accurate integration, 5) peptide's m/z should be above 500, and 6) peptide should not contain a "NG" or "NN" motif as it may be prone to deamidation, potentially consuming the unmodified peptide. Tryptic peptides containing methionine were included since the light/heavy ratio of

unmodified peptides in the glycation sample did not show a significant change when compared with the non-glycation control. For example, light/heavy ratio of FTISR, ASQGIR, EPQVYTLPPSR, LSCAASGFTFDDYAMHWVR, VTITCR and EEQYN[A2G0F]STYR peptides in IgG1 glycation sample were selected. The average light/heavy ratio of these peptides in the glycation sample was calculated to be 0.70. Thus, if a peptide did not undergo glycation, its light/heavy ratio in the glycation sample must be approximately 0.70 (Figure 4.3 panel A). Any decrease from this averaged value could indicate a decrease in the unmodified peptide, that could be attributed to glycation modification.

Furthermore, peptides that contained a glycation site or was next to one were analyzed. It was observed that the light/heavy ratio of these peptides in the glycation sample ranged from 0.01 for EVQLVESGGGLVQPGR (N-terminus peptide) to 0.60 for NSLYLQMNSLR, indicating that glycation at these sites progressed with variable extents. Glycation quantitation at AP**K**LLIYAASTLQSGVPSR site using our proposed heavy isotope-labeled internal standard method is described in Figure 4.3 panel B. The light/heavy ratio for LLIYAASTLQSGVPSR peptide in the glycation sample was calculated to be 0.1425 showing an 80% decrease from the previously calculated ratio of 0.70 (corresponding to least modified peptides). This 80% decrease in the unmodified peptide in the glycation sample was attributed to 80% glycation at this site. APK tryptic peptide was not chosen for calculation as its m/z is below 500 Da. Table 4.1 panel A demonstrates the glycation quantitation comparison between the published method and our proposed method in IgG1 sample from 3 replicates. It is worthwhile to mention that tryptic peptide K.VYACEVTHQGLSSPVTK.S in IgG1 has a lysine residue both before

it and at its C-terminus. Even so, the consumption of VYACEVTHQGLSSPVTK peptide was attributed to glycation at VYACEVTHQGLSSPVT**K**SFNR site since glycation at the lysine residue preceding the peptide was not detected. The percentage of relative glycation in IgG1 ranged from 14% at DNA**K**NSLYLQMNSLR site to 98% at **E**VQLVESGGGLVQPGR site, suggesting that this reaction was selective with different sites undergoing glycation to varying extents. In addition, the percentage of relative glycation obtained from our proposed heavy isotope-labeled internal standard approach was higher than that calculated using the published method. This difference could be due to under-representation of glycated peptide in the published method as glycated peptide may have a lower ionization efficiency compared to tryptic peptides. Moreover, higher glycation values in our proposed approach could be due to other possible side-reactions during glycation that could have led to the consumption of tryptic peptides.

Glycation quantitation on Natalizumab (IgG4) sample was performed next. The IgG4 sample was subjected to *in-vitro* glycation as described previously along with a parallel control. Heavy isotope-labeled IgG4 was added to both non-glycation control and glycation sample in a 1:1 molar ratio with the unlabeled protein. This mixture was subjected to trypsin digestion. % Relative quantitation was performed using both the published method[131] as well as the heavy isotope-labeled internal standard approach. On an average, the light/heavy ratio of peptides that did not contain or were adjacent to a glycation site from 3 replicates was calculated to be 0.87 (Figure 4.4 panel A). The light/heavy ratio of peptides containing/next to a glycation site ranged from 0.13 for DIQMTQSPSSLSASVGDR (N-terminus peptide) to 0.39 for VYACEVTHQGLSSPVTK. As have been mentioned in the case of IgG1,

VYACEVTHQGLSSPVTK peptide has a lysine residue at the C-terminus and is adjacent to a lysine residue that precedes it. The consumption of this peptide was attributed to glycation at VYACEVTHQGLSSPVT**K**SFNR site as glycation at the lysine residue preceding this peptide was not detected. Similarly, the consumption of VQWK peptide was attributed to glycation at EA**K**VQWK site since glycation at lysine present at the C-terminus of this peptide was not detected. The light/heavy ratio for VYACEVTHQGLSSPVTK peptide in IgG4 glycated sample was 0.4979 suggesting a 43% glycation at this site (Figure 4.4 panel B). Table 4.1 panel B shows the % relative glycation determined using both the published method and the proposed heavy isotope-labeled internal standard method. Similarly, the light/heavy ratio of least modified peptides in 'Frankenmab' (custom Ig2) glycation sample was determined to be 0.84 (Figure 4.5 panel A). The light/heavy ratio for peptides containing/next to a glycation site ranged from 0.01 (EVQLVESGGGLVQPGR) to 0.22 (APYTFGQGTK). For example, light/heavy ratio of TVAAPSVFIFPPSDEQLK in glycation sample was 0.2001 resulting in 76% glycation (Figure 4.5 panel B). Table 4.1 panel C displays % relative glycation determined using both the published method and heavy isotope-labeled internal standard method. % Relative glycation calculated by heavy isotope-labeled internal standard approach was observed to be higher than those calculated using published method.

Thus, to calculate % relative glycation in a protein, a known amount of heavy isotope-labeled variant of the protein can be added, followed by trypsin digestion for bottom-up approach. The light/heavy ratio of tryptic peptides that lack a glycation site and meet the previously mentioned criteria should be calculated and averaged. Light/heavy ratio of peptides containing/next to a glycation site can then be calculated.

Any decrease in this light/heavy ratio from the averaged value (for unmodified peptides) can be attributed to % relative glycation.

Further, absolute quantitation for glycation PTM was performed by multiplying the light/heavy ratio of peptides prone to glycation with the absolute amount of heavy isotope-labeled internal standard (normalized to 1 µmol). This value when subtracted from 1 µmol resulted in absolute quantitation. For instance, the amount of heavy isotope-labeled IgG1 used in this study was 6.76 µmol. This amount was normalized to 1 µmol. Therefore, the absolute quantitation at AP**K**LLIYAASTLQSGVPSR site in IgG1 was determined by multiplying the light/heavy ratio of 0.1425 (Figure 4.3 panel B) by 1 µmol that resulted in 0.1425 µmol. This value represented the amount of tryptic peptide remaining in the sample. The % absolute glycation at this site can then be calculated by subtracting 0.1425 from 1 µmol resulting in 0.86 µmol. Table 4.2 displays the absolute quantitation in (A) Adalimumab, (B) Natalizumab and (C) "Frankenmab" from 3 replicates.

Serial dilutions were performed to evaluate the linearity of our proposed heavy isotope-labeled quantitation approach. Mixtures of non-glycated control and glycated Adalimumab (IgG1) sample were prepared at control:glycated sample ratios 1:1, 1:0.75, 1:0.50, 1:0.25, 1:0.10 and 1:0.05, thereby decreasing the concentration of glycated species in the sample. These mixtures were then subjected to LC-MS analysis, and the detector's response was recorded to check the conformity with the performed dilutions. % Relative glycation for the undiluted glycation sample was normalized to 100%. Thus, % relative glycation at a particular site in the 1:1 mixture would theoretically be 50%. Glycation percentage would ideally be 37.5% in 1:0.75 mixture, 25% in 1:0.50, 12.5% in

1:0.25, 5% in 1:0.10 and 2.5% in 1:0.05 sample. % Relative glycation at different sites were calculated using both published method and heavy isotope-labeled quantitation approach. The experimental % relative glycation in the undiluted glycation sample was normalized to 100%, and experimental results for the dilutions were adjusted with respect to that. A plot of experimental vs theoretical % relative glycation was created (Figure 4.6) for each method. The red trace on the plot depicts the ideal scenario, that is a linear trend with y=x. Figure 4.6 panel A shows any deviations from the ideal trend for when the glycated peptides were quantified using the published method. Traces such as that of EVQLVESGGGLVQPGR deviated significantly from the ideal trend. Figure 4.6 panel B depicts how the glycation quantitation correlated with the ideal trend when the heavy isotope-labeled internal standard approach was used. Overall, it was discerned that data points closely aligned with the ideal trend in the heavy isotope-labeled internal standard approach as compared to when absolute peak area values were used in the published method. This observation indicated that the heavy isotope-labeled internal standard method had improved accuracy. The error bars were also seen to be lower in the case of heavy isotope-labeled quantitation approach indicating an improvement in precision.

Conclusions

This research aimed to quantify glycation, an essential PTM that can be introduced in biotherapeutic manufacturing and affect the safety and efficacy of therapeutic drugs. Both relative and absolute quantitation were performed on IgGs such as Adalimumab (IgG1), Natalizumab (IgG4) and 'Frankenmab' (custom IgG2). % Relative glycation was calculated by adding a known amount of heavy isotope-labeled variant (^{13}C and ^{15}N lysine and arginine) of the target protein, followed by trypsin

digestion for bottom-up HILIC-MS approach. The light/heavy ratio was calculated and averaged for tryptic peptides that did not possess a glycation site and met the criteria specified in the study. Light/heavy ratio of peptides containing/adjacent to a glycation site was then calculated. Any decrease in this light/heavy ratio from the averaged value (for unmodified peptides) was attributed to % relative glycation at that site. Absolute quantitation was performed by multiplying the light/heavy ratio of peptides prone to glycation with the absolute amount of heavy isotope-labeled internal standard used (normalized to 1 µmol). Subtracting this value from 1 µmol yielded absolute quantitation.

Dilutions were performed to evaluate the linearity of the proposed approach. Quantitation using a heavy isotope-labeled internal standard enhanced the accuracy and precision of glycation quantitation compared to one of the commonly used quantitation strategies, where the abundance of glycated missed cleavage peptides is compared with their tryptic peptide counterparts. While the results are demonstrated for glycation PTM, we expect this strategy could be employed to quantify other PTMs such as deamidation.

Acknowledgements

This work was supported in part by NIH grant numbers 2R42GM113666 and 2R44GM131533 to RO. The authors thank Dr. Barry Boyes (Advanced Materials Technology, Wilmington, DE) for providing Penta-HILIC columns.

(A)

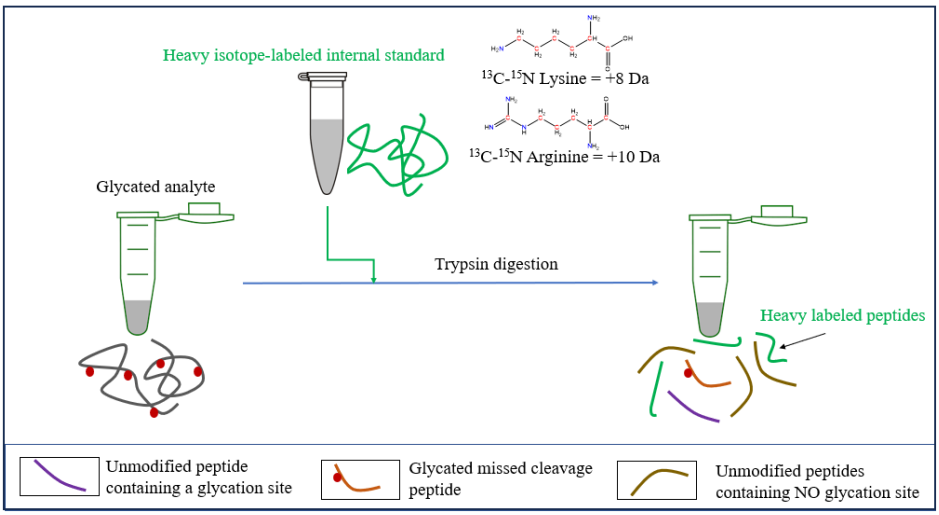

(B)

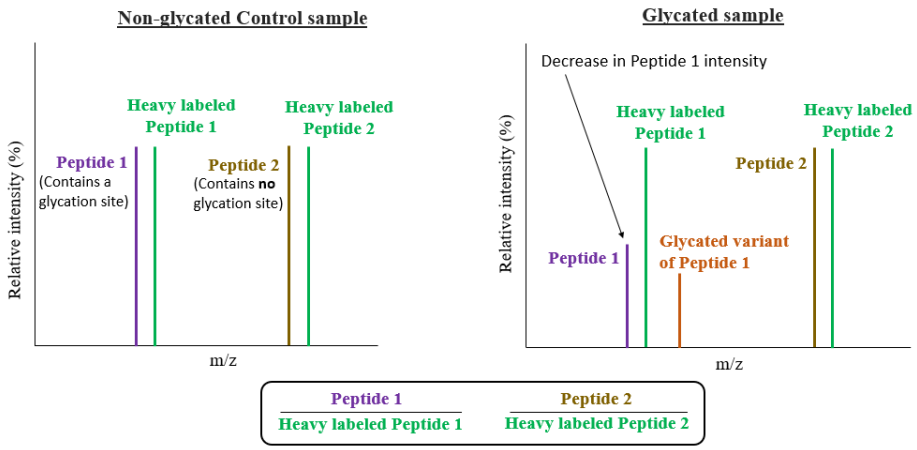

Figure 4.1: Glycation quantitation by using heavy isotope-labeled variant of the target protein. The heavy isotope-labeled variant contained ^{13}C and ^{15}N lysine and arginine residues and was added prior to trypsin digestion to serve as an internal standard **(A)**. The light/heavy ratio of unmodified tryptic peptides with a glycation site can be monitored to determine the extent of glycation at that site. To develop the proposed method, IgGs were glycated *in-vitro* to achieve detectable glycation. Light/heavy ratio of peptides with (Peptide 1) and without a glycation site (Peptide 2) was monitored to quantify glycation **(B)**. A decrease in light/heavy ratio of Peptide 1 was observed owing to the formation of its glycated variant.

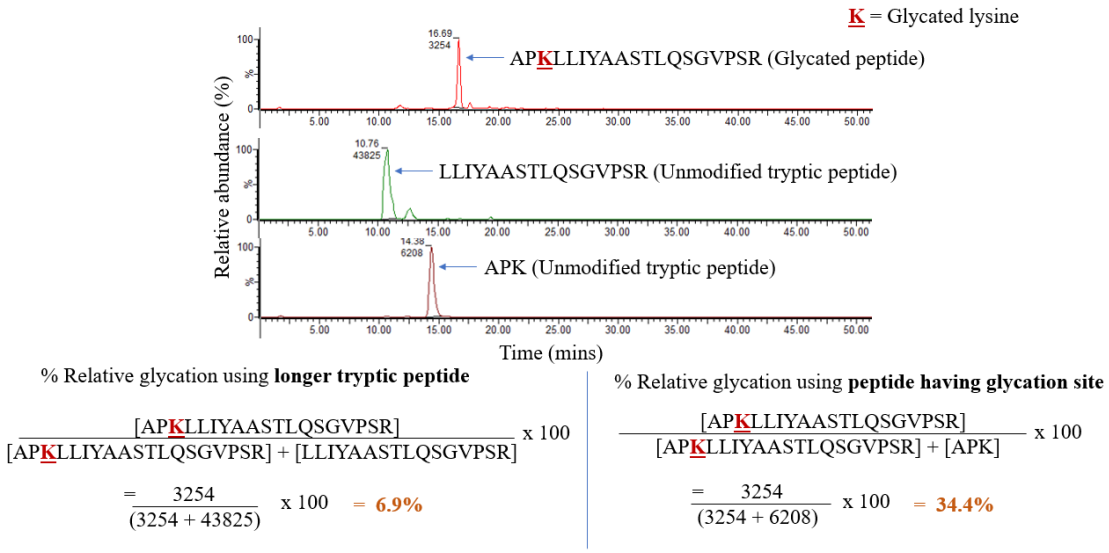

Figure 4.2: Extracted ion chromatograms (XICs) of glycated peptide (AP**K**LLIYAASTLQSGVPSR) and its unmodified counterparts (LLIYAASTLQSGVPSR and APK) in Adalimumab (human IgG1). % Relative glycation was performed using a published method. The accuracy of this method was observed to be dependent on the selection of unmodified peptide as different results were obtained in both the cases (6.9% versus 34.4%).

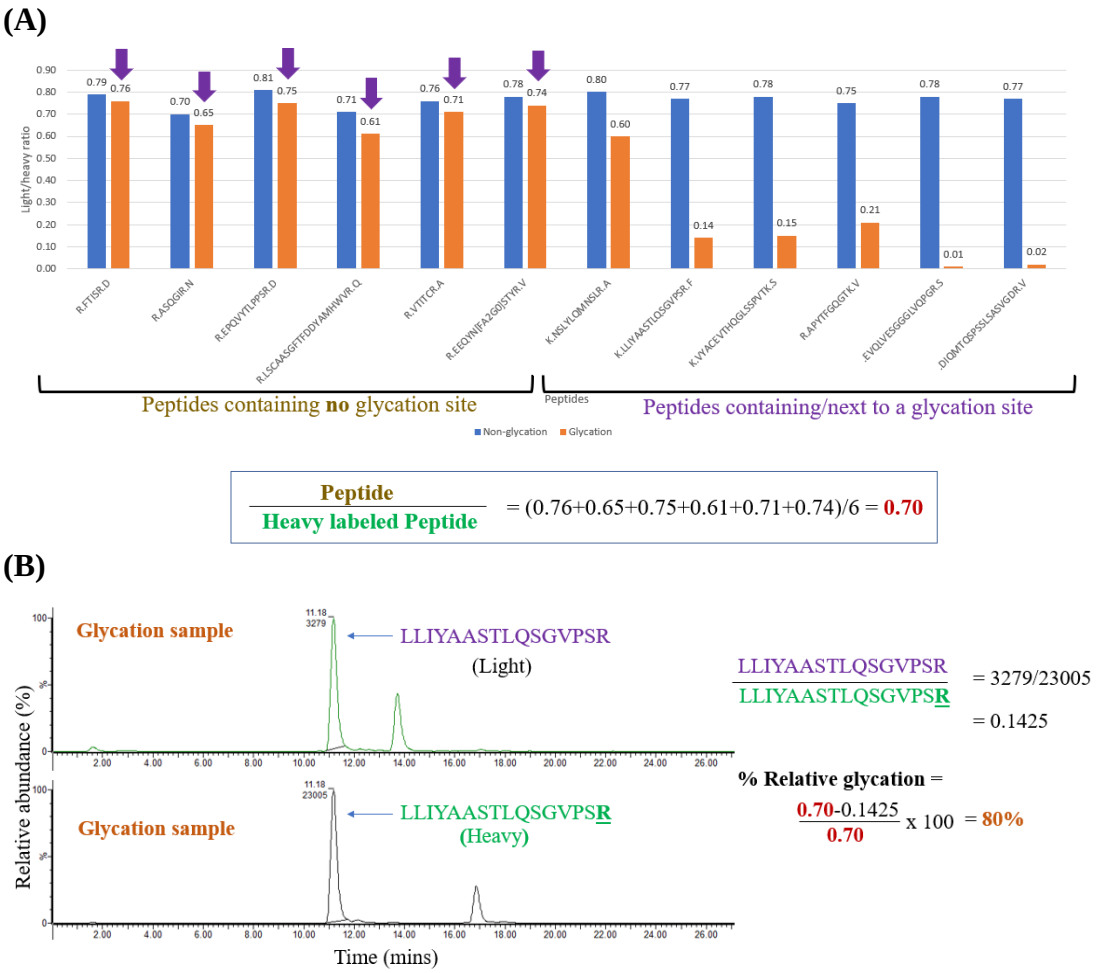

Figure 4.3: Glycation quantitation on Adalimumab using the proposed method. **(A)** displays light/heavy ratios of peptides with and without a glycation site in Adalimumab non-glycation control and glycation samples (from 3 replicates). The average light/heavy ratio for peptides that did not undergo significant modification was 0.70. **(B)** displays the XICs of unmodified light and heavy LLIYAASTLQSGVPSR tryptic peptides in glycation sample run. % Relative glycation at AP**K**LLIYAASTLQSGVPSR site was calculated to be 80% using heavy isotope-labeled internal standard approach. APK tryptic peptide was not chosen for calculation as it's m/z is below 400 Da.

(A)

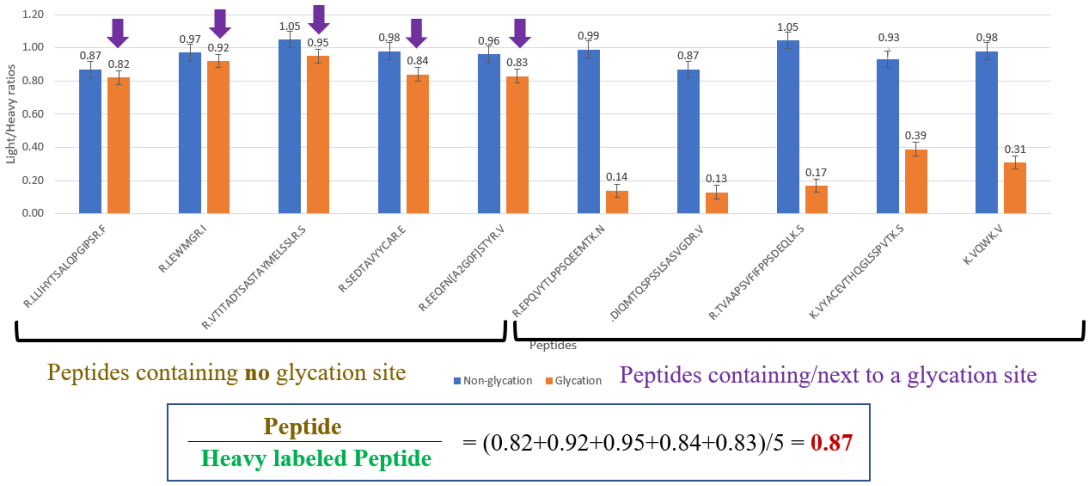

$$\frac{\textbf{Peptide}}{\textbf{Heavy labeled Peptide}} = (0.82+0.92+0.95+0.84+0.83)/5 = \mathbf{0.87}$$

(B)

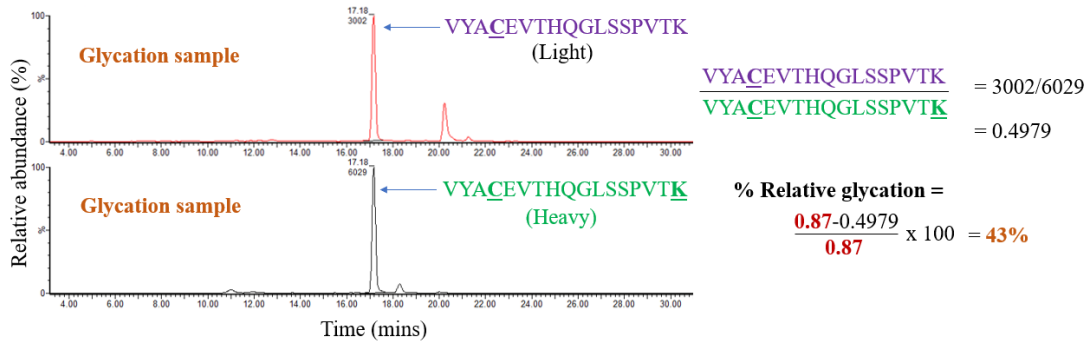

Figure 4.4: Glycation quantitation on Natalizumab (IgG4 expressed in CHO cell) using the proposed method. **(A)** displays light/heavy ratios of peptides with and without a glycation site in Natalizumab non-glycation control and glycation samples (from 3 replicates). The average light/heavy ratio for peptides that did not undergo significant modification was 0.87. **(B)** displays the XICs of unmodified light and heavy VYACEVTHQGLSSPVTK tryptic peptides in the glycation sample run. % Relative glycation at VYACEVTHQGLSSPVT**K**SFNR site was calculated to be 43% using heavy isotope-labeled internal standard approach.

(A)

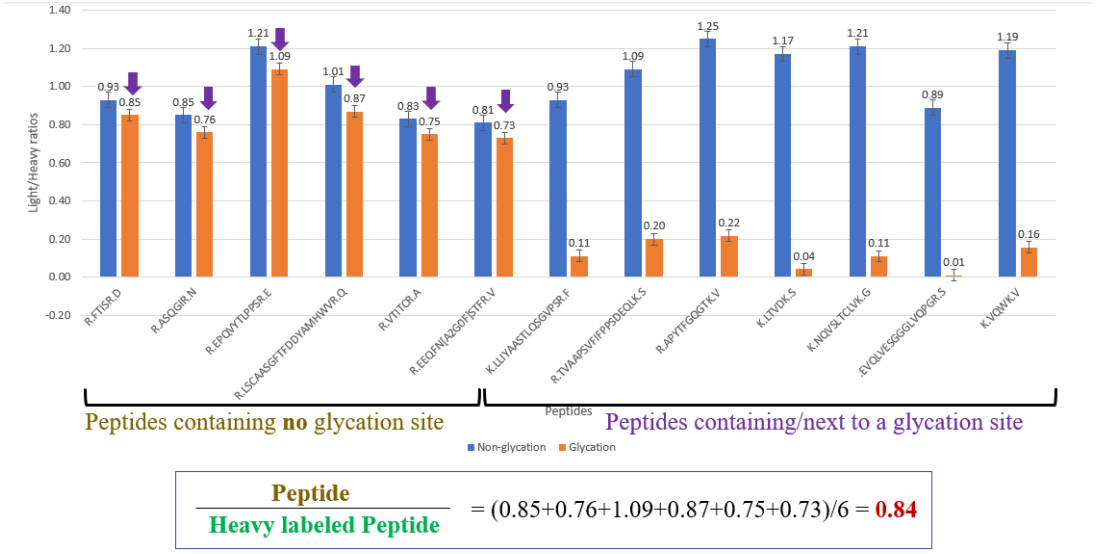

(B)

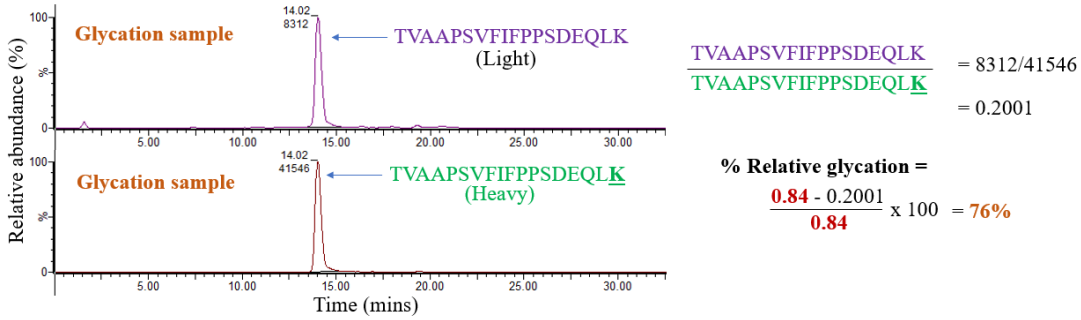

Figure 4.5: Glycation quantitation on 'Frankenmab' (custom IgG2) using the proposed method. **(A)** displays light/heavy ratios of peptides with and without a glycation site in 'Frankenmab' non-glycation control and glycation samples (from 3 replicates). The average light/heavy ratio for peptides that did not undergo significant modification was 0.84. **(B)** displays the XICs of unmodified light and heavy TVAAPSVFIFPPSDEQLK tryptic peptides in the glycation sample run. % Relative glycation at TVAAPSVFIFPPSDEQL**K**SGTASVVCLLNNFYPR site was calculated to be 76% using heavy isotope-labeled internal standard approach.

(A)

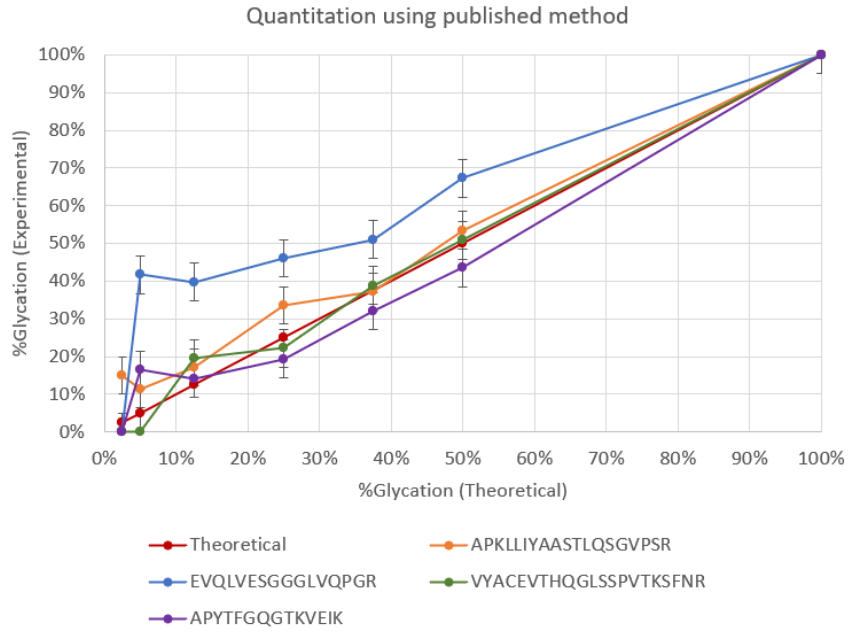

(B)

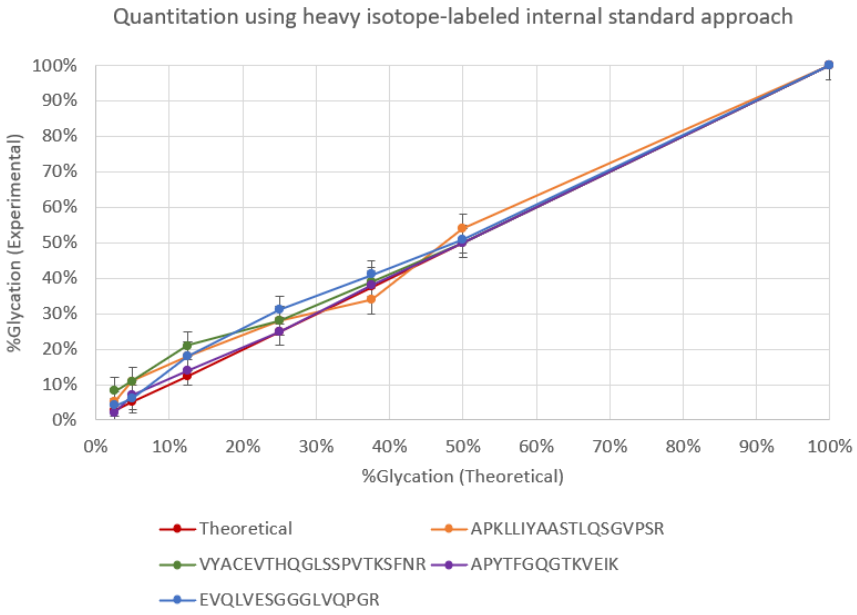

Figure 4.6: Experimental vs theoretical % relative glycation for dilution mixtures calculated using **(A)** published method and **(B)** the proposed internal standard method. A stronger correlation with the theoretical trend was observed when using heavy isotope-labeled internal standard approach demonstrating better accuracy. Smaller error bars in the internal standard approach indicated improvement in precision.

Table 4.1

% Relative glycation on **(A)** Adalimumab (human IgG1), **(B)** Natalizumab (IgG4) and **(C)** 'Frankenmab' (custom IgG2) samples calculated using the proposed heavy isotope-labeled internal standard approach as well as the published method. Higher % relative glycation values were observed using the internal standard approach.

(A)

Adalimumab (human IgG1)	**% Relative glycation**	
Peptides	Using heavy isotope-labeled internal standard approach	Using published method
VYACEVTHQGLSSPVT**K**SFNR	80%	37%
AP**K**LLIYAASTLQSGVPSR	80%	APK- 34%, LLIYAASTLQSGVPSR-7%
APYTFGQGT**K**VEIK	71%	35%
EVQLVESGGGLVQPGR	98%	41%
DIQMTQSPSSLSASVGDR	97%	39%
DNA**K**NSLYLQMNSLR	14%	Not detected

(B)

Natalizumab (IgG4)	**% Relative glycation**	
Peptides	Using heavy isotope-labeled internal standard approach	Using published method
EPQVYTLPPSQEEMT**K**NQVSLTCLVK	85%	14%
VYA**C**EVTHQGLSSPVT**K**SFNR	43%	11%
EA**K**VQWK	72%	8.6%
TVAAPSVFIFPPSDEQL**K**SGTASVVCLLNNFYPR	82%	10%
DIQMTQSPSSLSASVGDR	87%	19%
LTVD**K**SR	94%	14%

(C)

'Frankenmab' (custom IgG2)	**% Relative glycation**	
Peptides	Using heavy isotope-labeled internal standard approach	Using published method
AP**K**LLIYAASTLQSGVPSR	88%	15%
TVAAPSVFIFPPSDEQL**K**SGTASVV**C**LLNNFYPR	76%	12%
APYTFGQGT**K**VEIK	76%	15%
LTVD**K**SR	93%	18%
EEMT**K**NQVSLTCLVK	87%	10%
EVQLVESGGGLVQPGR	98%	21%
EA**K**VQWK	82%	17%

Table 4.2

Absolute glycation on **(A)** Adalimumab (human IgG1), **(B)** Natalizumab (IgG4) and **(C)** 'Frankenmab' (custom IgG2) samples. 6.76 µmol of heavy isotope-labeled internal standard was used, that was normalized to 1 µmol. Absolute glycation was calculated by multiplying the light/heavy ratio of peptides by the normalized absolute amount of heavy isotope-labeled internal standard used, followed by subtracting it from 1 µmol.

(A)

Adalimumab (human IgG1)	Absolute glycation (µmol)
VYACEVTHQGLSSPVTKSFNR	0.80
APKLLIYAASTLQSGVPSR	0.80
APYTFGQGTKVEIK	0.71
EVQLVESGGGLVQPGR	0.98
DIQMTQSPSSLSASVGDR	0.97
DNAKNSLYLQMNSLR	0.14

(B)

Natalizumab (IgG4)	Absolute glycation (µmol)
EPQVYTLPPSQEEMTKNQVSLTCLVK	0.85
VYACEVTHQGLSSPVTKSFNR	0.43
EAKVQWK	0.72
TVAAPSVFIFPPSDEQLKSGTASVVCLLNNFYPR	0.82
DIQMTQSPSSLSASVGDR	0.87
LTVDKSR	0.94

(C)

'Frankenmab' (custom IgG2)	Absolute glycation (µmol)
APKLLIYAASTLQSGVPSR	0.88
TVAAPSVFIFPPSDEQLKSGTASVVCLLNNFYPR	0.76
APYTFGQGTKVEIK	0.76
LTVDKSR	0.93
EEMTKNQVSLTCLVK	0.87
EVQLVESGGGLVQPGR	0.98
EAKVQWK	0.82

CHAPTER 5

EVALUATING THE QUANTITATIVE ASPECTS OF DIFFERENT N-GLYCAN PREPARATIVE STRATEGIES

Introduction

N-linked glycosylation represents an important post-translational modification (PTM) in which N-glycans are attached to proteins at specific asparagine (Asn) sites through an N-glycosidic covalent bond. This attachment occurs at sites that have a consensus sequence of N-X-S/T, where N stands for asparagine, X can be any amino acid except proline, and S/T indicates serine or threonine. N-glycosylation has been reported to affect protein's structure, folding, stability and activity. [168-176] Glycosylation is also an essential critical quality attribute (CQA) that must be considered in the development of biotherapeutics[177], necessitating their comprehensive characterization and quantitation. N-Glycans can be categorized into three main groups: high mannose, complex, and hybrid structures.

The current methods to identify N-glycosylation include analyzing the protein of interest using Liquid Chromatography coupled with Mass Spectrometry (LC-MS) via top-down[178,179], middle-up[177,179] and bottom-up approaches using fragmentation techniques such as electron transfer dissociation (ETD), electron capture dissociation (ECD), Collision-Induced Dissociation (CID).[180-183] While glycopeptide analyses offer information about the site of N-glycosylation, it may not provide structural information on linkage and branching in all cases.[184] In addition, poor ionization of glycopeptides in

the presence of more abundant non-glycosylated peptides could make the characterization more challenging and may often require a pre-enrichment step.[185,186] Thus, analyzing released N-glycans is a more practical approach for comprehensive glycomic profiling as they can be studied without any interference from the heterogeneity of the glycoprotein. N-glycans are typically released from the protein using PNGase F enzyme.[184] However, glycans have low ionization efficiency in mass spectrometry and lacks chromophore or fluorophore moieties, hampering its accurate detection.[187] Thus, released N-glycan is often labeled with a fluorophore at its reducing end to enhance glycan separation and detection. Some of the commonly used tags or labeling reagents include 2-aminobenzamide (2-AB) and 2-aminobenzoic acid (2-AA), Procainamide, ProZyme InstantPC, and Waters RapiFluor-MS.[187,188] The labeling procedure is frequently followed by a reductive amination step to form a more stable conjugate for detection. Reducing agents such as sodium cyanoborohydride ($NaBH_3CN$)[189], 2-Picoline borane[190] or 5-Ethyl-2-methylpyridine borane complex (EMP)[191] can be utilized for this purpose. While $NaBH_3CN$ is a toxic reagent[191], EMP is a less toxic, more stable, and organic soluble liquid. Subsequently, the N-glycan is subjected to clean-up/desalting step that employs size-exclusion columns[192] (PD MiniTrap G10 column) or polyamide columns such as Discovery Glycan SPE 50 mg column[193] (Millipore-Sigma). Size exclusion columns such as Cytiva PD MiniTrap G10 column containing Sephadex G-10 separate molecules based on differences in their size. On the other hand, polyamide columns such as Discovery Glycan SPE columns separate N-glycans by adsorbing them as a result of hydrogen bonding between hydrophilic -OH groups in N-glycan and amide groups of the polyamide resin through a reversed-phase mechanism.

As there are a variety of LC-MS sample preparation approaches to identify and quantify N-glycosylation PTM, this study focused on evaluating absolute and relative abundances of N-glycans obtained from a few of the protocols mentioned above. For instance, Procainamide labeling was chosen as the tagging agent and reducing agents such as $NaBH_3CN$ and EMP were utilized. In addition, sample clean-up strategies including the use of PD MiniTrap G10 size exclusion column and Discovery Glycan polyamide column were assessed. Further, abundances of N-glycans obtained from reduced maltotriose precipitation that does not involve a column desalting step were also analyzed and compared. Hydrophilic Interaction Liquid Chromatography (HILIC) that has been widely utilized to characterize hydrophilic modifications such as glycosylation was used in this study.[184, 188, 194-198] The more hydrophilic a glycan, the longer it can retain on the immobilized water surface on a HILIC column. Q-TRAP mass analyzer under precursor ion (Q1-mode) as well as Multiple reaction monitoring (MRM) modes were used for labeled N-glycan detection. The raw data files were then uploaded to Skyline software for peak area determinations.

Materials And Methods

Trypsin digestion

500 μg each of bovine Fetuin and human serum (from human male AB plasma) that were both purchased from Sigma Aldrich, St. Louis, MO, USA, were buffer exchanged with 50 mM ammonium bicarbonate (pH 7.8) to have a final concentration of 1 mg/mL. They were reduced with 200 mM Dithiothreitol (DTT) and alkylated using 1 M iodoacetamide, both purchased from Sigma Aldrich (St. Louis, MO, USA), to have a final concentration of 5 mM DTT and 8 mM iodoacetamide. Sequencing grade trypsin

from Promega (Madison, WI, USA) was then added at 20:1 ratio (w/w, protein/trypsin) and incubated at 37°C overnight.

N-glycan release

The digested protein samples were desalted using a JT Baker SPE octadecyl (C18) cartridge purchased from VWR International (Radnor, PA, USA). Firstly, acetic acid was added to the sample to bring it to 5% v/v. The C18 cartridge was washed with 3 mL of MeOH and equilibrated with 3 mL 5% acetic acid. The digested sample was loaded on the column. The cartridge was washed with 3 mL 5% acetic acid next. Further, peptides were eluted in 4 mL 60% acetonitrile with 5% acetic acid. The sample was dried using Speed vac. Tryptic peptides were resuspended in 50 mM ammonium bicarbonate. 2 µL of PNGase F (New England Biolabs, Ipswich, MA, USA) was added to it and was incubated overnight at 37^{o}C. Further, glycans were purified from peptides. Sample was dried down in Speed vac. 200 µL of 5% acetic acid was added and the sample was sonicated for 10-15 min before performing glycan purification. C18 cartridge was washed with 3 mL MeOH and equilibrated with 3 mL 5% acetic acid. Sample was loaded onto the column. N-glycans were eluted with 4 mL of 5% acetic acid as glycans do not retain on a C18 column. Sample was then divided into two parts and dried using Speed vac.

Procainamide labeling with $NaBH_3CN$ reductive amination

The first part was subjected to Procainamide labeling with sodium cyanoborohydride ($NaBH_3CN$) reductive amination. 60 µL of 0.4 M Procainamide.HCl (Sigma Aldrich, St. Louis, MO, USA), 0.8 M $NaBH_3CN$ (Sigma Aldrich, St. Louis, MO, USA) was added to this part, mixed in DMSO:acetic acid;7:3 (v/v) and incubated at 65°C overnight. The samples were again divided into two parts and each of them were dried

using SpeedVac. The first fraction was resuspended in 5% acetic acid (240µL) and cleaned on a PD MiniTrap G10 desalting column (Cytiva, Marlborough, MA, USA) using the manufacturer's protocol. The samples were then dried and resuspended in 80% ACN (1 mg/mL) for LC-MS analysis. The second fraction was subjected to Supelco Discovery Glycan polyamide column desalting (Supelco™ -Sigma Aldrich, Bellefonte, PA, USA). The sample was resuspended in 70% acetonitrile in water. Desalting was performed as per manufacturer's protocol, wherein the column was prepared by first washing it with water and then with 99% acetonitrile. The sample was loaded. The column was then washed with 99% acetonitrile and N-glycans were eluted with 20% acetonitrile in water. The samples were then dried and resuspended in 80% ACN (1 mg/mL) for LC-MS analysis.

Procainamide labeling with EMP reductive amination

The second part was subjected to Procainamide labeling with 5-Ethyl-2-methylpyridine borane complex (EMP) reductive amination, which was purchased from Millipore Sigma (Burlington, MA, USA). To the dried sample was added 35 µL of 0.4 M Procainamide solution containing 20% (1.5 M) EMP in 5% acetic acid/75% DMSO. The sample was incubated at 37^{o}C overnight. The sample was again divided into two fractions. The first fraction was desalted using a PD MiniTrap G10 size exclusion column as per manufacturer's protocol. The sample was resuspended in 80% ACN (1 mg/mL) for LC-MS analysis. The second fraction was cleaned up using reduced maltotriose precipitation. The reduced maltotriose solution was obtained from Advanced Materials Technology, Wilmington, DE, USA. 10 µL of reduced maltotriose was added to the sample. 0.7 mL of cold acetone was added to it and the sample was chilled in a -20^{o}C

freezer for 20 minutes. A white precipitate was observed. The sample was centrifuged at 5000 rpm for 20 minutes and dried using Speed vac. Lastly, the sample was resuspended in 80% ACN (1 mg/mL) for LC-MS analysis. 200 μg of Dextran (Mr 6,000) from Sigma Aldrich (St. Louis, MO, USA) was also subjected to Procainamide labeling with $NaBH_3CN$ as well as EMP reductive amination, each with PDG10 desalting using the method described above. Labeled dextran samples were then dried and resuspended in 80% ACN (1 mg/mL) for LC-MS analysis.

LC/MS settings and instrumentation

Data were acquired using an Nexera UFLC (Shimadzu, Kyoto, Japan) coupled to AB-SCIEX 4000 QqQ (Framingham, MA, USA) system with ESI source. Peptides were separated using a 2.1-mm × 150-mm HALO Penta-HILIC column packed with 2.7-μm diameter superficially porous particles that have a 90-Å pore diameter (Advanced Materials Technology, Wilmington, DE, USA) at 60 °C column temperature. The mobile phases used to perform separation were 50 mM ammonium formate in water with 0.1% Formic acid (Solvent A), and 0.1% Formic acid in Acetonitrile (Solvent B). A linear gradient of 80% to 40% Solvent B over 40 minutes (1%B per minute) at 0.2 mL/min flow rate was used for separation. Q1 and MRM experiments were conducted on AB-SCIEX 4000 QqQ. Absolute and relative abundance quantitation were performed utilizing peak areas obtained from Skyline software.

Results And Discussion

The study was initiated by performing relative and absolute quantitation on bovine fetuin. Fetuin was first treated with trypsin digestion prior to deglycosylation (Figure 5.1). N-glycans were released from the protein using PNGase F enzyme. The

released N-glycans were then labeled with Procainamide since it improves ionization and facilitates identification of N-glycans in mass spectrometry.[187] Labeling with Procainamide also ensures that the N-glycans are sufficiently retained on an LC column such as HILIC. The labeling step was followed by reductive amination. The sample was divided into two parts for reduction. One part was subjected to $NaBH_3CN$ reduction, which is one of the standard methods of performing reduction[189]. The other part was subjected to EMP reducing agent. EMP has been reported to be less toxic than $NaBH_3CN$ reagent[191]. The $NaBH_3CN$ fraction was further divided into two parts, with one part desalted using PD MiniTrap G-10 column, whereas the other part was desalted using Supelco Discovery Glycan polyamide column. PD MiniTrap G-10 column is a size-exclusion column whereas the separation in the polyamide column is mainly based on hydrogen bonding with the hydrophilic N-glycans. The EMP fraction was similarly divided into two parts, one went through PD MiniTrap-G10 column whereas the other was treated with reduced maltotriose precipitation, thus avoiding the use of a desalting column.

These labeled N-glycans from all four fractions were subjected to LC-MS analysis. HILIC column that has been utilized for the analysis of hydrophilic modifications[184, 188, 194-198] was used to study N-glycosylation. The more an N-glycan is hydrophilic, the longer it would be retained on a HILIC column owing to the interactions between the N-glycan and water enriched hydrophilic stationary phase in HILIC column. MRM and Q1 experiments were conducted on AB-SCIEX 4000 QqQ instrument using the transitions for each N-glycan precursor, as well as daughter ions such as 441.2708 m/z (core GlcNAc linked to Procainamide), 204.0866 m/z (HexNAc oxonium ion) and

366.1395 m/z (Hexose+HexNAc). Absolute and relative abundance quantitation were performed utilizing peak areas obtained from Skyline software.

Firstly, the choice of reducing agent during Procainamide labeling was evaluated. Most abundant glycans with compositions A2G1, A2G2, A3G3, A2G2Neu5Ac1, A2G2Neu5Ac2, A3G3Neu5Ac1, A3G3Neu5Ac2, A3G3Neu5Ac3 and A3G3Neu5Ac4 in bovine fetuin were analyzed. Therefore, abundances of these N-glycans obtained from the fraction that was subjected to $NaBH_3CN$ reduction followed by PD MiniTrap G-10 column desalting step (referred as $NaBH_3CN$-PDG10) was compared with the fraction that was subjected to EMP reduction and PD MiniTrap G-10 desalting (referred as EMP-PDG10). LC traces for $NaBH_3CN$-PDG10 and EMP-PDG10 are depicted in Figure 5.2 panel A. Peak areas of individual N-glycans in both fractions were determined using Skyline software and plotted on Microsoft excel to compare the absolute abundances (Figure 5.2 panel B). The sialylated N-glycans produced multiple peaks in the chromatogram due to the differences in sialic acid linkage, such as 2,3- and 2,6- linkages as well as due to the presence of positional isomers. The peak area of multiple peaks corresponding to a particular composition were summed up and considered for analysis. It was observed that the overall abundance of N-glycans was higher when $NaBH_3CN$ was utilized as a reducing agent compared to EMP. $NaBH_3CN$ has been reported to be a stronger reducing agent than EMP[191], which may have led to greater absolute abundances of N-glycans. An interesting observation was that the relative abundance of N-glycans increased in the case of highly sialylated N-glycans when bovine fetuin was treated with EMP reduction, as shown in Figure 5.2 panel C. For instance, the relative abundance of A2G2Neu5Ac2, A3G3Neu5Ac1, A3G3Neu5Ac2, A3G3Neu5Ac3 and A3G3Neu5Ac4

glycans was higher in the case of EMP reduction when compared to $NaBH_3CN$ reduction. One of the plausible reasons for this observation is that reductive amination with $NaBH_3CN$ was performed at a higher temperature (65^oC, overnight) compared to EMP reductive amination, which was performed at 37^oC (overnight). The higher temperature in $NaBH_3CN$ reductive amination may have caused the sialic acid to fall out from the N-glycan[199], whereas this degradation was not significant in the case of EMP reductive amination conditions.

The absolute and relative abundances of N-glycans were then compared between EMP reduction with PD MiniTrap G10 desalting (EMP-PDG10) and EMP reduction subjected to reduced maltotriose precipitation (EMP-Precipitation) protocol in bovine fetuin sample. LC-Q1 traces of N-glycans released using EMP–PDG10 and EMP-Precipitation protocols are depicted in Figure 5.3 panel A. Overall absolute and relative abundances of N-glycans were observed to be comparable between the two protocols based on their peak area (Figures 5.3 panels B and C). t-test statistical analysis was performed to discern if this observation was statistically significant. A p-value of 0.277802, which is greater than 0.05 indicated that the differences in the peak area of N-glycans obtained from the two protocols were not statistically significant.

Finally, the abundance of N-glycans obtained from various sample clean-up conditions were evaluated. More specifically, fetuin N-glycans tagged with Procainamide and reduced with $NaBH_3CN$ were subjected to either PD MiniTrap G10 size exclusion column ($NaBH_3CN$-PDG10) or Supelco polyamide column ($NaBH_3CN$-Polyamide). It was observed that the abundance of all detected N-glycans, as determined from peak area, were comparable in both the protocols (Figure 5.4). t-test statistical analysis was

performed to determine if the slight differences in abundances were statistically significant or not. It was discerned that the peak area differences for N-glycans in both protocols were not statistically significant.

Analysis on Procainamide labeled dextran (glucose polymer) was carried out next to understand if prevalence of larger glycans obtained from EMP reducing agent in Fetuin was size or charge dependent as sialylated glycans introduced negative charge in the glycan structure. Therefore, dextran was labeled with Procainamide and the sample was split into two parts. One part went through standard $NaBH_3CN$ reduction and PDG10 desalting, whereas the other part went through EMP reduction and PDG10 desalting, thus differing in only the choice of reducing agent used. LC-SRM traces of dextran obtained from both protocols are displayed in Figure 5.5. Higher relative abundance of larger dextran molecules such as GU9 (GU = Glucose Unit), GU10, GU11, and GU12 compared to lower molecular weight dextran molecules suggested that the prevalence of heavier sialylated N-glycans by EMP reducing agent observed in fetuin N-glycans was not charge-dependent. The higher GU molecules may have remained more stable when reduction of Dextran was performed at a lower temperature of 37^{o}C in EMP protocol, compared to being subjected to a high temperature of 65^{o}C in $NaBH_3CN$ protocol.

The study was further extended to analysis of more complex human serum samples. Most abundant N-glycans with compositions A2G1, FA2G1, A2G2, A2G2Neu5Ac1, FA2G2Neu5Ac1, A2G2Neu5Ac2, FA2G2Neu5Ac2, A3G3Neu5Ac2, A3G3Neu5Ac3 and FA3G3Neu5Ac3 were studied. The trend obtained in the case of human serum N-glycans were similar to those observed in the case of fetuin N-glycans. Overall absolute abundance of N-glycans were observed to be higher when they were

obtained using $NaBH_3CN$-PDG10 protocol compared to the EMP-PDG10 protocol based on peak area (Figure 5.6 panel A), highlighting that the choice of reducing agent can have a significant effect on N-glycan abundances. In addition, the evaluation of relative abundances of human serum N-glycans obtained from $NaBH_3CN$-PDG10 and EMP-PDG10 protocols revealed that larger N-glycans were observed to have higher relative abundances when EMP was utilized (Figure 5.6 panel B). Further, Figure 5.7 panel A displays the evaluation of absolute abundances of human serum N-glycans obtained from EMP-PDG10 and EMP-maltotriose precipitation protocols. The overall absolute abundance of human serum N-glycans were again observed to be comparable between the two protocols. The evaluation of relative abundances of human serum N-glycans obtained from EMP-PDG10 and EMP-precipitation protocols are depicted in Figure 5.7 panel B. The relative abundances were comparable in both cases. t-test analysis (p-value > 0.05) indicated that the differences between the abundances of N-glycans obtained from both protocols were statistically insignificant.

Evaluation of abundances of $NaBH_3CN$ reduced human serum N-glycans obtained from PD Mini Trap G10 column desalting ($NaBH_3CN$-PDG10) and Polyamide column desalting ($NaBH_3CN$-Polyamide) were performed next (Figure 5.8). Overall absolute and relative abundances of N-glycans were observed to be comparable in both cases depicting that a change in a desalting column did not introduce inaccuracies in quantitation. t-test analysis (p-value > 0.05) indicated that the differences between the abundances of N-glycans obtained from both protocols were statistically insignificant.

Thus, the choice of LC-MS sample preparation protocol can impact the abundances of N-glycans and can result in inaccuracies in their absolute and relative

quantitation. For example, the absolute and relative abundances of N-glycans varied between $NaBH_3CN$ reductive amination and EMP reductive amination during Procainamide labeling step. Each protocol has its own advantages and disadvantages. For instance, $NaBH_3CN$ is a stronger reducing agent than EMP, but EMP is a safer and less toxic alternative. EMP reaction conditions were also observed to be less harsh than $NaBH_3CN$ reduction possibly preventing sialic acids to fall out of N-glycans. The key takeaway is that it is vital to choose one specific protocol and utilize it consistently throughout the study to achieve reproducible and accurate absolute and relative quantification of N-glycans.

Conclusions

Experimentally determined absolute and relative abundances appeared to be altered by the choice of the N-glycan sample preparation protocol, especially when selecting the reducing agent during the glycan labeling step. For instance, the absolute abundance of fetuin and human serum N-glycans were higher when $NaBH_3CN$ was used during Procainamide labeling, compared to EMP. Further, the relative abundance of heavier sialylated N-glycans were higher when EMP was chosen. The $NaBH_3CN$ reductive amination step was carried out at a higher temperature (65^oC) than EMP protocol (37^oC) that may have caused the sialic acid to fall out of N-glycans, thus decreasing the abundances of heavier sialylated N-glycans. The difference in N-glycan abundances were not significant when desalting/clean-up strategies were compared.

Thus, the selection of an LC-MS sample preparation method can influence the quantitation of N-glycans. While each method has its own pros and cons, it is crucial to

carefully select a sample preparation approach and maintain its consistency throughout a study to enhance reproducibility and accuracy of N-glycan quantitation.

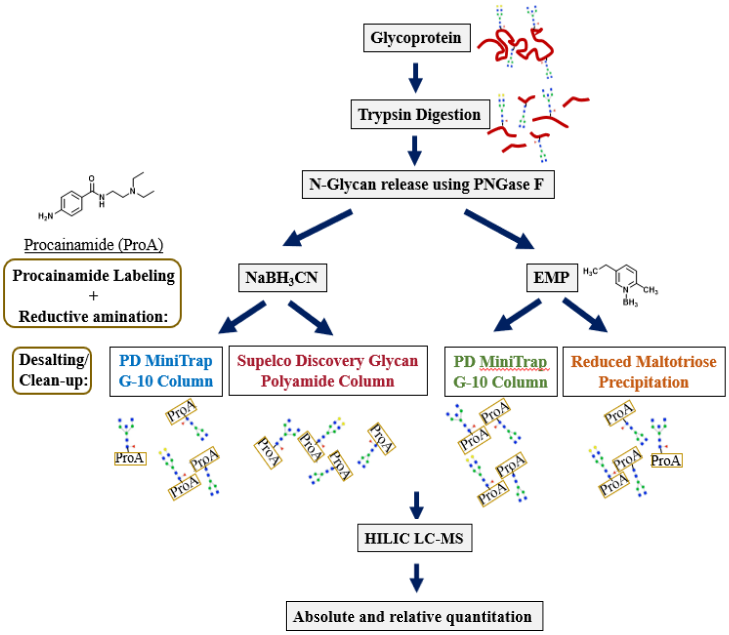

Figure 5.1: Experimental design followed in this study. Glycoprotein was digested using trypsin followed by N-glycan release using PNGase F. The released N-glycans were then labeled with Procainamide and reductively aminated using either $NaBH_3CN$ or EMP. N-glycans labeled and reductively aminated by $NaBH_3CN$ were then divided into two fractions. The first fraction was desalted using PD MiniTrap G-10 size exclusion column, and the second fraction with a polyamide column. N-glycans that were reductively aminated with EMP were also divided into two fractions, where one fraction was subjected to PD MiniTrap G-10 column desalting and the other was treated with reduced maltotriose precipitation. All fractions were subjected to HILIC LC-MS. Absolute and relative abundances of N-glycans were compared between different protocols.

(A)

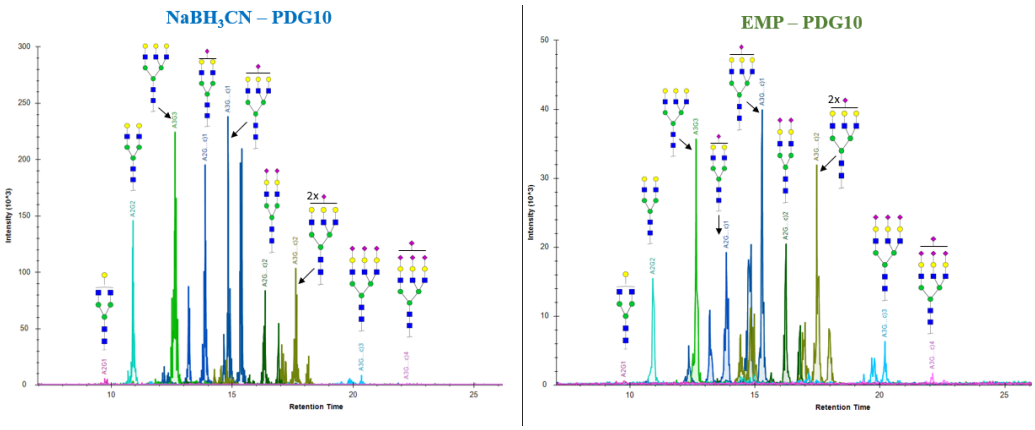
NaBH3CN – PDG10
EMP – PDG10
Intensity (10^3)
Retention Time
2x

(B)

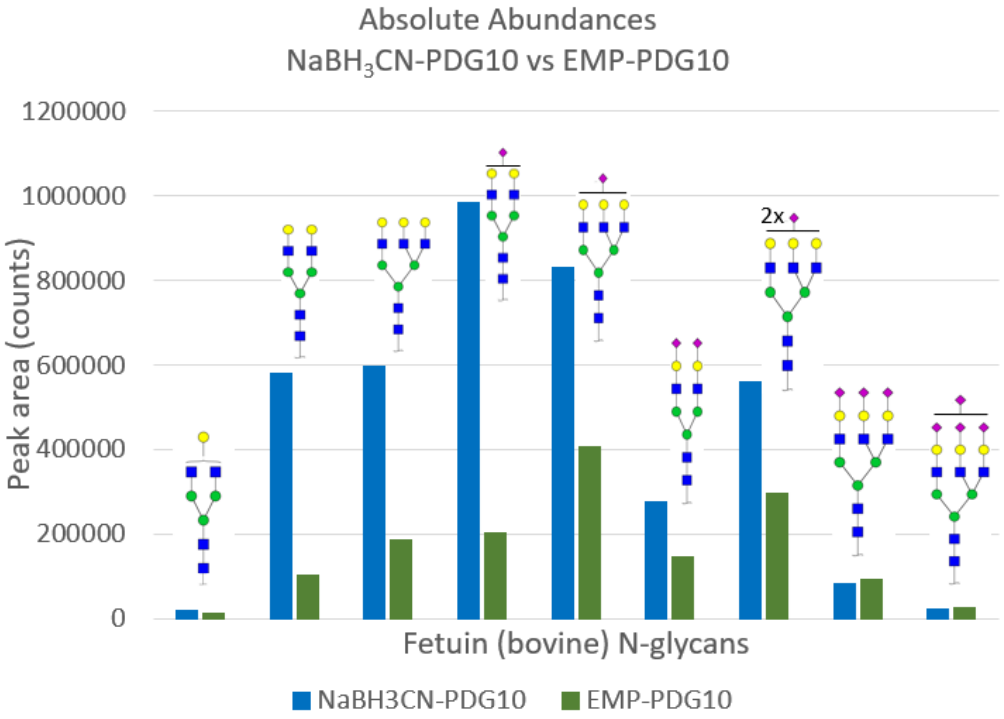
Absolute Abundances
NaBH3CN-PDG10 vs EMP-PDG10
Peak area (counts)
1200000
1000000
800000
600000
400000
200000
0
2x
Fetuin (bovine) N-glycans
NaBH3CN-PDG10
EMP-PDG10

(C)

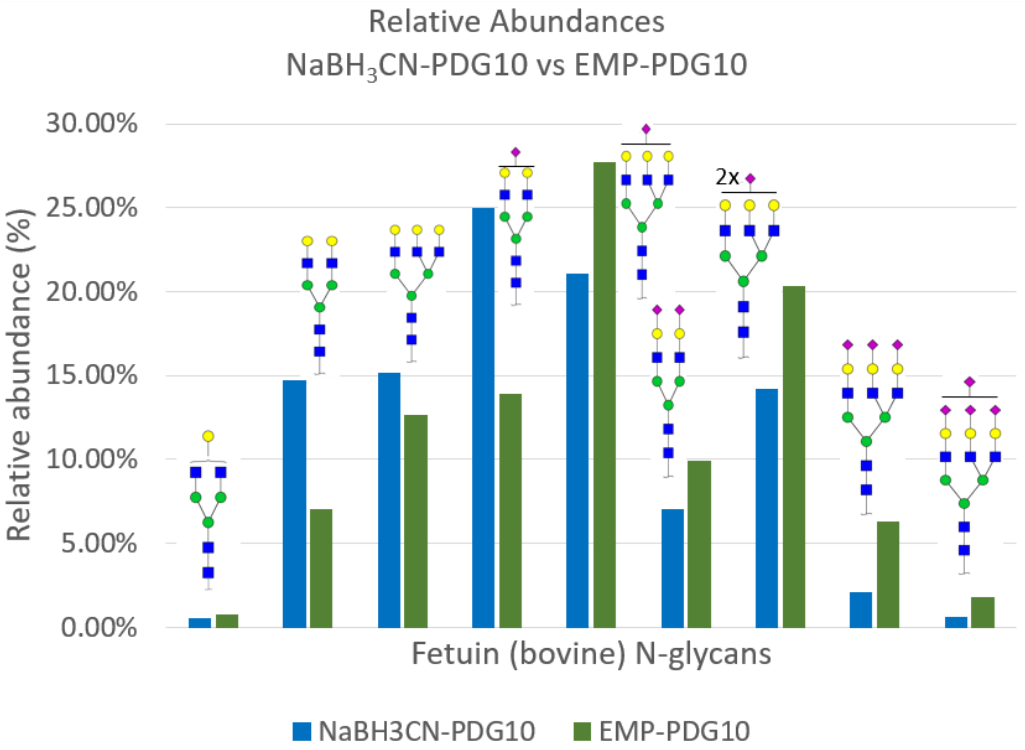

Figure 5.2: LC-Q1 traces of N-glycans released from bovine Fetuin using $NaBH_3CN$–PDG10 and EMP-PDG10 protocols **(A)**. Absolute abundance of N-glycans, displayed in **(B)** were observed to be higher in the case of $NaBH_3CN$–PDG10 protocol. Larger sialylated N-glycans were more abundant relative to smaller N-glycans in EMP-PDG10 protocol, as shown in **(C)**.

(A)

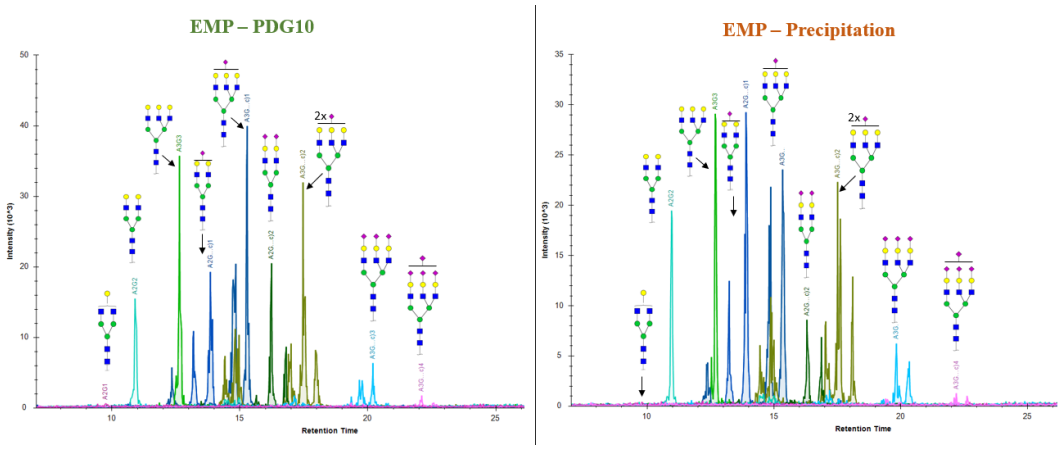
EMP – PDG10
EMP – Precipitation
Intensity (10^3)
Retention Time
2x

(B)

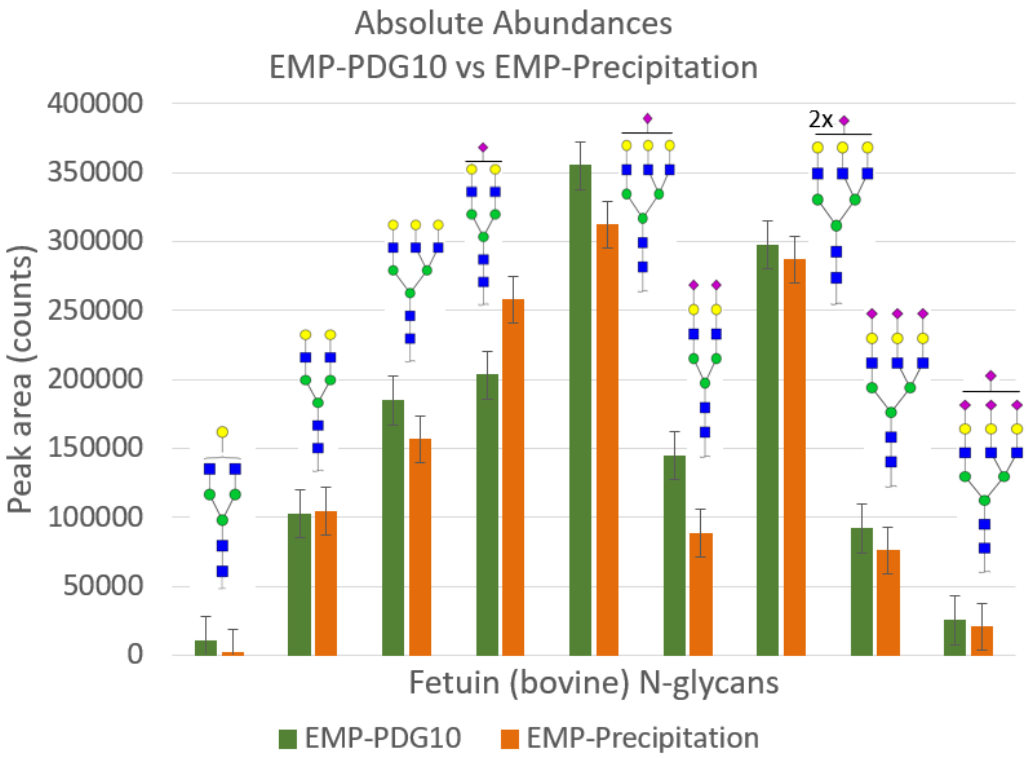
Absolute Abundances
EMP-PDG10 vs EMP-Precipitation
Peak area (counts)
400000
350000
300000
250000
200000
150000
100000
50000
0
2x
Fetuin (bovine) N-glycans
EMP-PDG10
EMP-Precipitation

(C)

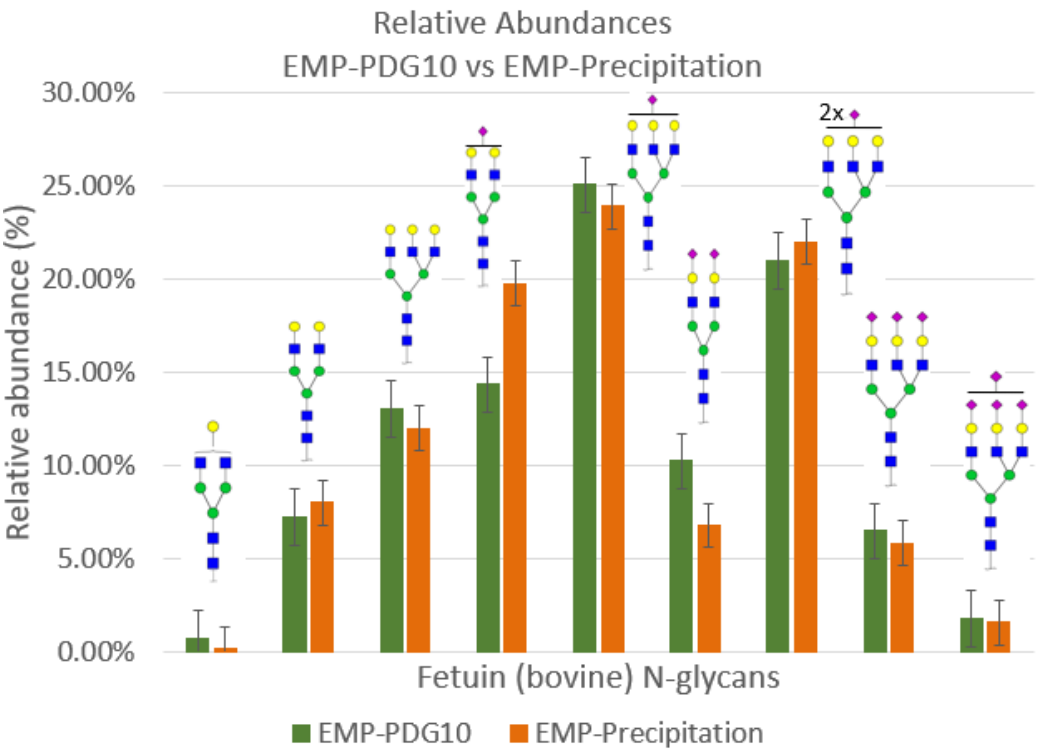

Figure 5.3: LC-Q1 traces of N-glycans released from bovine Fetuin using EMP–PDG10 and EMP-maltotriose precipitation protocols **(A)**. The absolute abundance of N-glycans displayed in **(B)** and relative abundance of N-glycans displayed in **(C)** were observed to be comparable between the two protocols.

(A)

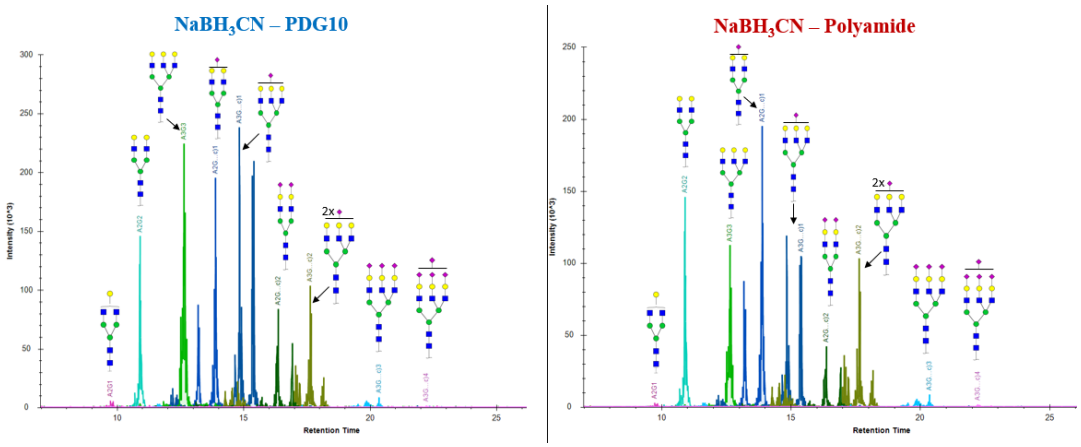
NaBH3CN – PDG10
NaBH3CN – Polyamide
Intensity (10^3)
Retention Time
2x

(B)

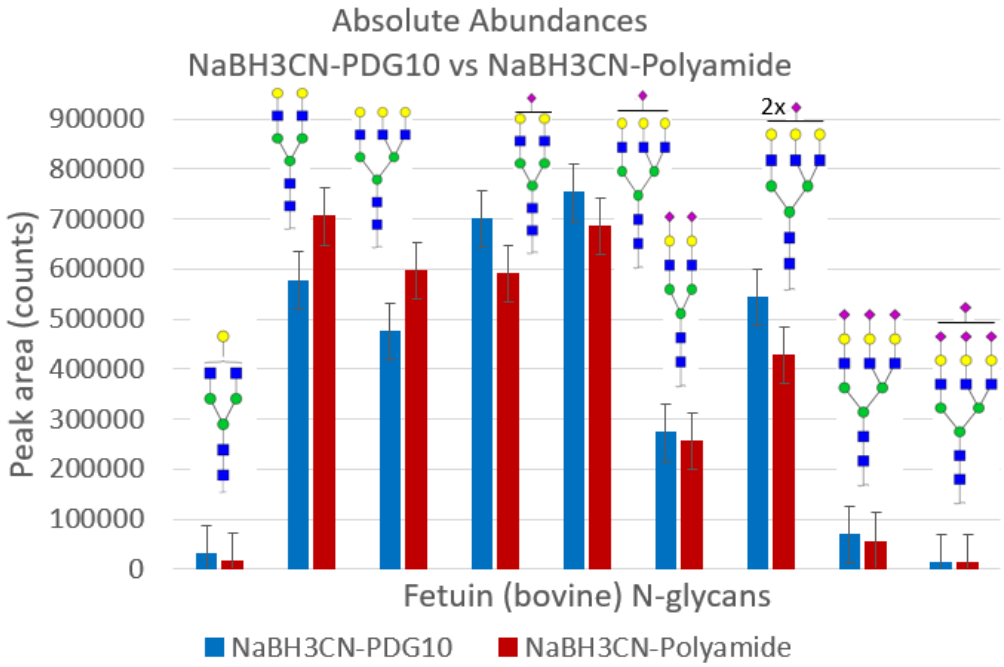
Absolute Abundances
NaBH3CN-PDG10 vs NaBH3CN-Polyamide
Peak area (counts)
900000
800000
700000
600000
500000
400000
300000
200000
100000
0
2x
Fetuin (bovine) N-glycans
NaBH3CN-PDG10
NaBH3CN-Polyamide

(C)

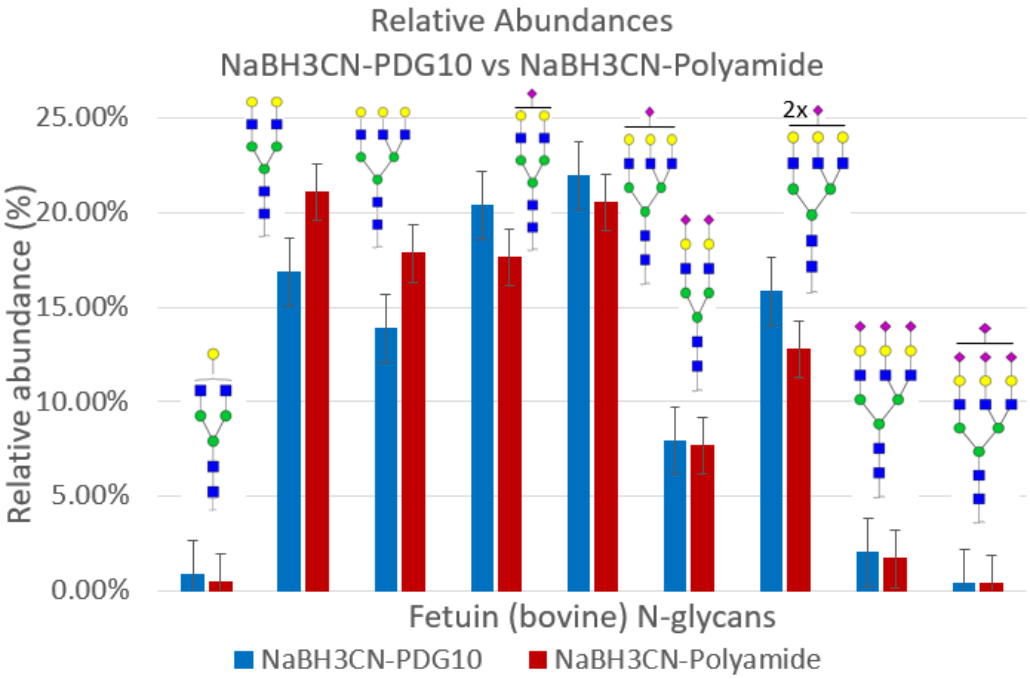

Figure 5.4: LC-Q1 traces for $NaBH_3CN$-PDG10 and $NaBH_3CN$-Polyamide protocols **(A)**. Evaluation of absolute (**B**) and relative (**C**) abundances of N-glycans obtained from $NaBH_3CN$-PDG10 and $NaBH_3CN$-Polyamide desalting protocols are also depicted. Overall absolute and relative abundances of N-glycans in bovine fetuin were observed to be comparable in both protocols.

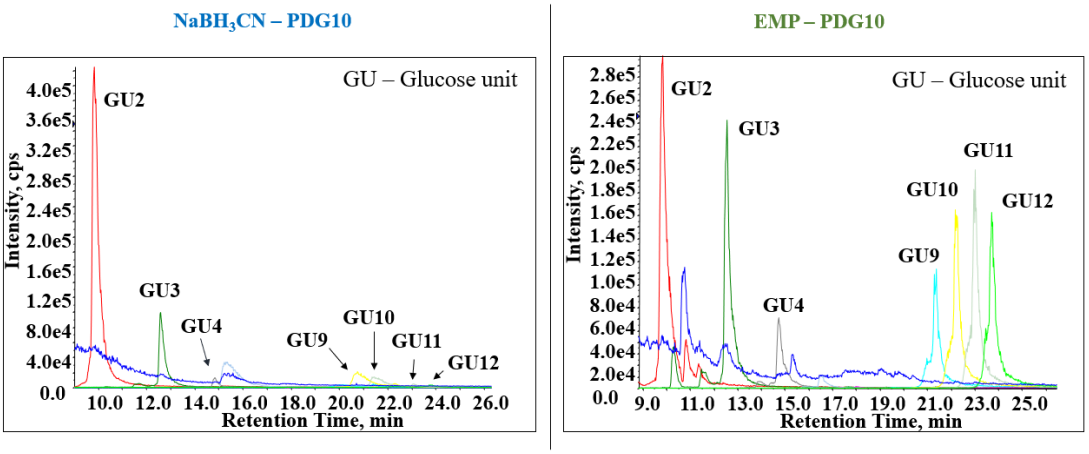

Figure 5.5: LC-SRM traces of dextran obtained from $NaBH_3CN$-PDG10 and EMP-PDG10 protocols. Analysis on dextran was carried out to understand if the prevalence of larger glycans by EMP reducing agent in Fetuin was size or charge dependent. Higher relative abundance of larger dextran molecules in EMP-PDG10 protocol suggested that the prevalence of heavier sialylated N-glycans in Fetuin was not charge dependent.

(A)

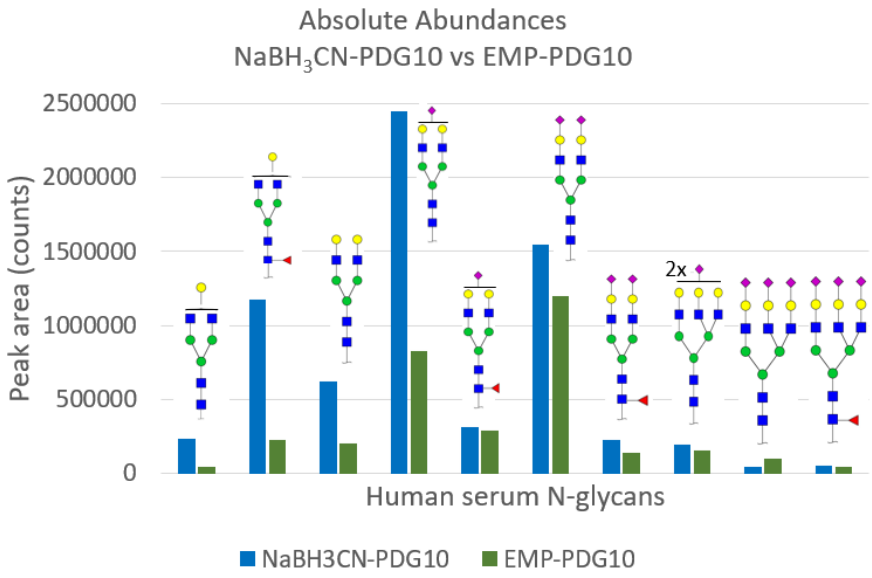

(B)

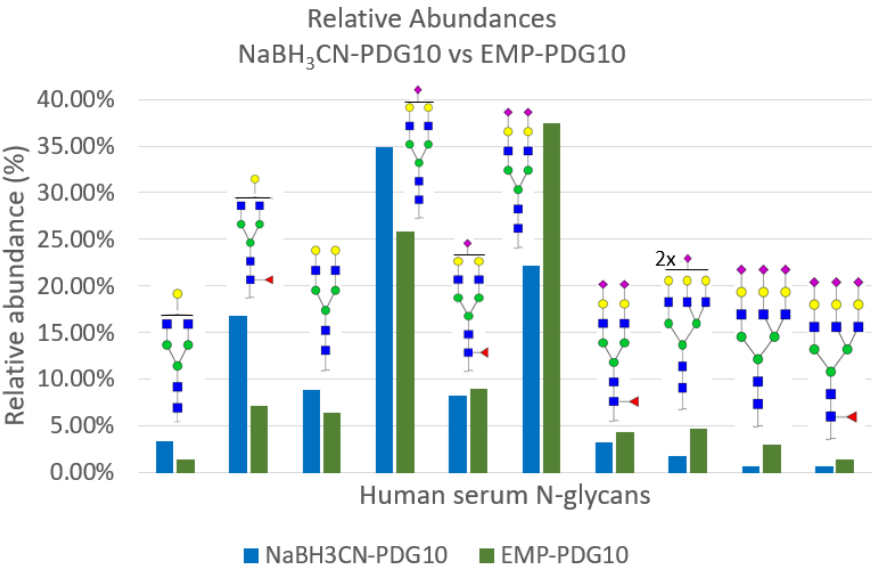

Figure 5.6: Evaluation of absolute abundances of human serum N-glycans obtained from $NaBH_3CN$-PDG10 and EMP-PDG10 protocols **(A)**. Overall absolute abundance of N-glycans were observed to be higher for $NaBH_3CN$-PDG10 protocol based on their peak area. **(B)** illustrates the evaluation of relative abundances of human serum N-glycans obtained from $NaBH_3CN$-PDG10 and EMP-PDG10 protocols. Larger N-glycans were observed to have higher relative abundances when EMP was utilized.

(A)

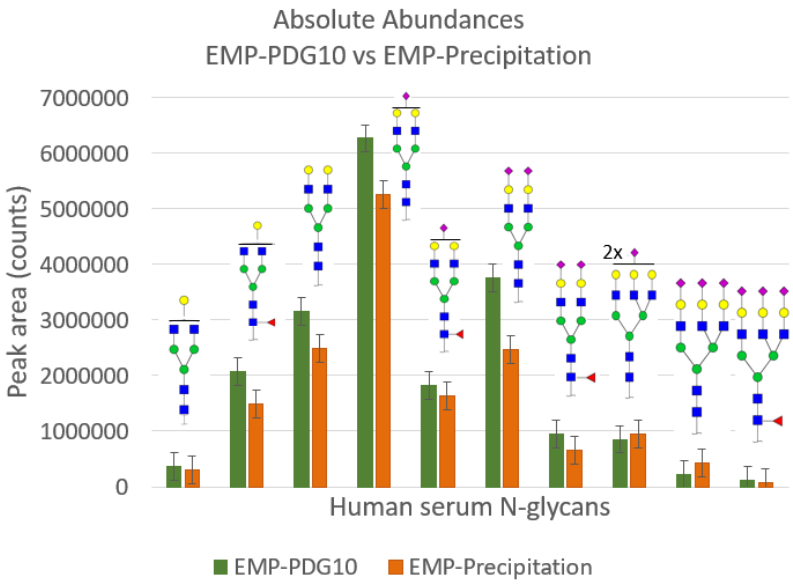

(B)

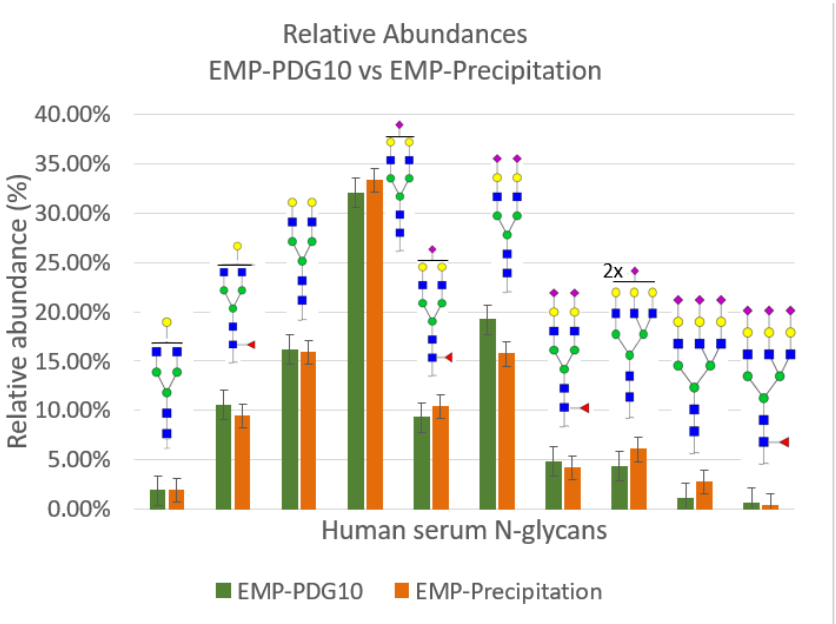

Figure 5.7: Evaluation of absolute (**A**) and relative (**B**) abundances of human serum N-glycans obtained from EMP-PDG10 and EMP-maltotriose precipitation protocols. Overall absolute and relative abundances of N-glycans were observed to be similar between the two protocols based on peak area.

(A)

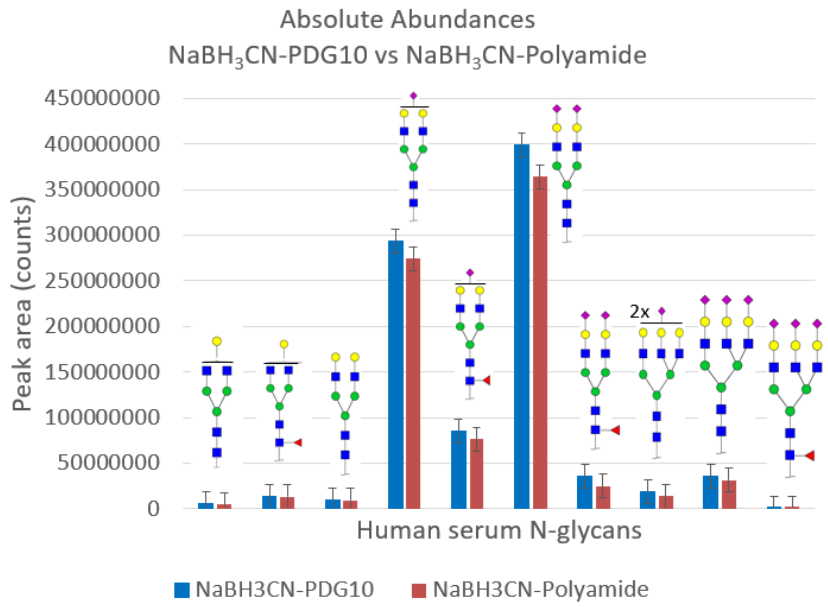

(B)

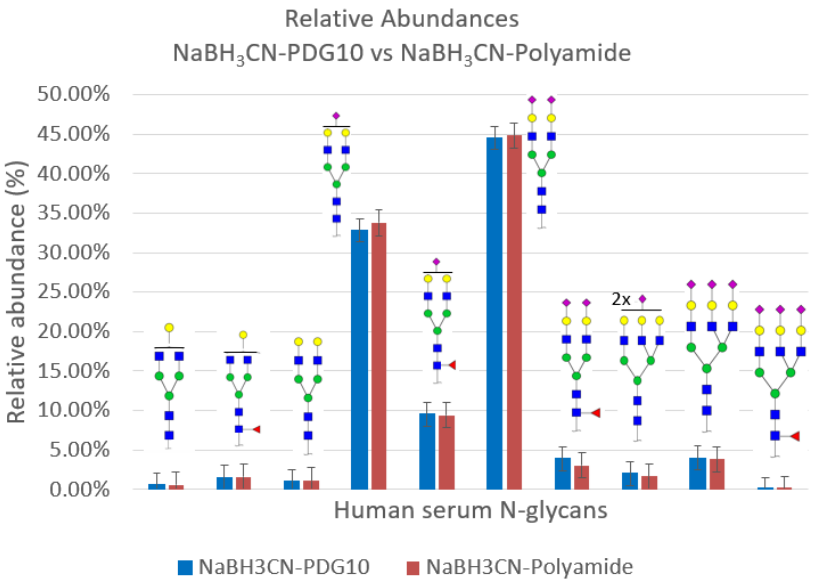

Figure 5.8: Evaluation of absolute (**A**) and relative (**B**) abundances of human serum N-glycans obtained from $NaBH_3CN$-PDG10 and $NaBH_3CN$-Polyamide column desalting protocols. Overall absolute and relative abundances of N-glycans were observed to be comparable in both protocols.

CHAPTER 6

A SURVEY ON CORE FLOW CYTOMETRY FACILITIES: INSTRUMENT MAINTENANCE, USAGE AND FUNDING[3]

[3] Priya, S., Brundage, K., and Orlando, R. Accepted by *The Journal of Biomolecular Techniques*. Reprinted here with permission of the publisher, October 29, 2023.

Abstract

Flow cytometry is a powerful tool that finds applications in various fields such as immunology, molecular biology, cancer biology, virology, and infectious disease monitoring. A significant portion of the research in these disciplines is supported by Flow Cytometry Shared Resource Labs (SRLs). There are several types of flow cytometers available for use in SRLs including analyzers, sorters, imaging flow cytometers and mass cytometers. Each type has different challenges when it comes to maintenance and life expectancy. An independent online survey was conducted to better understand instrument maintenance and turnover in Flow Cytometry SRLs. Questions regarding instrument uptime (availability), its usage, routine maintenance, and cost associated with it were addressed. The respondents also answered questions pertaining to frequency of deep cleaning of the instrument and quality control. In addition, the survey queried about the source of funding used to purchase the instruments and possible reasons for a replacement. Presented herein are the results compiled from 146 core facilities that provide a look at the operation within a typical SRL with the responses reflecting researchers' experiences with handling flow cytometers.

Introduction

No matter which technology or equipment a Shared Resource Lab (SRL) specializes in, they all share common concerns regarding instrument maintenance and life expectancy. SRL managers and directors contemplate the optimal strategies for maintaining an instrument, determining the right time to replace an instrument, and obtaining the necessary funding for service contracts or for acquiring new instruments. To gain deeper insights into how SRLs address these challenges, we opted to conduct a

survey specifically among SRLs that are focused on flow cytometry. We believe that the responses gathered in this survey from flow cytometry SRLs can be extrapolated to SRLs focused on other technologies and instrumentation.

Flow cytometry technology has been around since the 1950's. Over the years, the instrumentation, the cell types analyzed, and the assays performed have become more diverse and complex. [200-214] What started out as a way to count cells has developed into a technology where tens of thousands of cells are analyzed per second for expression of multiple proteins, viability, and function. Today fluorescent antibody panels containing 15 or more antibodies are routinely used to identify unique cell populations with very distinct properties and functions.

Flow cytometers can be divided into 2 broad categories based on their function: analyzers, and sorters.[215,216] As their name implies, analyzers assess the cells in the sample and the assayed cells are not recovered. Sorters make up the second category of flow cytometers. Sorters possess comparable capabilities to analyzers but also contains an additional attribute. Sorters can separate cells into different purified populations based on their fluorescent signature. These purified populations can then be used for downstream applications such as single cell RNA sequencing and western blots. These purified cell populations are often reintroduced into culture for expansion or functional studies.

An alternative method of categorizing flow cytometers is based on how the signal is detected. Employing this way to categorize flow cytometers results in 4 different types of flow cytometers: traditional flow cytometers, mass cytometers[217-219], imaging flow cytometers[220-222] and full spectrum flow cytometers.[223,224] When most individuals think of flow cytometers, they think of the traditional flow cytometers. These types of instruments

use both diodes and photomultiplier tubes (PMTs)[225] to detect the fluorescent signal with a single fluorescent molecule being detected at each detector. Longpass and bandpass filters are placed in front of the detectors to narrow the wavelength detected. Mass cytometers have been around since the early 2000's and combines a flow cytometer with a mass spectrometer.[217-219] Unlike the other three types of flow cytometers, cells intended for analysis using a mass cytometer are labeled with antibodies conjugated to isotopes of rare earth metals. As with a traditional flow cytometer, when assaying cells on a mass cytometer, the labeled cells are brought to the detection device within a fluidic stream. The distinction lies in the fact that the cells upon reaching the detection device are atomized and sent through a mass spectrometer. Time of flight is utilized to identify the antibodies that are bound to the cell. Imaging flow cytometers combine flow cytometry with microscopy. These instruments use fluorescent-labeled antibodies and images of each cell, and bright field and fluorescence are taken as the cells go through the detection region. The newest type of flow cytometer is the full spectrum flow cytometer.[223,224] These types of flow cytometers have truly demonstrated their potential over the past five years. These instruments use a series of avalanche photodiodes as detectors. The detectors are set up for each laser starting at 15 - 30 nm from the laser wavelength and at 15 – 30 nm intervals until 815 nm. This implies that instead of identifying each fluorochrome with a single detector, the system provides a comprehensive value across the entire range, yielding the dye spectrum or a fingerprint. The majority of fluorescent dyes possess unique spectra that allows one to distinguish them from each other.

Even though today's flow cytometers have better sensitivity, can detect more markers, and collect data more rapidly than those of 25 years ago, the old instruments

still generate good and reliable data. Since the 1980's, flow cytometry data generated on any instrument produced by any company uses a standard data format that is open source and readable in third party software. In many cases, researchers do not need the latest and advanced flow cytometer to answer their research questions. Flow cytometers entail a considerable financial investment, with costs ranging from $50,000 to $750,000 or beyond, based upon the desired features and specifications. Thus, figuring out when and how to replace an older instrument is a major issue for most Flow Cytometry shared resource labs (SRLs) [226-228]/core facility directors. The majority of institutions lack the available funds to acquire the most current and advanced flow cytometers. For this reason, most if not all flow cytometry SRLs expend substantial efforts to prolong the operational lifespan of their existing instrumentation.

Information Sought and Aim of Study:

The survey whose results are presented below was designed to better understand instrument maintenance and turnover in Flow Cytometry SRLs. It assessed the age of the instruments in the facilities, whether instruments were maintained using service contracts, and who operates the instruments, i.e., users or staff. The survey also examined why new instruments were purchased and which funding sources were utilized for the procurement of these new instruments. We anticipate that the outcomes presented and discussed in this study will serve as a valuable point of reference for SRL labs in their capital purchase discussions as well as in devising strategic plans related to lab operations.

Methods

An independent online survey was developed and shared using internet survey provider SurveyMonkey (www.surveymonkey.com/r/ABRFFlowCytometrySurvey). The

survey was made available on June 6, 2020 and was open for a total of 3 weeks. The goal of the survey was to obtain comprehensive information about flow cytometer facilities including the type of staffing, funding, instrument usage, frequency of routine maintenance and the average annual maintenance cost associated with operating a lab among various other factors. The survey consisted of four multi-part questions, including a mix of open-ended and multiple-choice options. Respondents' answers were kept anonymous. The original survey can be found in the supporting information (Table 6.1). To gain a better understanding of the types of instruments used, the survey was divided into three categories: newest, oldest, and most used instruments. If the instrument fell into two categories, the responses were collected based on the length of time the instrument was most occupied. Keywords that were commonly used in this study are defined in Table 6.2. All monetary data has been converted to US currency to facilitate comparisons between countries.

Data were collated and analyzed using Microsoft Excel. Statistical significance of differences between means was determined by performing t-test for unpaired data.

Results And Discussion

Demographic of Respondents

The survey achieved participation from 146 respondents residing in 14 countries across 4 continents (Figure 6.1 panel A). The majority of survey participants were core facility directors (39.7%) or managers (34.3%, Figure 6.1 panel B) who worked at universities (64.6%), hospitals (8.9%), private institutions (6.3%) and companies (6.3%, Figure 6.1 panel C). At the time of the survey, 27.8% of the survey respondents identified themselves as members of ABRF whereas the majority of participants (72.2%)

were not (data not shown). The number of respondents and their demographics aligned with what would be expected based on the known distribution of Flow Cytometry SRLs across the world.

Instrumentation

As expected, the two major types of flow cytometers in their SRLs were analyzers (54.4%) and sorters (37.9%, Figure 6.1 panel D). Fewer SRLs had imaging flow cytometers (5.2%) and mass cytometers (2.5%, Figure 6.1 panel D). Figure 6.1 panel E illustrates the age distribution of these instruments in the period 1980-2020. The results were grouped for 1980-1990-year range owing to fewer instruments purchased prior to 1990 and still in use. Subsequent responses for later years were grouped in 5-year periods. The respondents reported that the average age of the analyzers was 9 years old and spanned from 1980 to 2020. Sorters which became commercially available after 1990 had an average age of 8.5 years. Imaging and mass flow cytometers became available in 2005 and 2009, respectively. The "newness" of these types of instruments is reflected in the average age of the instruments in SRLs; 5 years for imaging flow cytometers and 1.5 years for mass cytometers.

Who Operates the Instruments?

As far as the staffing was considered, 49.9% of laboratory staff in Flow Cytometry SRLs were technicians (BS or MS level), 30.1% were Ph.D. scientists and 20.0% had other levels of education (Figure 6.1 panel F). It was inferred from the data that the average lab staffing was 2 PhD scientists, 3 technicians and 1-2 other staff members.

As to who operated the instruments, the majority of analyzers were operated by both users and SRL staff (58.1%) (Figure 6.2 panel A). A smaller percentage was operated by only user (37.7%) or only staff (4.2%) (Figure 6.2 panel A). This was not true for sorters, where 47.4% of sorters were operated by both user and staff, 44.9% operated by only staff while 7.7% of these were operated by only users (Figure 6.2 panel A). Imaging flow cytometers were predominantly operated by both user and staff (62.5%), while 25.0% of these were operated by only users and 12.5% operated by only staff (Figure 6.2 panel A). All of the four mass cytometers were staff-operated exclusively, probably due to the mass spectrometer aspect of the instrument (Figure 6.2 panel A). What these results clearly demonstrate is that the more complex the instrumentation the more likely it will be operated by a trained SRL staff.

To understand how instrument age and usage level affects personnel decisions, the respondents were asked specific questions related to their oldest, newest, and most used instruments in their SRL. Respondents indicated that majority of newer analyzers were operated by both user and staff (62.9%), while older analyzers were just as likely to be user operated (46.9%) as both user and staff operated (46.9%) (Figure 6.2 panel B). The most used analyzers in the facility were predominantly operated by both user and staff (64.3%) (Figure 6.2 panel B). It is evident from Figure 6.2 panel C that the newer analyzers were majorly being operated by both user and SRL staff.

When it came to newer sorters in the SRLs (Figure 6.2 panel D), they were primarily operated by both user and staff (65.4%), while a majority of older sorters were operated by staff only (52.8%). This difference is most likely due to the fact that manufacturers in the past few years have started to produce sorters that are designed to

require less adjustments and operator intervention. Of course, these types of sorters are not designed for overly complex sorts. Interestingly, the most used sorters were observed to be mainly staff-operated (56.2%), which may indicate that users prefer experienced SRL staff when it comes to sorting their samples even though this is associated with a higher cost. The distribution of user type vs. the year of purchase for sorters is depicted in Figure 6.2 panel E, which shows that the older sorters were predominantly staff-operated whereas the newer ones were operated by both users and staff.

Maintenance

The average annual maintenance costs for analyzers (from 138 responses), sorters (69 responses), imaging flow cytometers (5 responses) and mass cytometers (3 responses) were $14318, $25,328, $10,272, and $72,500 respectively (Table 6.5). When the annual maintenance costs were analyzed with respect to the year of purchase of instruments (Figure 6.3), it was evident that the newer analyzers and sorters (discerned from ten newest instruments), had a higher maintenance cost as compared to older instruments (discerned from ten oldest instruments). The average maintenance cost for ten newest and ten oldest analyzers were $12791.50 and $5168.2 respectively. The average maintenance cost for ten newest and oldest sorters were $26,141.90 and $16,637.80 respectively (Table 6.6). One plausible reason for this observation is that the cost of a service contract is tied to the price of instruments, thus more expensive newer instruments by default may have a higher annual service contract. Another possibility is that the newer instruments can perform more complex tasks resulting in higher repair costs.

The cost of maintenance in user-operated and staff-operated instruments were not observed to be significantly different (p-value > 0.05) in the case of both analyzers and

sorters. The average maintenance cost for user-operated, staff-operated and both user and staff-operated analyzers were seen to be $13,651, $14,860 and $15,742 respectively. The maintenance costs were $22,917, $22,772, and $21,780 for user-operated, staff-operated and both user and staff-operated sorters respectively (Table 6.7).

Analyzers with the highest usage in the SRLs were purchased between years 2004 and 2019 (average age = 6.5 years), while the most used sorters were purchased between 2003 and 2015 (average age = 10 years). The survey also indicated that 68.3% of newest analyzers, 41.1% of most used and 25% of older analyzers were under warranty/service contract. For sorters, 65.4% of newer instruments, 46.7% of most used and 22.2% older instruments were under warranty/service contract (Table 6.8). A lower percentage of older analyzers and sorters being under contract could potentially be attributed to manufacturers no longer offering service contracts for those models.

A majority of respondents had mentioned that they maintained their analyzers by involving Original Equipment Manufacturer (OEM) (62.9%) followed by in-house (institutional) staff (28.7%) and third-party service provider (8.3%). The same trend held true for sorters with 68.5% laboratories reporting OEM, 22.2% of them stating in-house staff and the remaining 9.3% respondents mentioning third-party service provider (Table 6.9). Interestingly, more in-house maintenance was observed for older analyzers and sorters, whereas more OEM maintenance was incorporated for newer analyzers and sorters (Figure 6.4). It’s reasonable to infer that older analyzers and sorters were likely maintained by in-house staff, as manufacturers no longer offered service contracts for them.

The annual maintenance cost for analyzers was $12,761 in facilities contracting with OEM, $10,772 with a Third-party service provider, and $3,189 when performed by in-house staff. The average annual maintenance costs for sorters were $21,199 using the OEM, $24200 with a Third-party service provider, and $8,289 when performed by in-house staff (Table 6.10). It was surprising to observe that using a third-party service provider did not provide significant cost savings compared to receiving service from the OEM. A reason for the lower cost associated with in-house service could be that the salary of the person providing the service, or labor charge is not being included in this cost, hence comparing the cost of in-house maintenance to that provided by an external vendor may not be an even comparison. The survey also aimed to find out if the in-house maintenance that costs less than OEM and third-party service provider results in a longer instrument wait time. It was inferred that the wait times for in-house were not significantly longer than OEM or Third-part maintenance as percentage of time an analyzer was waiting to be repaired was 4.7% for OEM, 9.0% for Third-party and only 4.2% for in-house maintenance. Similarly, the percentage of time a sorter was waiting to be repaired was 5.7% for OEM, 4.2% for Third-party and 5.5% for in-house maintenance. The p-values obtained from t-tests (p-value > 0.05) suggested that these differences in percent wait times were not statistically significant in the case of both analyzers and sorters (Table 6.10).

The average annual cost of consumables for analyzers, sorters, imaging flow cytometers and mass cytometers were observed to be $4,101 (from 105 entries), $5,555 (65 entries), $1,069 (6 entries) and $23,333 (3 entries) respectively. The fact that mass cytometers incurred the highest consumable costs is not surprising, given that they are a

combination of flow cytometry and mass spectrometer, which by itself has been known for its expensive operational costs.

The cost of consumables was also found to be higher for newer instruments (as per ten newest instruments) compared to older instruments (as per ten oldest instruments) in the case of both analyzers and sorters (Table 6.11). The average cost of consumables for the ten newest and ten oldest analyzers were $3750 and $955.9 respectively. The average cost of consumables for the ten newest and ten oldest sorters were $5392.9 and $3930.2 respectively.

An aspect the survey investigated was how frequently the laboratories schedule routine maintenance (preventative maintenance/staff maintenance). Respondents were given the following choices: monthly, every couple of months, twice a year and annually. Respondents indicated that typically a lab housing analyzers and/or sorters scheduled preventative maintenance twice a year (analyzers- 56.2% and sorters- 52.6%) as shown in Table 6.13. This observation was fairly consistent for instruments regardless of when the instrument was purchased (Figure 6.5).

Typically, flow cytometers undergo a brief daily cleaning at day's end or between users. In addition to this routine cleaning, manufacturers often advise a more thorough and extensive cleaning (referred to as deep cleaning) every month or two. The survey queried about the deep cleaning of the instruments. Respondents indicated that a majority of facilities performed deep cleaning of analyzers, sorters and imaging flow cytometers (Figure 6.6) on a monthly basis (analyzers- 48.8%, sorters- 44.7%, imaging flow cytometers- 71.4%). In addition, the quality control (QC) was primarily performed on a daily basis for analyzers (62.1%) and sorters (65.8%) as shown in Figure 6.7.

Survey respondents were asked to provide information about common reasons to perform instrument maintenance (Figure 6.8). The most common reasons for performing non-routine/scheduled maintenance on analyzers were failure to pass quality control (24.6%) and to ensure an acceptable coefficient of variation (CV) value (24.1%) followed by clogging (14.9%), high background (11.4%) and low instrument sensitivity (10.6%). An acceptable CV value is very critical to ensure reproducibility of flow cytometry results particularly when results are important for medical diagnosis. The common reasons for performing non-routine/scheduled maintenance on sorters were similar to the reasons for analyzers with the additional reason of contamination issues (15.4%). Maintaining cleanliness in a sorter is essential because often the cells returned to the researcher are cultured or injected into animals.

The survey was also designed to query about what were the likely reasons for replacing an instrument (Figure 6.9). The following options were provided: instrument no longer serviced by company/keeps having issues/too few features/users' needs have changed/not upgradeable/other. The most common reason that facilities considered for replacing an analyzer was because the manufacturer was no longer going to service the instrument (27.1%). Other common reasons included users' needs had changed (19.6%), instrument kept having issues (18.2%), and that their instrument was not upgradeable (14.6%). A similar trend was observed in the case of sorters with the most common reasons for instrument replacement being instrument no longer serviced by the company (31.5%), users' needs had changed (21.3%), instrument kept having issues (21.3%) and instrument was not upgradeable (15.8%).

Instrument Usage

To get a better understanding of instrument uptime (available time) vs. used time, the survey asked respondents what percent of time the instrument was out of service waiting to be repaired, percent of time the instrument was unavailable for use due to routine maintenance, and percent of time the instrument was actually used. The answers were based on the past year (2019).

The percent of instrument uptime for analyzers averaged to 91.4% with the remaining 4.6% of the time being out of service waiting to be repaired and 4.1% of the time unavailable for use due to routine maintenance. While there was no significant variation in instrument uptime over the years, it was interesting to note that older instruments purchased between 1980 and 1995 demonstrated an average instrument uptime of around 90% (data not shown). The comparison between the operational time of user and staff-operated instruments (Table 6.16 panel A) indicated that the percent uptime for user-operated analyzers was higher (92.5%) than for analyzers operated by both user and staff (87.9%). The statistical difference between the data was confirmed by performing an un-paired t-test (p-value = 0.0052). This may indicate the significance of regular maintenance, as well as the potential influence of user training, and the guidance provided to users regarding the operation of the instruments. The survey indicated that the percent of time the instruments were out of service as well as unavailable for use due to routine maintenance were 3.63% and 3.66% respectively for user-operated analyzers, whereas 5.4% and 3.4% respectively for staff-operated analyzers. Finally, analyzers operated by both user and staff were 4.7% of the time out of service, and 5.14% of the time occupied to perform routine maintenance.

The average operable time for sorters was observed to be 89.5%, with the remaining 5% of the time being out of service waiting to be repaired and 5.7% of the time unavailable for use due to their routine maintenance. Similar to the trend discerned in the case of analyzers, the uptime of newer sorters were comparable to the oldest sorters (purchased between 1995 and 2000) that provided around 88% instrument uptime (data not shown). The operational time for user-operated, staff-operated and both user and staff-operated instruments (Table 6.16 panel B) were comparable (91.7%, 88% and 88.8% respectively). The percent of time the user-operated sorters were out of service as well as unavailable for use due to routine maintenance were 3.3% and 5.0% respectively, they were 5.4% and 6.5% respectively for staff-operated sorters and were 6.4% and 5.7% respectively for both user and staff-operated instruments. The instruments' availability, duration of it being out of service and occupied for routine maintenance were quite similar between analyzers and sorters.

Funding Source

The last section of the survey dealt with sources of funds used to purchase instruments in Flow Cytometry SRLs. Respondents indicated that the majority of facilities used in-house (institutional) funds (57.3%) followed by government instrumentation grant (15.2%), government research grant (12.8%), and private foundation (6.7%) among others (7.9%) to purchase their analyzers (Figure 6.10 panel A). There was a similar distribution of funding source for sorters (Figure 6.10 panel B), imaging flow cytometers (Figure 6.10 panel C) and mass cytometers (Figure 6.10 panel D). 55.3% of sorters were funded by in-house funds, 23.7% by government instrumentation grant, 13.2% by government research grant, 5.3% by private foundation

and 2.6% from other funding sources. The SRLs using an imaging flow cytometer (7 responses) obtained their funding from in-house funds (42.9%) and government instrumentation grant (42.9%), followed by government research grant (14.3%). The 4 respondents with mass cytometers in there SRL indicated that in-house funds (50%) were most frequently used to purchase the instrument followed by government instrumentation grant (25%) and other funding sources (25%).

Respondents residing in the United States were queried if the instruments were specifically purchased using NIH shared instrumentation grant (NIH S10 award) or NIH high-end instrumentation grant. The majority of survey respondents who used the US government funds to acquire their instruments purchased their analyzers (94.3%) and sorters (80%) using NIH S10 award (Figure 6.10 panels E and F). Overall, 27% of all flow cytometers in the US SRLs were funded by NIH S10 award (25% of analyzers and 34% of sorters). In addition, 14.4% of all analyzers and 17.8% of all sorters used by respondents from across the world were funded by NIH S10 award. The survey data suggested that the number of flow cytometers funded by NIH S10 award seemed to have increased from 1996 to 2020 (Figure 6.11) revealing the increasing reliance of core labs on S10 award to purchase the instruments, and the importance of NIH S10 award in facilitating cutting-edge research in flow cytometry SRLs. Data has been reported from 1996 to 2020 due to fewer responses about instruments purchased prior to 1996 (Table 6.18). The average annual NIH S10 budget that was allocated for the purchase of flow cytometers between 2014 and 2021 was $4,257,880 (determined from NIH Office of Research Infrastructure Programs data).[229] This represented 5% of the total annual budget allocated for various instrument types. Flow cytometers comprised 7% of all funded

instruments. The annual budget and number of instruments funded by NIH S10 award between 2014 and 2021 are listed in Table 6.19. With continued budget allocation by NIH to purchase flow cytometers in the recent years, and an overall increase in number of flow cytometers being funded by NIH S10 grant from 1996 to 2020, we believe that the S10 award will continue to support core SRLs in the future in procuring state-of-the-art flow cytometers and expanding flow cytometry core labs across the US.

Conclusions

An independent online survey was created to acquire comprehensive information about SRLs that use Flow cytometers (analyzers, sorters, imaging flow cytometers and mass cytometers). Survey achieved participation from 14 countries across 4 continents, primarily from core facility directors and managers working in universities, private institutions and companies. The majority of analyzers in SRLs were operated by both user and staff. Older analyzers were often user-operated or both user and staff operated. Both user and staff operation were also common for sorters, but the most used sorters were observed to be mainly staff-operated, suggesting a preference for experienced SRL staff. Recent sorters were mainly operated by both users and staff (65.4%), with older sorters largely operated by staff (52.8%), likely due to the emergence of sorter designs that require less operator involvement in recent years. Similarly, imaging flow cytometers were primarily operated by both users and staff, while all mass cytometers were exclusively staff-operated likely due to their mass spectrometry aspect of the instrument.

Maintenance costs varied by instrument type, with an average annual cost of $14,922 for analyzers, $25,328 for sorters, $10,271 for imaging flow cytometers, and $72,500 for mass cytometers. Newer analyzers and sorters incurred higher maintenance

expenses that may be attributed to service contract costs being tied to instrument prices, resulting in higher annual costs for newer and more expensive instruments. The survey indicated that a significant portion of the newest analyzers (68.3%) and sorters (65.4%) were under warranty or service contracts. A lower percentage of older analyzers and sorters being under contract could potentially be due to manufacturers discontinuing service contracts for older models. Most respondents depended on the OEM for maintenance. Older analyzers and sorters had more in-house (institutional) maintenance, while newer ones relied on the OEM. The study found that the cost to service analyzers and sorters through OEM was not observed to be significantly higher than contracting with a third-party service provider. The survey also checked if affordable in-house maintenance caused longer instrument wait times. Results showed that in-house maintenance wait times were comparable to OEM or third-party maintenance. It was also found that typically a lab housing analyzers and/or sorters scheduled preventative maintenance twice a year regardless of instrument's purchase date. Most facilities conducted monthly deep cleaning and daily quality control for their analyzers, sorters, and imaging flow cytometers. Further, survey respondents indicated that the common reasons for performing non-routine maintenance on analyzers and sorters included addressing quality control failures and maintaining acceptable CV values among others. The survey also revealed that the common reasons for instrument replacement included manufacturer's discontinuing service, evolving user needs, persistent issues with the instrument, and lack of upgradeability. The average uptime was 91.4% for analyzers and 89.5% for sorters, with older instruments from 1980 to 2000 still being operable (analyzers = 90%, sorters = 88%). No noticeable differences in downtime were found

between user-operated and staff-operated instruments. This suggested the significance of routine maintenance and the potential influence of user training and guidance in instrument usage.

The survey queried about funding sources for instrument purchase in Flow Cytometry SRLs. In-house funds were commonly used. Further, it was observed that the analyzers and sorters used by respondents in the US were predominantly supported by NIH S10 award, suggesting that the NIH S10 grant program greatly contributed to advancing research in these labs. Due to consistent budget allotment from NIH for acquiring flow cytometers, along with a general rise in the number of flow cytometers funded through NIH S10 award between 1996 and 2020, we believe that the S10 award will continue supporting core SRLs in the future. This support will enable the procurement of cutting-edge flow cytometers and further expansion of core labs across the United States. We anticipate that the outcomes presented in this study will serve as a valuable resource for establishing a core lab, along with aiding in the long-term planning and management of core lab operations.

Acknowledgements

The authors gratefully acknowledge The Association of Biomolecular Resource Facilities and Ken Schoppmann for sharing the online survey on SurveyMonkey. We would also like to thank the scientific community for their contributions to the data collected for this study.

(A)

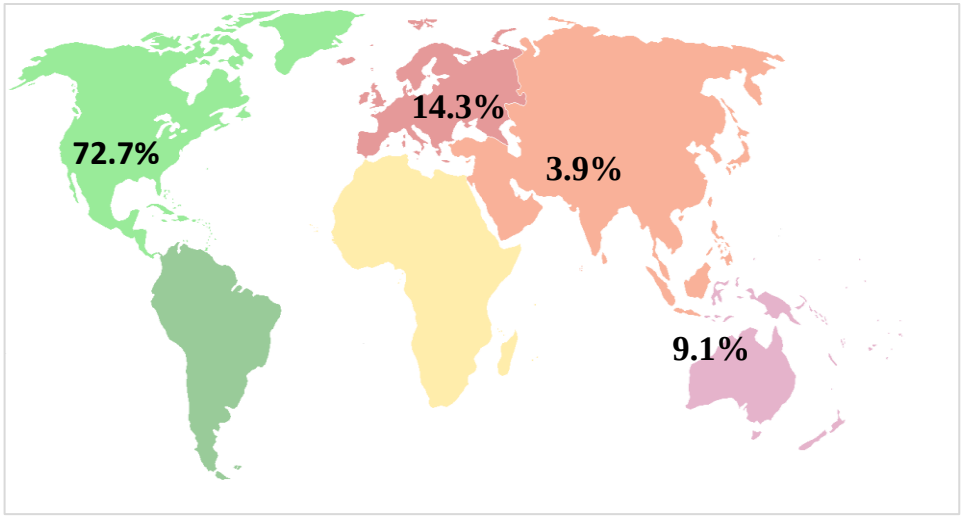
72.7%
14.3%
3.9%
9.1%

(B)

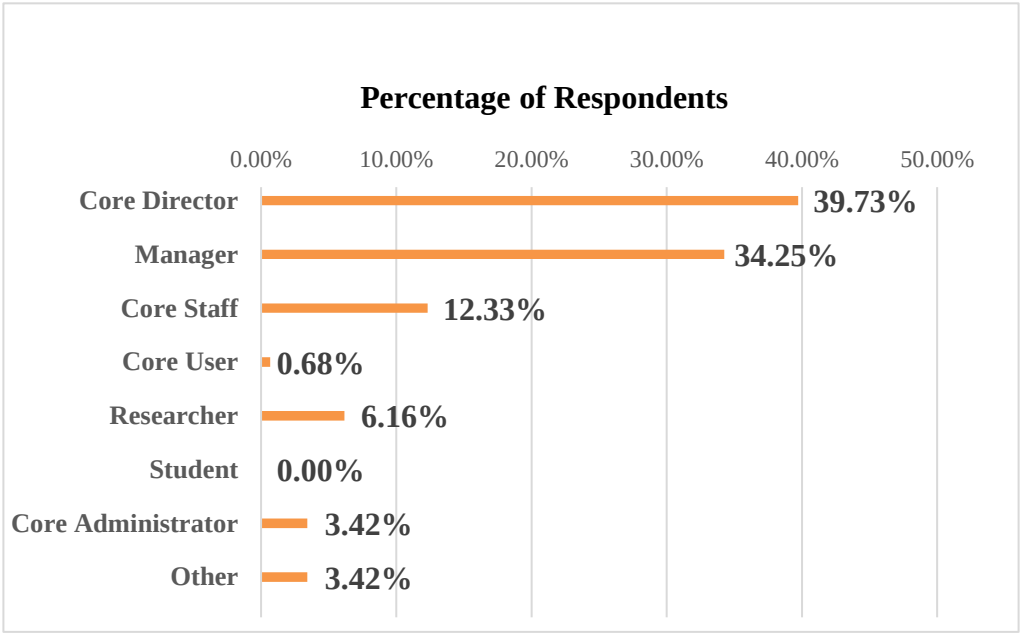
Percentage of Respondents
0.00%
10.00%
20.00%
30.00%
40.00%
50.00%
Core Director
39.73%
Manager
34.25%
Core Staff
12.33%
Core User
0.68%
Researcher
6.16%
Student
0.00%
Core Administrator
3.42%
Other
3.42%

(C)

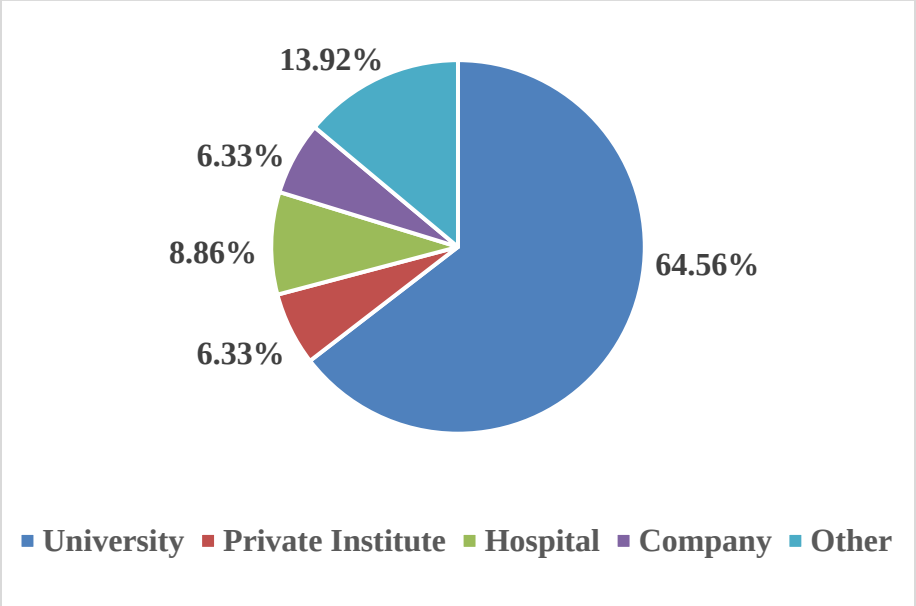
13.92%
6.33%
8.86%
64.56%
6.33%
University
Private Institute
Hospital
Company
Other

(D)

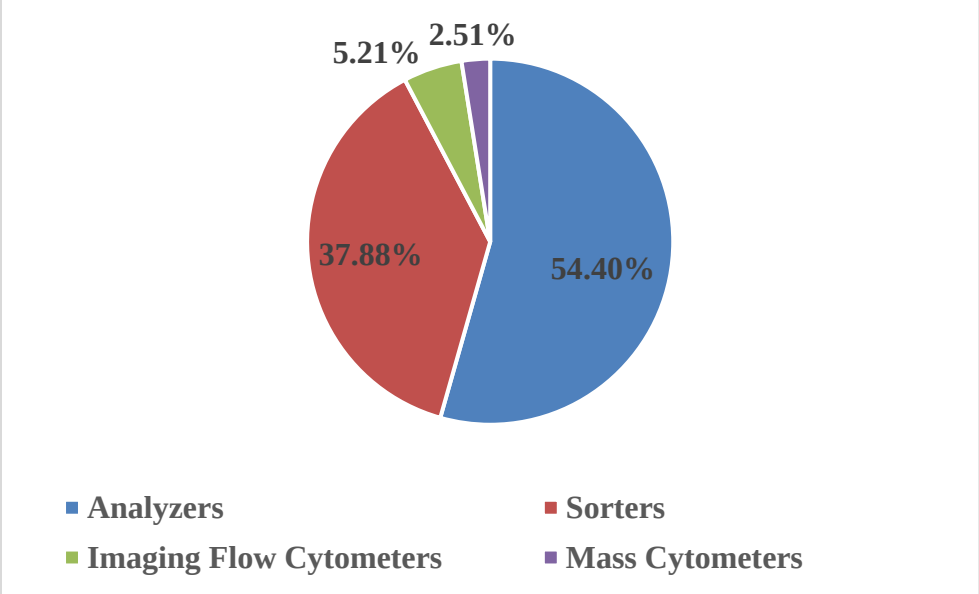
5.21%
2.51%
37.88%
54.40%
Analyzers
Sorters
Imaging Flow Cytometers
Mass Cytometers

(E)

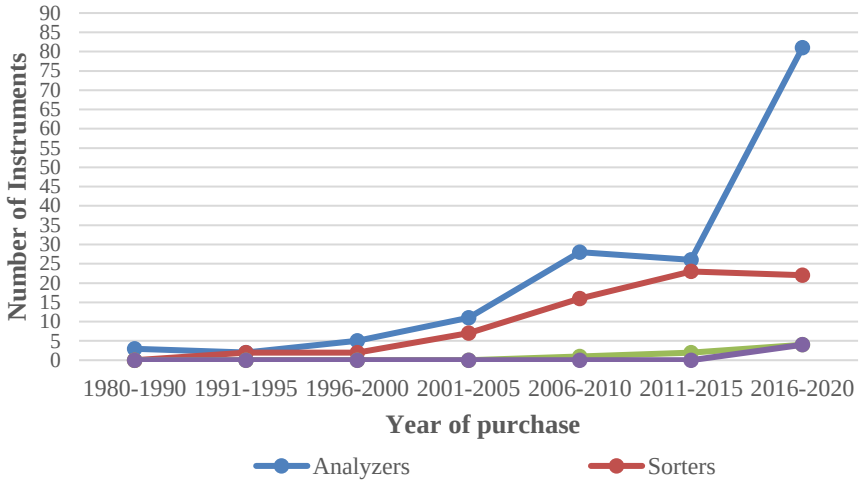

(F)

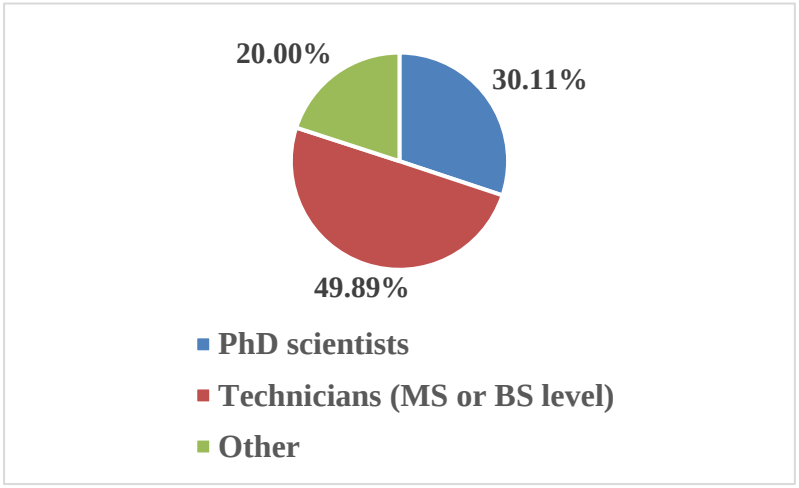

Figure 6.1: (A) Demographic information of the respondents that spanned across four continents (from 77 responses). **(B)** depicts the job title of the respondents (146 responses). The type of institution (from 79 responses) that respondents were associated with are represented in **(C)**. Most respondents were core directors and managers from universities and hospitals among others. **(D)** depicts the types of instruments that were taken into consideration such as analyzers, sorters, imaging flow cytometers and mass cytometers. **(E)** shows the year of purchase of different instruments, and **(F)** depicts institution staffing such as PhD scientists, technicians, and others.

(A)

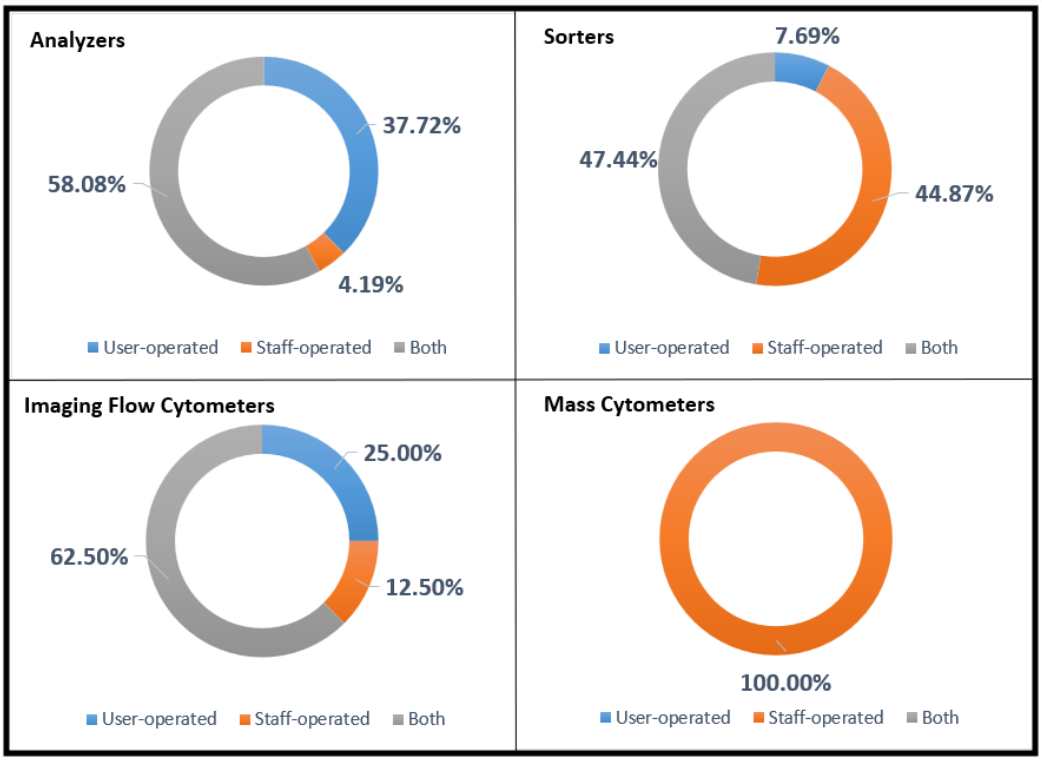
Analyzers
37.72%
58.08%
4.19%
User-operated
Staff-operated
Both
Sorters
7.69%
47.44%
44.87%
User-operated
Staff-operated
Both
Imaging Flow Cytometers
25.00%
62.50%
12.50%
User-operated
Staff-operated
Both
Mass Cytometers
100.00%
User-operated
Staff-operated
Both

(B)

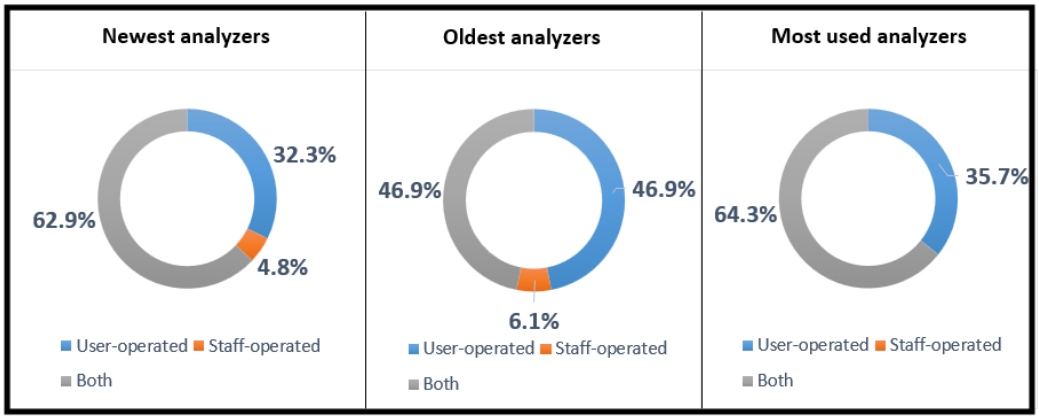
Newest analyzers
32.3%
62.9%
4.8%
User-operated
Staff-operated
Both
Oldest analyzers
46.9%
46.9%
6.1%
User-operated
Staff-operated
Both
Most used analyzers
35.7%
64.3%
User-operated
Staff-operated
Both

(C)

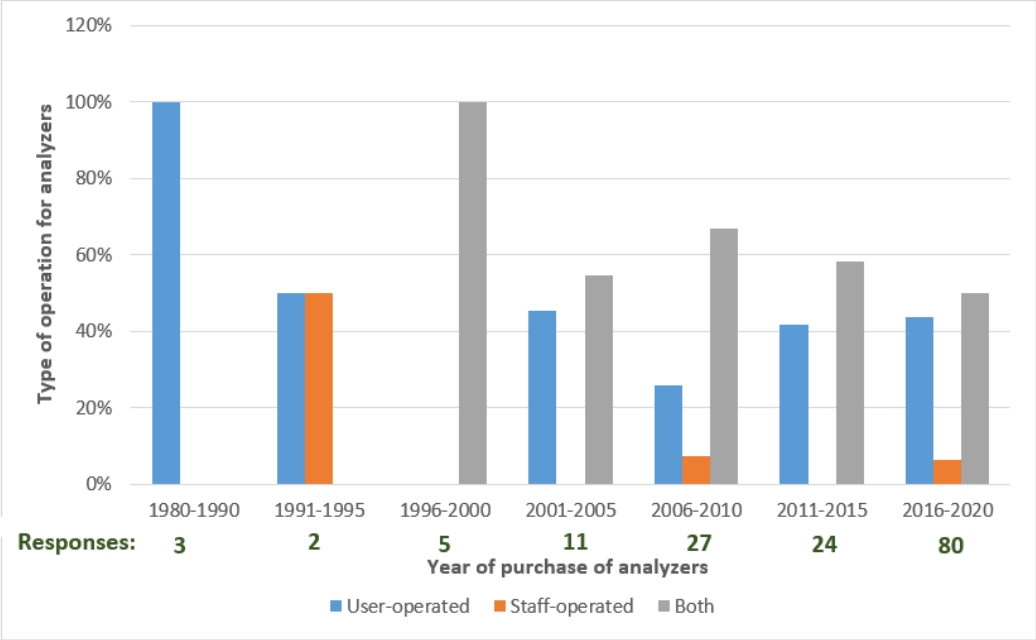
120%
100%
80%
60%
40%
20%
0%
Type of operation for analyzers
1980-1990
1991-1995
1996-2000
2001-2005
2006-2010
2011-2015
2016-2020
Responses:
3
2
5
11
27
24
80
Year of purchase of analyzers
User-operated
Staff-operated
Both

(D)

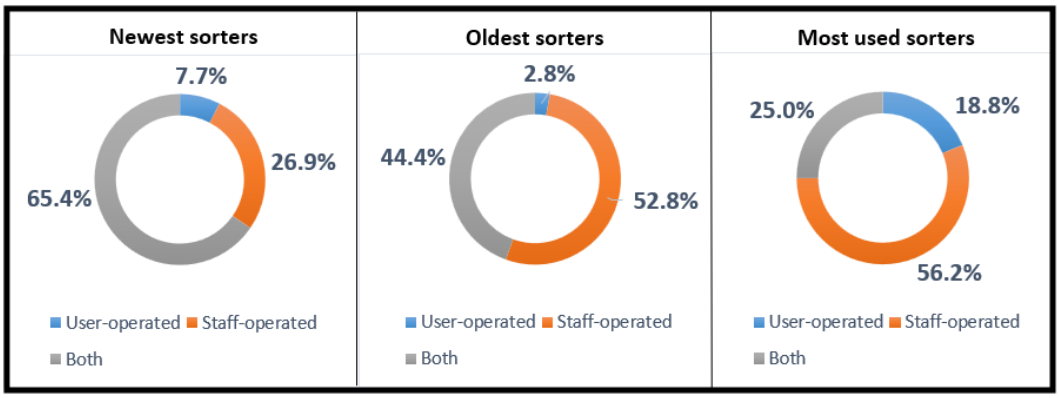
Newest sorters
7.7%
26.9%
65.4%
User-operated
Staff-operated
Both
Oldest sorters
2.8%
44.4%
52.8%
User-operated
Staff-operated
Both
Most used sorters
25.0%
18.8%
56.2%
User-operated
Staff-operated
Both

(E)

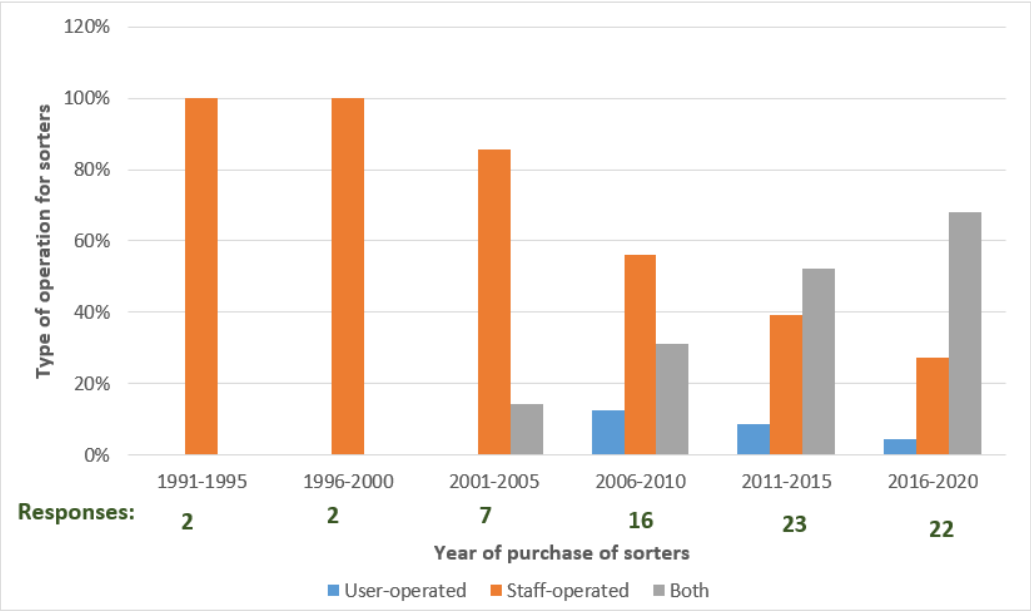

Figure 6.2: (A) Type of operation for analyzers (167 responses), sorters (78 responses), imaging flow cytometers (8 responses) and mass cytometers (4 responses). A majority of analyzers, sorters and imaging flow cytometers were operated by both user and staff whereas all 4 mass cytometers were operated by staff members. **(B)** shows the instrument usage of newest, oldest and most used analyzers. **(C)** depicts the type of operation vs. year of purchase of analyzers. Newer analyzers were majorly being operated by both user and SRL staff. **(D)** shows instrument usage of newest, oldest, and most used sorters and **(E)** depicts type of operation such as user-operated, staff-operated or both user and staff operated vs. year of purchase of sorters. Older sorters were predominantly staff-operated whereas the newer ones were operated by both users and staff.

(A)

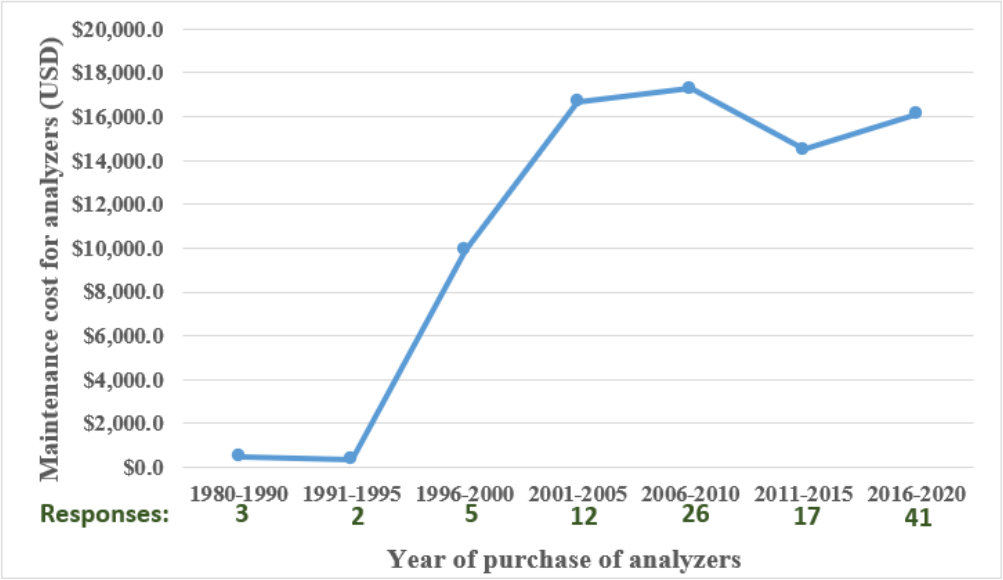

(B)

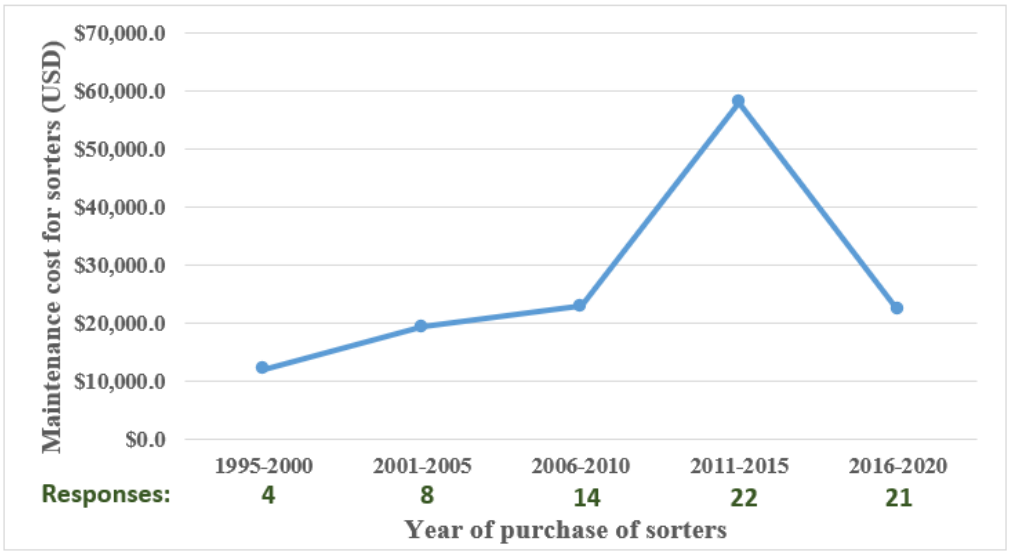

Figure 6.3: Maintenance cost vs. year of purchase of **(A)** analyzers and **(B)** sorters. All monetary data has been converted to US currency to facilitate comparisons between countries. Overall, the newest analyzers and sorters costed more in maintenance as compared to oldest analyzers and sorters.

(A)

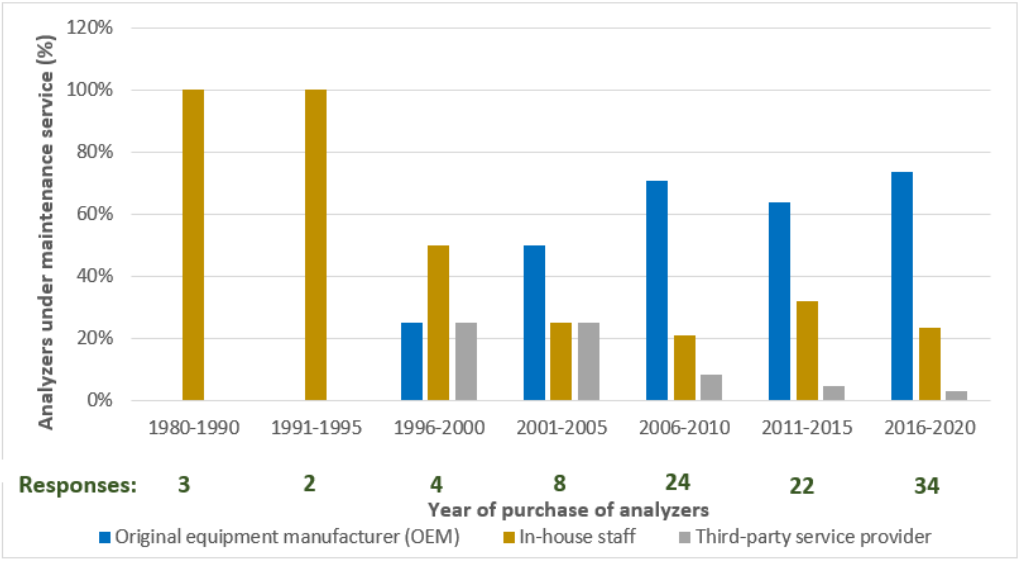

(B)

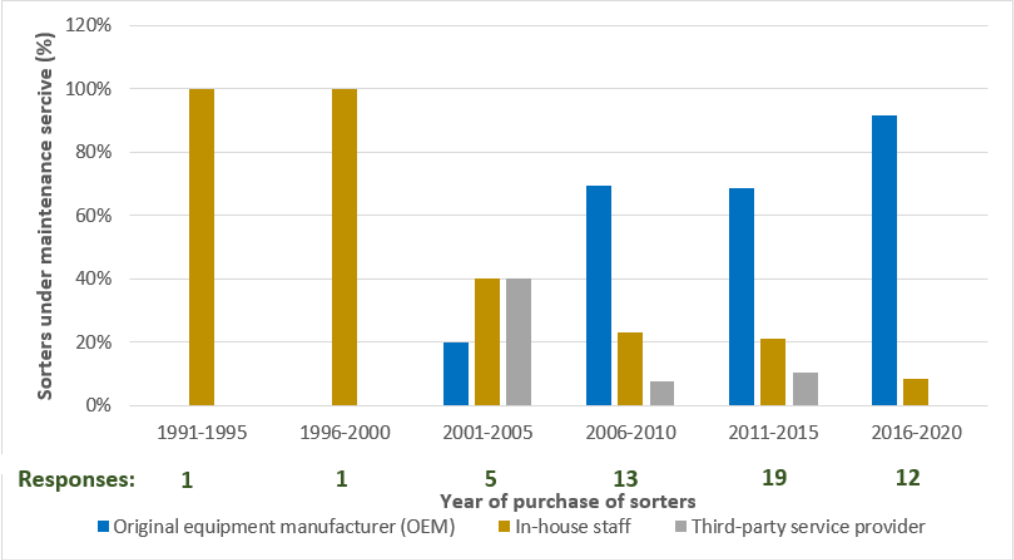

Figure 6.4: Type of maintenance service such as Original Equipment Manufacturer (OEM), in-house (institutional) and third-party service provider vs. year of purchase of **(A)** analyzers and **(B)** sorters. In-house maintenance was majorly observed for older analyzers and sorters, whereas OEM maintenance was predominantly incorporated for newer analyzers and sorters.

(A)

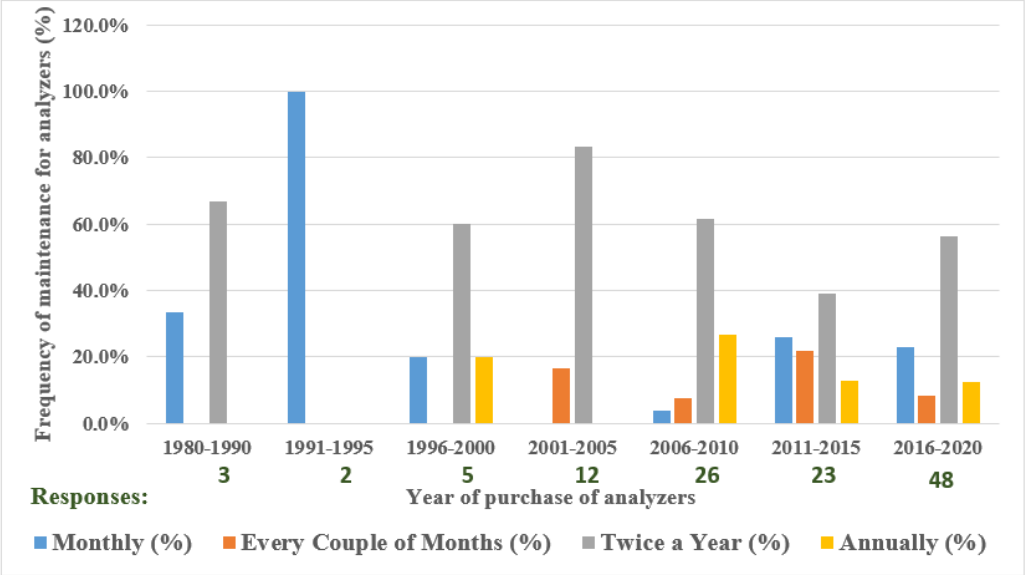

(B)

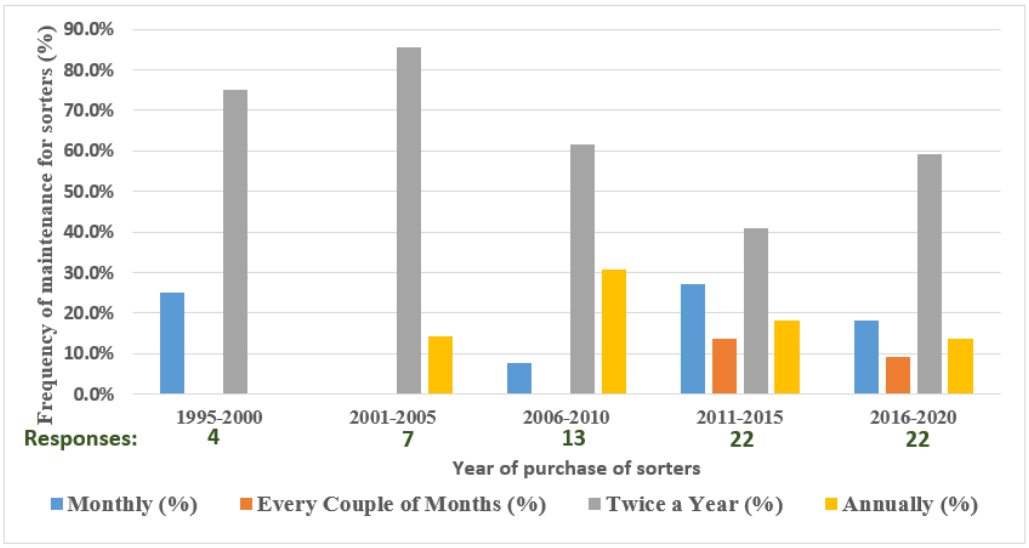

Figure 6.5: Frequency of maintenance vs. year of purchase of **(A)** analyzers and **(B)** sorters. Typically, a lab housing analyzer and/or sorter scheduled preventative maintenance twice a year regardless of when the instrument was purchased.

(A)

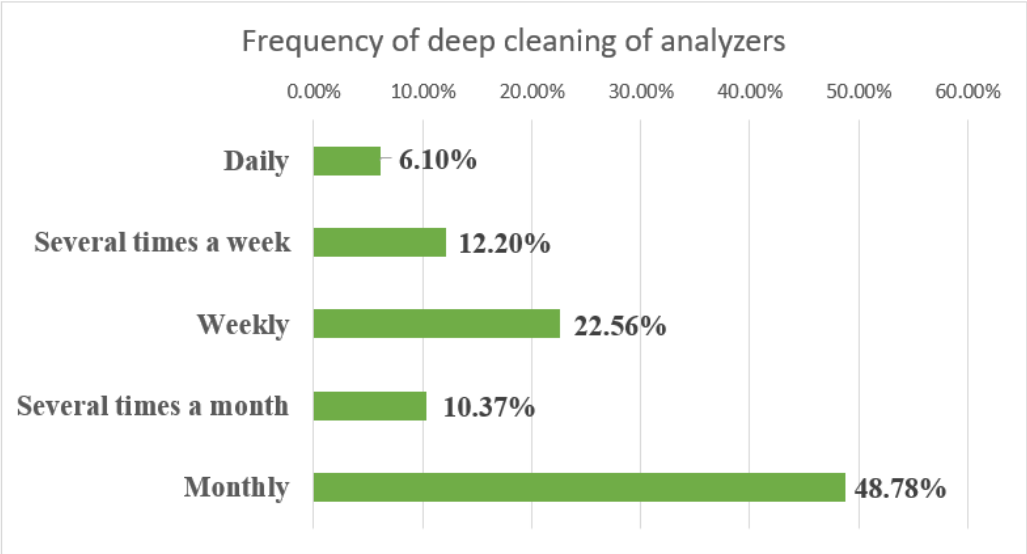
Frequency of deep cleaning of analyzers
0.00%
10.00%
20.00%
30.00%
40.00%
50.00%
60.00%
Daily
6.10%
Several times a week
12.20%
Weekly
22.56%
Several times a month
10.37%
Monthly
48.78%

(B)

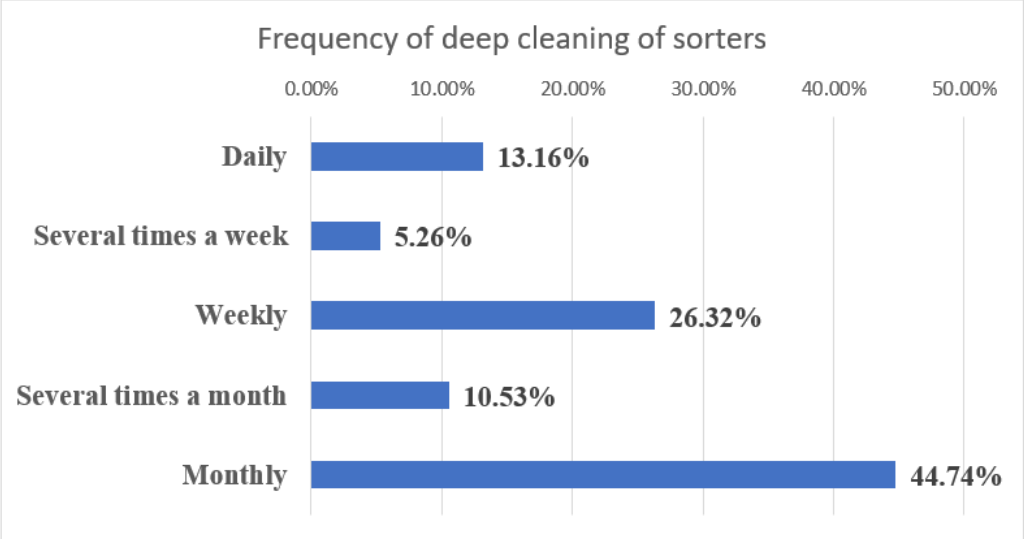
Frequency of deep cleaning of sorters
0.00%
10.00%
20.00%
30.00%
40.00%
50.00%
Daily
13.16%
Several times a week
5.26%
Weekly
26.32%
Several times a month
10.53%
Monthly
44.74%

(C)

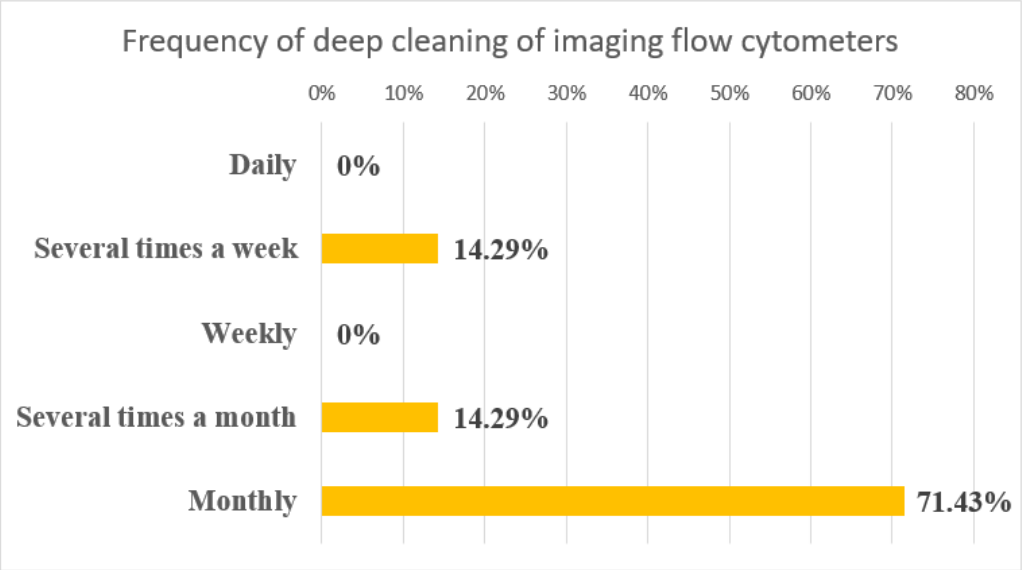

Figure 6.6: Frequency of deep cleaning of **(A)** analyzers, **(B)** sorters and **(C)** imaging flow cytometers. A majority of facilities performed deep cleaning of their analyzers, sorters and imaging flow cytometers on a monthly basis.

(A)

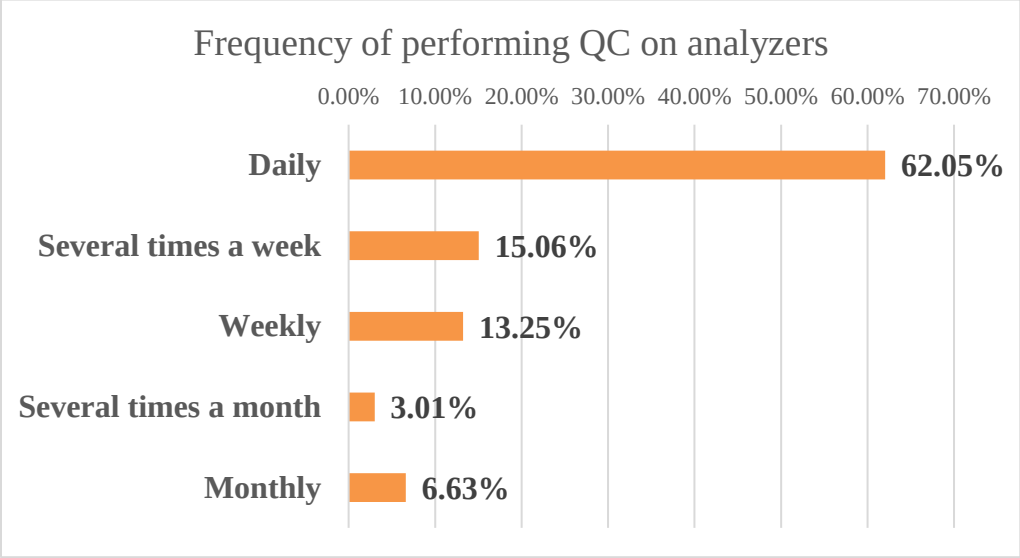

(B)

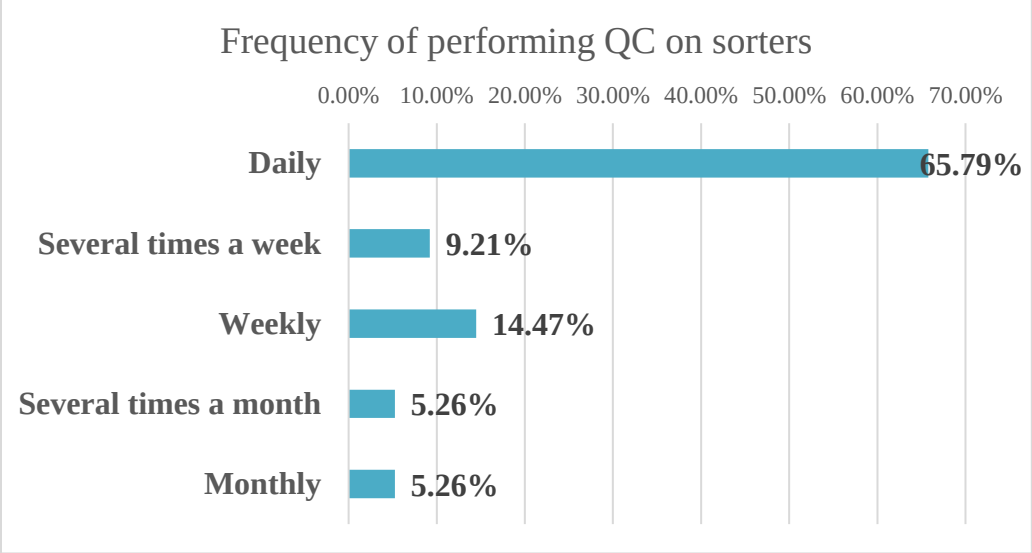

Figure 6.7: Frequency of performing quality control (QC) on **(A)** analyzers and **(B)** sorters. The quality control was primarily performed on a daily basis for analyzers and sorters.

(A)

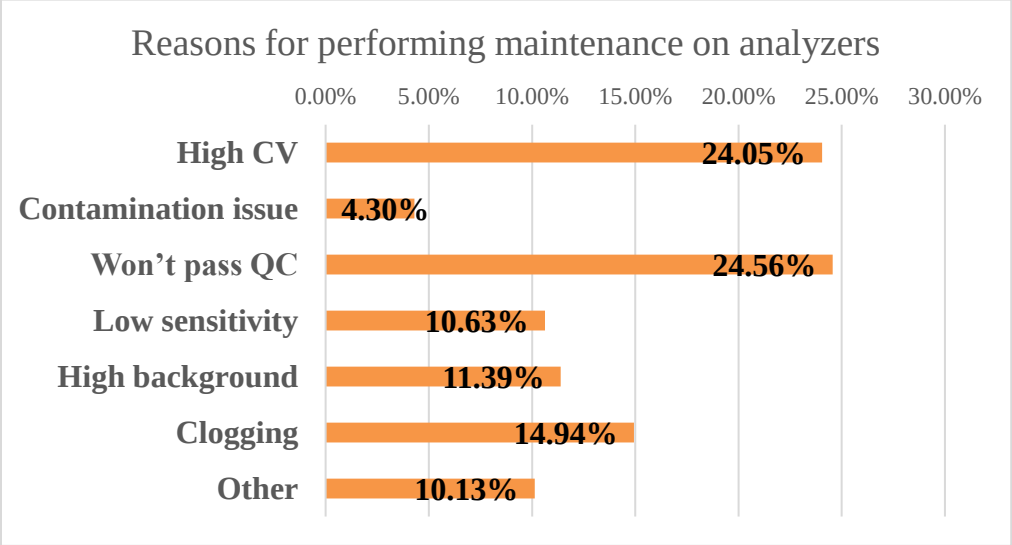

(B)

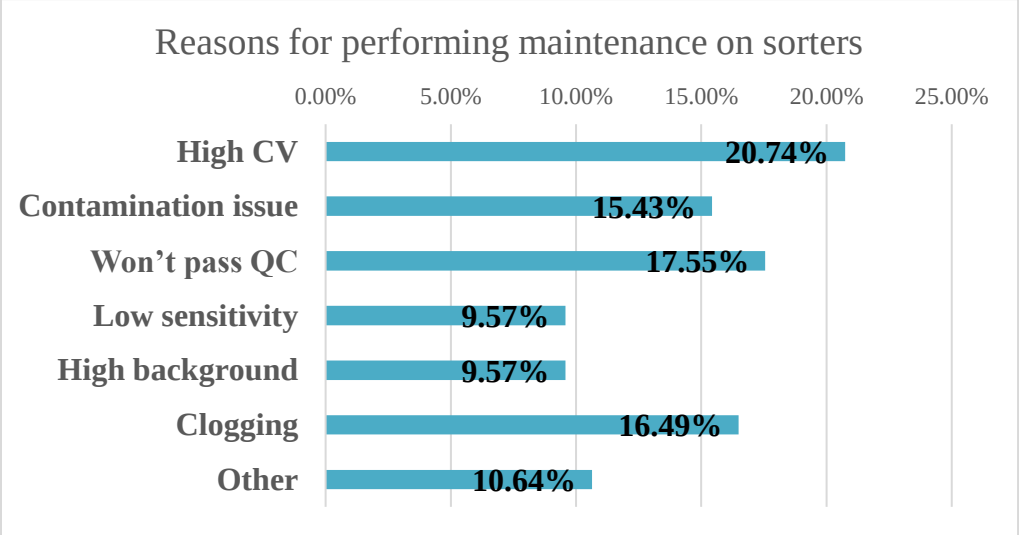

Figure 6.8: Reasons why SRLs typically perform maintenance on **(A)** analyzers and **(B)** sorters. The most common reasons for performing non-routine/scheduled maintenance on analyzers and sorters were failure to pass quality control, to ensure an acceptable coefficient of variation (CV) value and due to clogging.

(A)

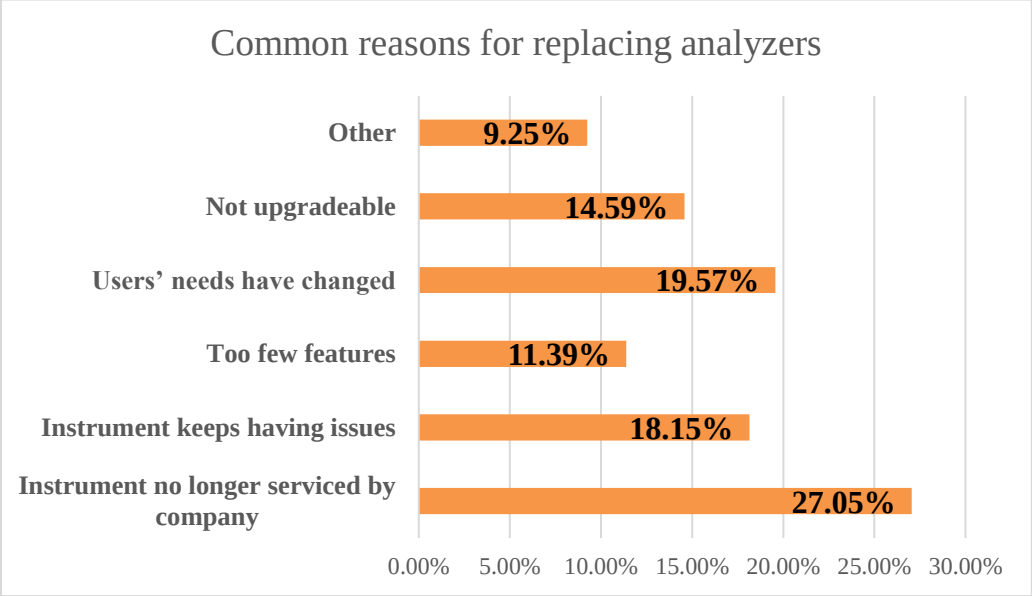

(B)

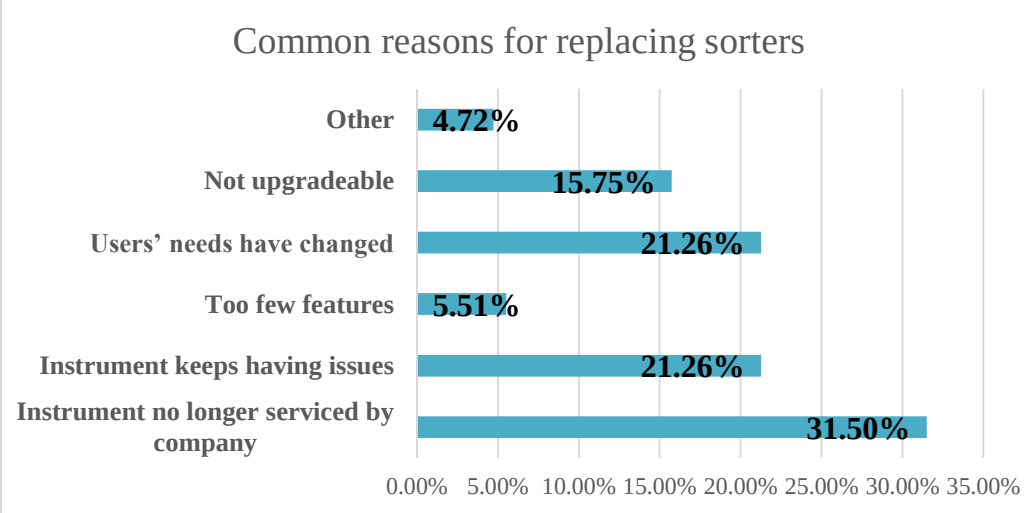

Figure 6.9: Common reasons for replacing **(A)** analyzers and **(B)** sorters in SRLs. The probable reasons for replacing an analyzer and sorter were because the instrument was no longer serviced by the manufacturer, users' needs had changed and due to instrument consistently experiencing issues.

(A)

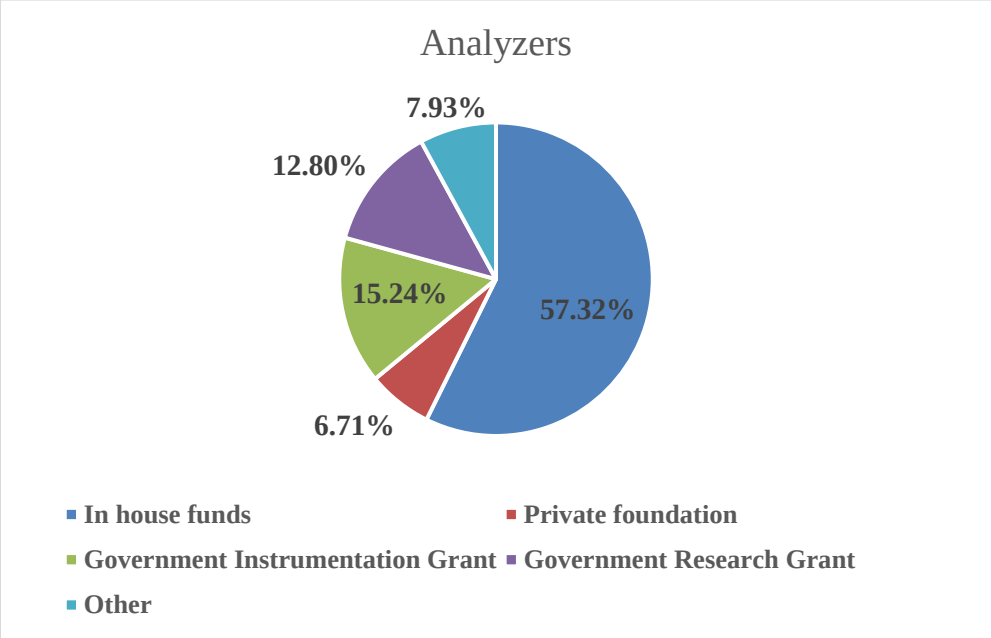
Analyzers
7.93%
12.80%
15.24%
57.32%
6.71%
In house funds
Private foundation
Government Instrumentation Grant
Government Research Grant
Other

(B)

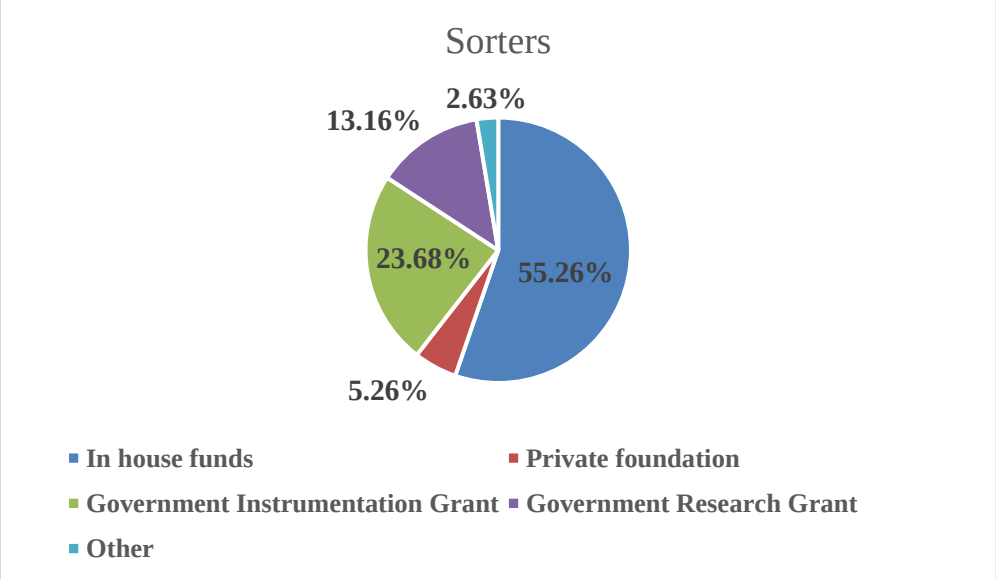
Sorters
2.63%
13.16%
23.68%
55.26%
5.26%
In house funds
Private foundation
Government Instrumentation Grant
Government Research Grant
Other

(C)

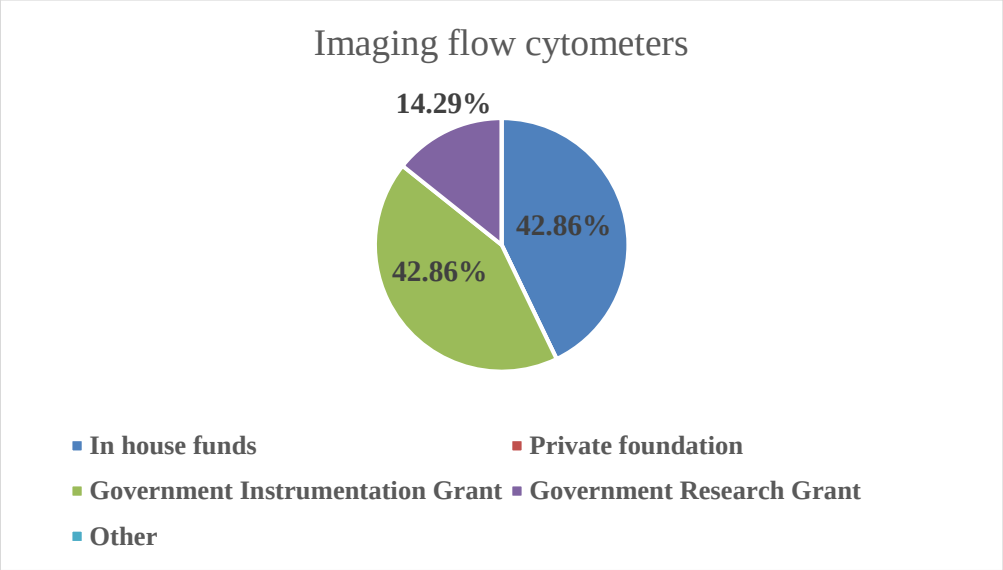
Imaging flow cytometers
14.29%
42.86%
42.86%
In house funds
Private foundation
Government Instrumentation Grant
Government Research Grant
Other

(D)

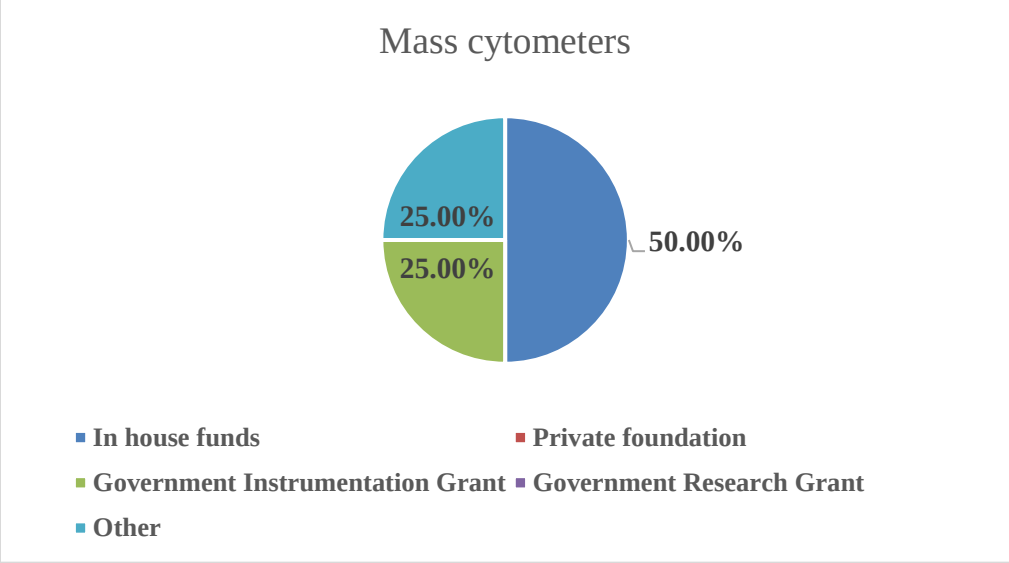
Mass cytometers
25.00%
25.00%
50.00%
In house funds
Private foundation
Government Instrumentation Grant
Government Research Grant
Other

(E)

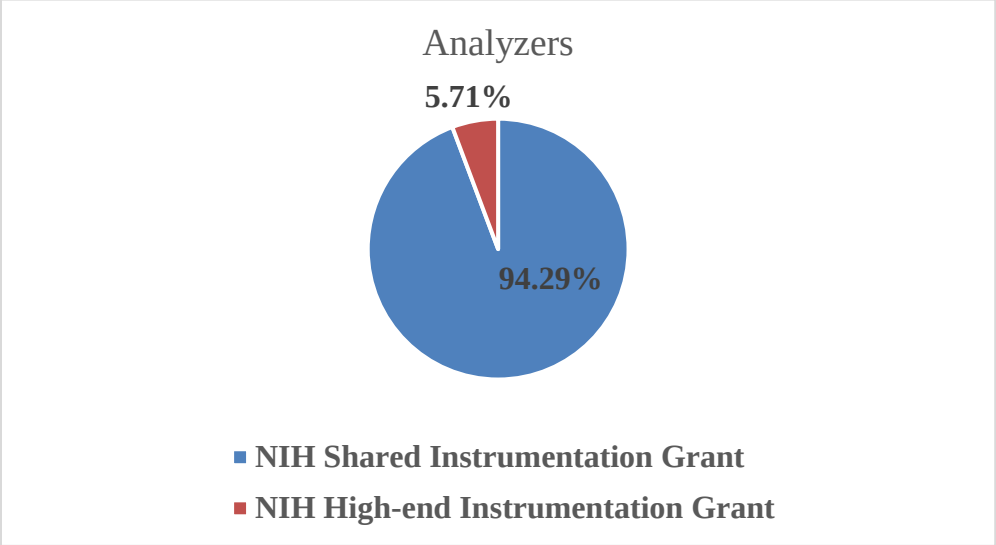

(F)

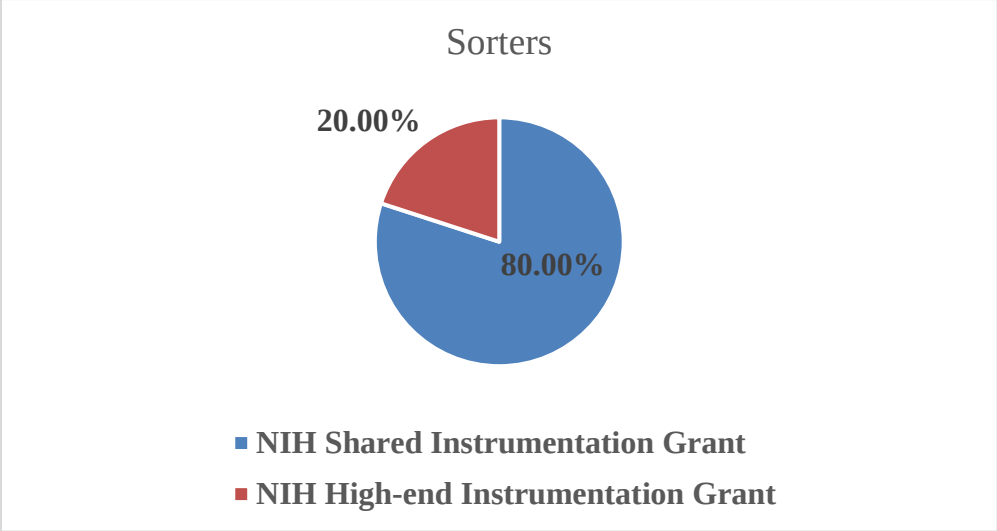

Figure 6.10 Sources of funding for **(A)** analyzers, **(B)** sorters, **(C)** imaging flow cytometers and **(D)** mass cytometers. The most common source of funding was observed to be in-house funds followed by government instrumentation grant among other sources. Additionally, NIH instrumentation grant information for **(E)** analyzers and **(F)** sorters are shown. Most US survey participants who utilized government funds to buy analyzers and sorters obtained them through the NIH S10 shared instrumentation grant.

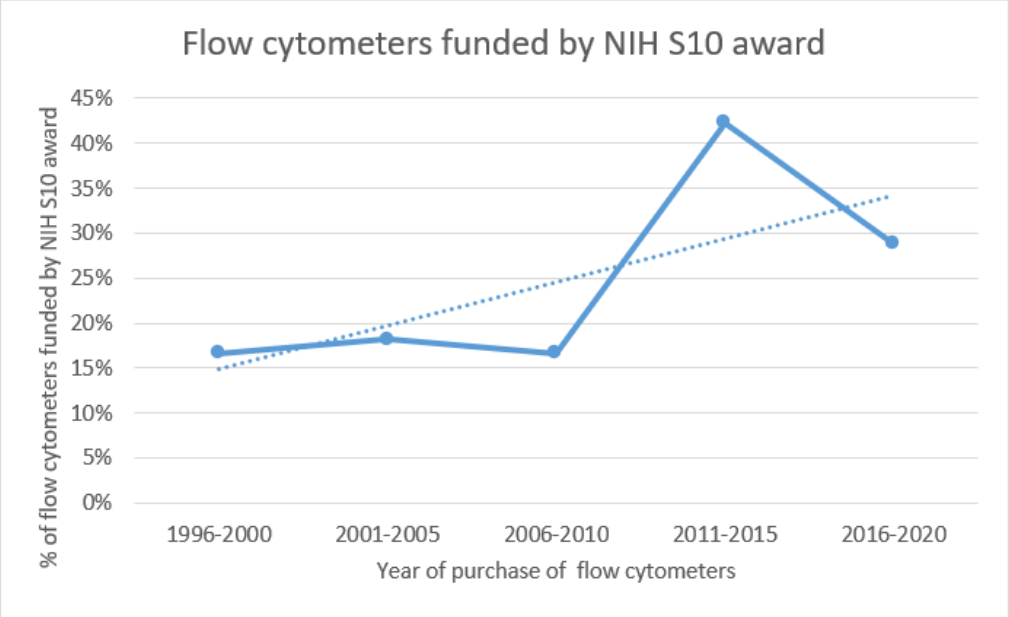

Figure 6.11: Percentage of flow cytometers in the US SRLs that were purchased using NIH S10 award. Data has been shown for flow cytometers purchased between 1996 and 2020 as fewer responses were obtained for flow cytometers acquired prior to 1996. An overall increase in the number of flow cytometers funded by NIH S10 award was observed from 1996 to 2020.

Table 6.1

Survey questions

Question	Description
General Questions:	
1a)	What is your job title? [Choices: Core Director/Manager/Core Staff/Core User/Researcher/Student/Core Administrator]
1b)	What is your primary field of work? [Short answer]
1c)	What is the staffing in your core facility/lab/company? PhD scientists (#) = Technicians (MS or BS level) (#) = Other (#) =
1d)	Where is your lab located? [Choices: University/Company/Private Institute/Hospital/Other]
1e)	Are you a member of ABRF (Association of Biomolecular Resource Facilities)? (Y/N) If not, enter your email address if you would like information about ABRF.
1f)	Enter the number of each of these instruments you have in your lab: Analytical flow cytometers - Sorters - Imaging flow cytometers - Mass cytometers –
Instrumentation:	
To gain a better understanding of the types of instruments used, the next set of questions will be broken apart into three categories: ‘Newest’, ‘Oldest’, and	

'Most Used' instrument. If your instrument falls into two categories, please answer based on the length of time the instrument is most occupied.	
2.	**For your Newest instrument:**
2a)	Type of instrument: [Choices: Analyzer/Sorter/Imaging flow cytometer/Mass cytometer]
2b)	Vendor:
2c)	Model:
2d)	Year of purchase:
2e)	Is the instrument user-operated or staff-operated or both? Please mention the percentage time for each.
2f)	Is the instrument under warranty? (Y/N) If yes, skip question (g)
2g)	How do you maintain your instrument? [Choices: In-house staff/Original Equipment Manufacturer (OEM)/Third-party service provider/Multi-vendor service provider]
2h)	How much is the average maintenance cost for the instrument? (i.e., the cost of service contract and parts if that is how you maintain your instrument)
2i)	How often do you schedule routine maintenance (preventative maintenance/staff maintenance)? [Choices: monthly, every couple of months, twice a year, yearly]
2j)	How often do you perform deep cleaning of the instrument? [Choices: daily/several times a week/weekly/several times a month/monthly]
2k)	How often do you perform quality control? [Choices: daily/several times a week/weekly/several times a month/monthly]

2l)	When do you expect the instrument to be replaced?
2m)	What is/are the likely reason(s) for replacing the instrument (check all that applies): [Choices: Instrument no longer serviced by company/keeps having issues/too few features/users' needs have changed/not upgradeable/Other]
2n)	What is the approximate annual cost for consumables such as for sheath fluids, filters, tubing, QC beads, probes, fluid tanks etc.?
2o)	Where were the funds for this instrument obtained from? [Choices: In-house funds/private foundation/government instrumentation grant/government research grant/other] Do you live in the US? If yes, then was this specifically purchased using: NIH shared instrumentation grant? NIH high-end instrumentation grant?
2p)	What are the common reasons for performing maintenance? [Choices: High CVs/contamination issue/won't pass QC/low sensitivity/high background/clogging/other]
To get a better understanding of the time the instrument is operational vs the time the instrument is in use, please answer the next set of questions based on operational and amount of time the instrument has been in use in the past year: (Total percent time should sum up to 100%)	
2q)	What percentage of time is the instrument out of service waiting to be repaired?
2r)	What percentage of time is the instrument unavailable for use due to routine maintenance?
2s)	What percentage of time is the instrument operable?
3.	**For your Oldest instrument:**
3a)	Type of instrument:

	[Choices: Analyzer/Sorter/Imaging flow cytometer/Mass cytometer]
3b)	Vendor:
3c)	Model:
3d)	Year of purchase:
3e)	Is the instrument user-operated or staff-operated or both? Please mention the percentage time for each.
3f)	Is the instrument under warranty? (Y/N) If yes, skip question (g)
3g)	How do you maintain your instrument? [Choices: In-house staff/Original Equipment Manufacturer (OEM)/Third-party service provider/Multi-vendor service provider]
3h)	How much is the average maintenance cost for the instrument? (i.e., the cost of service contract and parts if that is how you maintain your instrument)
3i)	How often do you schedule routine maintenance (preventative maintenance/staff maintenance)? [Choices: monthly, every couple of months, twice a year, yearly]
3j)	How often do you perform deep cleaning of the instrument? [Choices: daily/several times a week/weekly/several times a month/monthly]
3k)	How often do you perform QC? [Choices: daily/several times a week/weekly/several times a month/monthly]
3l)	When do you expect the instrument to be replaced?
3m)	What is/are the likely reason(s) for replacing the instrument (check all that applies):

	[Choices: Instrument no longer serviced by company/keeps having issues/too few features/users' needs have changed/not upgradeable/Other]
3n)	What is the approximate annual cost for consumables such as for sheath fluids, filters, tubing, QC beads, probes, fluid tanks etc.?
3o)	Where were the funds for this instrument obtained from? [Choices: In-house funds/private foundation/government instrumentation grant/government research grant/other] Do you live in the US? If yes, then was this specifically purchased using: NIH shared instrumentation grant? NIH high-end instrumentation grant?
3p)	What are the common reasons for performing maintenance? [Choices: High CVs/contamination issue/won't pass QC/low sensitivity/high background/clogging/other]
To get a better understanding of the time the instrument is operational vs the time the instrument is in use, please answer the next set of questions based on operational and amount of time the instrument has been in use in the past year: (Total percent time should sum up to 100%)	
3q)	What percentage of time is the instrument out of service waiting to be repaired?
3r)	What percentage of time is the instrument unavailable for use due to routine maintenance?
3s)	What percentage of time is the instrument operable?
4.	**For your Most Used instrument:**
4a)	Type of instrument: [Choices: Analyzer/Sorter/Imaging flow cytometer/Mass cytometer]
4b)	Vendor:

4c)	Model:
4d)	Year of purchase:
4e)	Is the instrument user-operated or staff-operated or both? Please mention the percentage time for each.
4f)	Is the instrument under warranty? (Y/N) If yes, skip question (g)
4g)	How do you maintain your instrument? [Choices: In-house staff/Original Equipment Manufacturer (OEM)/Third-party service provider/Multi-vendor service provider]
4h)	How much is the average maintenance cost for the instrument? (i.e., the cost of service contract and parts if that is how you maintain your instrument)
4i)	How often do you schedule routine maintenance (preventative maintenance/staff maintenance)? [Choices: monthly, every couple of months, twice a year, yearly]
4j)	How often do you perform deep cleaning of the instrument? [Choices: daily/several times a week/weekly/several times a month/monthly]
4k)	How often do you perform QC? [Choices: daily/several times a week/weekly/several times a month/monthly]
4l)	When do you expect the instrument to be replaced?
4m)	What is/are the likely reason(s) for replacing the instrument (check all that applies): [Choices: Instrument no longer serviced by company/keeps having issues/too few features/users' needs have changed/not upgradeable/Other]

4n)	What is the approximate annual cost for consumables such as for sheath fluids, filters, tubing, QC beads, probes, fluid tanks etc.?
4o)	Where were the funds for this instrument obtained from? [Choices: In-house funds/private foundation/government instrumentation grant/government research grant/other] Do you live in the US? If yes, then was this specifically purchased using: NIH shared instrumentation grant? NIH high-end instrumentation grant?
4p)	What are the common reasons for performing maintenance? [Choices: High CVs/contamination issue/won't pass QC/low sensitivity/high background/clogging/other]
To get a better understanding of the time the instrument is operational vs the time the instrument is in use, please answer the next set of questions based on operational and amount of time the instrument has been in use in the past year: (Total percent time should sum up to 100%)	
4q)	What percentage of time is the instrument out of service waiting to be repaired?
4r)	What percentage of time is the instrument unavailable for use due to routine maintenance?
4s)	What percentage of time is the instrument operable?

Table 6.2

Keyword definitions

Keyword	**Definition**
Flow cytometry	A powerful technique used to analyze and measure properties of individual cells or particles
Shared Resource Labs (SRLs)	Facilities that provide specialized equipment and expertise to researchers within an institution
Analyzers	Flow cytometers that analyze cells but do not recover them
Sorters	Flow cytometers that analyze and can separate cells into different populations
Imaging flow cytometers	Instruments that combine flow cytometry with fluorescence microscopy
Mass cytometers	Flow cytometers that use mass spectrometry to analyze cells
Uptime	The percentage of time an instrument is available and operational
Staffing	The number and types of personnel working in a facility
Funding source	The origin of financial support for purchasing instruments such as in-house funds (institutional), government instrumentation grant, government research grant and private foundation
Government instrumentation grant	Grant issued by the government to purchase instruments
Government research grant	Grant issued by the government to support research projects
NIH shared instrumentation grant	NIH S10 award that assists in purchases of state-of-the-art commercially available instruments to enhance research of NIH-funded labs
Instrument usage	The extent to which instruments are utilized and operational
Quality control (QC)	Procedures to ensure accurate and reliable instrument performance
User-operated	Flow cytometers that are operated by researchers or individuals outside the facility's staff
Staff-operated	Flow cytometers that are operated by the facility's staff members
Both user and staff operated	Flow cytometers that are operated by both researchers and the facility's staff members
Original Equipment Manufacturer (OEM)	Instrument manufacturer

Table 6.3

Distribution of instrument operators

(A) Analyzer –

User-operated	**Staff-operated**	**Both**
(63/167) *100 = **37.72%**	(7/167) *100 = **4.19%**	(97/167) *100 = **58.08%**

(B) Sorter –

User-operated	**Staff-operated**	**Both**
(6/78) *100 = **7.69%**	(35/78) *100 = **44.87%**	(37/78) *100 = **47.44%**

(C) Imaging Flow cytometer –

User-operated	**Staff-operated**	**Both**
(2/8) *100 = **25%**	(1/8) *100 = **12.5%**	(5/8) *100 = **62.5%**

(D) Mass cytometer –

User-operated	**Staff-operated**	**Both**
(0/4) *100 = **0%**	(4/4) *100 = **100%**	(0/4) *100 = **0%**

Table 6.4

Operators for Newest, Oldest and Most used instruments

(A) Analyzer –

	User-operated	**Staff-operated**	**Both**
Newest	(20/62) *100 = **32.25%**	(3/62) *100 = **4.83%**	(39/62) *100 = **62.9%**
Oldest	(23/49) *100 = **46.93%**	(3/49) *100 = **6.12%**	(23/49) *100 = **46.93%**
Most Used	(20/56) *100 = **35.71%**	(0/56) *100 = **0%**	(36/56) *100 = **64.28%**

(B) Sorter-

	User-operated	**Staff-operated**	**Both**
Newest	(2/26) *100 = **7.69%**	(7/26) *100 = **26.92%**	(17/26) *100 = **65.38%**
Oldest	(1/36) *100 = **2.77%**	(19/36) *100 = **52.77%**	(16/36) *100 =**44.44%**
Most Used	(3/16) *100 = **18.75%**	(9/16) *100 = **56.25%**	(4/16) *100 = **25.00%**

Table 6.5

Cost of maintenance for Newest, Oldest and Most Used instruments

(A) Analyzer –

	Price range	**Average maintenance cost**
Newest	$1000 - $40000	738246/47 = **$15707**
Oldest	$0 - $50000	420686/41 = **$10260**
Most Used	$115 - $36000	849549/50 = **$16989**

Combined average: **$14,318.67**

(B) Sorter-

	Price range	**Average maintenance cost**
Newest	$3400 - $50000	728605/24 = **$30358**
Oldest	$0 - $72000	748895/34 = **$22026**
Most Used	$2000 - $55000	259614/11 = **$23601**

Combined average: **$25,328**

(C) Imaging cytometer –

	Price range	**Average maintenance cost**
Newest	$1000 - $46000	52677/3 = **$17559**
Oldest	$500 - $4968	5968/2 = **$2984**
Most Used	-	-

Combined average: **$10,271.5**

(D) Mass cytometer –

	Price range	**Average maintenance cost**
Newest	$60000 - $110000	170000/2 = **$85000**
Oldest	-	-
Most Used	$60000	60000/1 = **$60000**

Combined average: **$72,500**

Table 6.6

Average maintenance cost vs. year of purchase of instrument

(A) Analyzer –

Instruments	Year range	Average maintenance cost
Oldest 10	1980-2000	**$5168.2**
Newest 10	2019-2020	**$12791.50**

(B) Sorter –

Instruments	Year range	Average maintenance cost
Oldest 10	1995-2006	**$16,637.80**
Newest 10	2019-2020	**$26,141.90**

Table 6.7

Correlation of maintenance cost with user-operated, staff-operated and both user and staff-operated instruments

(A) Analyzer –

User-operated	**Staff-operated**	**Both**
Range: $0 - $50000 Average: 737172/54 = **$13651.33**	Range: $1800 - $30000 Average: 74300/5 = **$14860**	Range: $231 - $100000 Average: 1322352/27 = **$15742.29**

t-test:
Between User and Staff operated = 0.821484284 (p-value > 0.05)
Between User and Both User & Staff operated = 0.332430493 (p-value > 0.05)
Between Staff and Both User & Staff operated = 0.8662891 (p-value > 0.05)

(B) Sorter –

User-operated	**Staff-operated**	**Both**
Range: $3478 - $35000 Average: 91668/4 = **$22917**	Range: $0 - $55000 Average: 728708/32 = **$22772.13**	Range: $2000 - $42000 Average: 718738/33 = **$21779.94**

t-test:
Between User and Staff operated = 0.985551325 (p-value > 0.05)
Between User and Both User & Staff operated = 0.883070813 (p-value > 0.05)
Between Staff and Both User & Staff operated = 0.784024576 (p-value > 0.05)

Table 6.8

Warranty on Newest, Oldest and Most used instruments

(A) Analyzer –

	Instruments under warranty/service contract
Newest	(43/63) *100 = **68.25%**
Oldest	(12/48) *100 = **25.00%**
Most Used	(23/56) *100 = **41.07%**

(B) Sorter –

	Instruments under warranty/service contract
Newest	(17/26) *100 = **65.38%**
Oldest	(8/36) *100 = **22.22%**
Most Used	(7/15) *100 = **46.66%**

Table 6.9

Maintenance cost varying with type of service contract

(A) Analyzer –

Original Equipment Manufacturer (OEM)		**Third-Party service provider**		**In-house staff**	
%	Maintenance cost	%	Maintenance cost	%	Maintenance cost
83/132 = **62.88%**	Range: 1800-50000 Average: 390822/83 = **$12761**	11/132 = **8.33%**	Range: 1000-25000 Average: 13500/11 = **$10772.72**	38/132 = **28.72%**	Range: 100-22300 Average: 121195/38 = **$3189.34**

(B) Sorter-

Original Equipment Manufacturer (OEM)		**Third-Party service provider**		**In-house staff**	
%	Maintenance cost	%	Maintenance cost	%	Maintenance cost
37/54 = **68.5%**	Range: 3400-72000 Average: 847977/40 = **$21199.43**	5/54 = **9.26%**	Range: 12000-32000 Average: 121000/5 = **$24200**	12/54 = **22.22%**	Range: 0-17392 Average: 82892/10 = **$8289**

Table 6.10

Instrument wait time for different types of maintenance services

(A) Analyzer –

Maintenance type	Annual Maintenance cost	Percent of time instrument is waiting to be repaired (%)	Percent of time instrument is operable (%)
OEM	$12,761	**4.7**	89.3
Third Party service provider	$10,772	**9.0**	79.2
In-house staff	$3,189	**4.2**	89.6

t-test:
Between In-house staff and OEM = 0.696372363 (p-value > 0.05)
Between In-house staff and Third-party = 0.282866248 (p-value > 0.05)
Between OEM and Third-party = 0.317921816 (p-value > 0.05)

(B) Sorter –

Maintenance type	Annual Maintenance cost	Percent of time instrument is waiting to be repaired (%)	Percent of time instrument is operable (%)
OEM	$21,199	**5.7**	80.4
Third Party service provider	$24,200	**4.2**	88.6
In-house staff	$8,289	**5.5**	89.7

t-test:
Between In-house staff and OEM = 0.924963321 (p-value > 0.05)
Between In-house staff and Third-party = 0.500633019 (p-value > 0.05)
Between OEM and Third-party = 0.211857391 (p-value > 0.05)

Table 6.11

Average cost of consumables vs. year of purchase of instrument

(A) Analyzer –

Instruments	Year range	Average cost of consumables
Oldest 10	1980-2003	**$955.9**
Newest 10	2019-2020	**$3750**

(B) Sorter –

Instruments	Year range	Average cost of consumables
Oldest 10	1995-2005	**$3930.2**
Newest 10	2019-2020	**$5392.9**

Table 6.12

Average cost of consumables for newest and oldest instruments compared to instrument use

(A) Analyzer –

	Year range	Consumable cost (USD)	Percent of time instrument is operable (%)
Oldest 10	1980-2003	956	93.4
Newest 10	2019-2020	3750	90.8

t-test:
Between Oldest 10 and Newest 10 analyzers = 0.255235255 (p-value > 0.05)

(B) Sorter –

	Year range	Consumable cost (USD)	Percent of time instrument is operable (%)
Oldest 10	1995-2005	3930	88.6
Newest 10	2019-2020	5393	86.7

t-test:
Between Oldest 10 and Newest 10 sorters = 0.680617658 (p-value > 0.05)

Table 6.13

Correlation between maintenance frequency and maintenance cost

(A) Analyzer –

Frequency of Preventative/Staff maintenance	**Number of facilities**	**Cost of maintenance (USD)**
Monthly	22 Percent: (22/160) *100 = **13.75**%	Range: 100-40000 Average: 228837/22 = **$10401.68**
Every couple of months	20 Percent: (20/160) *100 = **12.5**%	Range: 0 – 35000 Average: 166791/20 = **$8339.55**
Twice a year	90 Percent: (90/160) *100 = **56.25**%	Range: 500-40000 Average: 1400056/90 = **$15556.17**
Annually	28 Percent: (28/160) *100 = **17.5%**	Range: 500-50000 Average: 259225/28 = **$9258.04**

t-Test

Cost: Twice a year vs. Annually = 0.051559878 (hence, they are statistically different)

(B) Sorter-

Frequency of Preventative/Staff maintenance	**Number of facilities**	**Cost of maintenance (USD)**
Monthly	18 Percent: (18/76) *100 = **23.68%**	Range: 2000-36000 Average: 328410/18 = **$18245**
Every couple of months	6 Percent: (6/76) *100 = **7.89%**	Range: 17379-54711 Average: 156090/6 = **$26015**
Twice a year	40 Percent: (40/76) *100 = **52.63%**	Range: 3478-50000 Average: 832824/40 = **$20820.6**
Annually	12 Percent: (12/76) *100 = **15.78%**	Range: 0-72000 Average: 256790/12 = **$21399.16**

Table 6.14

Frequency of deep cleaning of the instruments

(A) Analyzer – (164 entries)

Frequency of deep cleaning	**Facilities**
Daily	10 Percent: (10/164) *100 = **6.10%**
Several times a week	20 Percent: (20/164) *100 = **12.20%**
Weekly	37 Percent: (37/164) *100 = **22.56%**
Several times a month	17 Percent: (17/164) *100 = **10.37%**
Monthly	80 Percent: (80/164) *100 = **48.78%**

(B) Sorter – (76 entries)

Frequency of deep cleaning	**Facilities**
Daily	10 Percent: (10/76) *100 = **13.16%**
Several times a week	4 Percent: (4/76) *100 = **5.26%**
Weekly	20 Percent: (20/76) *100 = **26.32%**
Several times a month	8 Percent: (8/76) *100 = **10.53%**
Monthly	34 Percent: (34/76) *100 = **44.74%**

(C) Imaging Flow cytometer – (7 entries)

Frequency of deep cleaning	**Facilities**
Daily	0 Percent: (0/7) *100 = **0%**
Several times a week	1 Percent: (1/7) *100 = **14.29%**
Weekly	0 Percent: (0/7) *100 = **0%**
Several times a month	1 Percent: (1/7) *100 = **14.29%**
Monthly	5 Percent: (5/7) *100 = **71.43%**

Table 6.15

Frequency of performing Quality Control (QC)

(A) Analyzer – (166 entries)

Frequency of performing QC	**Facilities**
Daily	103 Percent: (103/166) *100 = **62.05%**
Several times a week	25 Percent: (25/166) *100 = **15.06%**
Weekly	22 Percent: (22/166) *100 = **13.25%**
Several times a month	5 Percent: (5/166) *100 = **3.01%**
Monthly	11 Percent: (11/166) *100 = **6.63%**

(B) Sorter – (76 entries)

Frequency of performing QC	**Facilities**
Daily	50 Percent: (50/76) *100 = **65.79%**
Several times a week	7 Percent: (7/76) *100 = **9.21%**
Weekly	11 Percent: (11/76) *100 = **14.47%**
Several times a month	4 Percent: (4/76) *100 = **5.26%**
Monthly	4 Percent: (34/76) *100 = **5.26%**

Table 6.16

Average instrument uptime on user, staff and both user and staff-operated instruments

(A) Analyzer –

User-operated (% time)	**Staff-operated (% time)**	**Both (% time)**
Out of service Range: 0-10 Average: 214/59 = **3.63** Routine Maintenance Range: 0-10 Average: 216/59 = **3.66** Operable (% time) Range: 75-100 Average: 5457.5/59 = **92.50**	Out of service Range: 2-10 Average: 27/5 = **5.40** Routine Maintenance Range: 0-7 Average: 17/5 = **3.40** Operable (% time) Range: 90-94 Average: 460/5 = **92.0**	Out of service Range: 0-50 Average: 455.9/97 = **4.70** Routine Maintenance Range: 0-50 Average: 499.1/97 = **5.14** Operable (% time) Range: 0-100 Average: 8532/97 = **87.95**

t-Test

Operable: User vs. Both user and staff-operated = 0.005160653

Analyzers- average uptime: 91.37%; routine maintenance- 4.06%; out of service- 4.57%

(B) Sorter-

User-operated (% time)	**Staff-operated (% time)**	**Both (% time)**
Out of service Range: 0-10 Average: 20/6 = **3.33** Routine Maintenance Range: 1-15 Average: 30/6 = **5.0** Operable (% time) Range: 75-99 Average: 550/6 = **91.66**	Out of service Range: 0-25 Average: 179.5/33 = **5.44** Routine Maintenance Range: 1-15 Average: 214.5/33 = **6.50** Operable (% time) Range: 70-99 Average: 2906/33 = **88.06**	Out of service Range: 0-30 Average: 217.7/34 = **6.40** Routine Maintenance Range: 0-20 Average: 194.3/34 = **5.71** Operable (% time) Range: 60-99 Average: 3018/34 = **88.76**

Sorters- average uptime: 89.5%; routine maintenance- 5.74%; out of service – 5.03%

Table 6.17

Sources of funding

(A) Analyzer –
Number of entries: **164**

Funding Source	**Facilities**
In house funds	57.32%
Government Instrumentation Grant	15.24%
Government Research Grant	12.80%
Private foundation	6.71%
Other	7.93%

(B) Sorter –
Number of entries: **76**

Funding Source	**Facilities**
In house funds	55.26%
Government Instrumentation Grant	23.68%
Government Research Grant	13.16%
Private foundation	5.26%
Other	2.63%

(C) Imaging Flow Cytometer –
Number of entries: **7**

Funding Source	**Facilities**
In house funds	42.86%
Government Instrumentation Grant	42.86%
Government Research Grant	14.29%
Private foundation	0.00%
Other	0.00%

(D) Mass cytometer –
Number of entries: **4**

Funding Source	**Facilities**
In house funds	50.00%
Government Instrumentation Grant	25.00%
Government Research Grant	0.00%
Private foundation	0.00%
Other	25.00%

Table 6.18

Flow cytometers funded by NIH shared instrumentation grant (S10 award)

(A) Analyzer –

Year range	Number of analyzers funded by NIH S10 award	Number of analyzers in the US SRLs	% of analyzers funded by NIH S10 award
1996-2000	1	5	20%
2001-2005	1	9	11%
2006-2010	3	21	14%
2011-2015	5	15	33%
2016-2020	12	41	29%

(B) Sorter -

Year range	Number of sorters funded by NIH S10 award	Number of sorters in the US SRLs	% of sorters funded by NIH S10 award
1996-2000	0	1	0%
2001-2005	1	2	50%
2006-2010	2	9	22%
2011-2015	6	11	55%
2016-2020	3	11	27%

(C) Total flow cytometers -

Year range	Flow cytometers funded by NIH S10 award	Number of flow cytometers in the US SRLs	% of flow cytometers funded by NIH S10 award
1996-2000	1	6	17%
2001-2005	2	11	18%
2006-2010	5	30	17%
2011-2015	11	26	42%
2016-2020	15	52	29%

Total number of flow cytometers funded by S10 award	Number of flow cytometers in the US	% of flow cytometers funded by NIH S10 award
34	125	27%

Table 6.19

Funding offered by NIH S10 award as per ORIP-NIH website

(A) Instruments funded by NIH S10 award from 2014 to 2021

Award year	NIH S10 total budget	Total number of instruments funded
2014	$71,024,659	116
2015	$70,265,102	110
2016	$68,416,022	107
2017	$71,387,628	109
2018	$83,238,060	120
2019	$81,134,038	131
2020	$89,618,744	123
2021	$99,071,561	128

(B) Flow cytometers funded by NIH S10 award from 2014 to 2021

Award year	NIH S10 budget for flow cytometers	Number of flow cytometers funded
2014	$3,416,370	7
2015	$3,722,465	8
2016	$4,846,804	10
2017	$2,632,943	5
2018	$6,228,862	11
2019	$4,922,122	11
2020	$4,907,185	11
2021	$3,386,286	8

CHAPTER 7

CONCLUSIONS

The proposed work aimed to improve the characterization and quantitation of protein post-translational modifications (PTMs) such as glycation, glycosylation, and pyroglutamate formation. A detailed characterization of these PTMs is especially important as they may affect protein stability, conformation, and biological functions among others. For instance, glycation is a PTM that could be introduced during the manufacturing of biotherapeutic drugs and may impact the safety, efficacy, and potency of drug products. HILIC LC-MS was observed to be a powerful technique in characterizing these modifications via bottom-up approach.

Chapter 3 demonstrated that glycated peptides can be effectively separated from their unmodified counterparts through HILIC chromatography. Glycation involves the addition of a hydrophilic glucose molecule to a protein, which could increase HILIC retention. Conversely, neutralizing the positive charge on the primary amine could decrease retention. The interplay between these two factors had in fact resulted in a slight overall increase in HILIC retention. Standard peptides and proteins were utilized to determine the average shift in HILIC retention upon glycation (in GU). Dextran ladder was used as a retention calibrant. This shift in retention (in GU) was then integrated into Badgett's peptide retention prediction model to calculate the HILIC retention coefficient for glycation. Further, this coefficient was effectively employed to predict and characterize glycation in complex mAb samples such as Adalimumab (human IgG1),

Natalizumab (IgG4), and 'Frankenmab' (custom IgG2). Remarkably, the experimental retention times of glycated peptides closely matched the predicted values. HILIC retention coefficient for glycation was calculated to be +0.52 GU. This meant that on an average a glycated peptide eluted later than its unmodified variant by 0.52 GU. Furthermore, the model was successfully applied to predict the retention times of glycated peptides generated by Glu-C enzymatic digestion of Adalimumab. For such cases, the HILIC coefficient of 0.52 GU was added to the experimental retention time of the unmodified variants. Pyroglutamation PTM was also studied wherein it was observed that the average retention shift upon this modification was -2.10 GU in the HILIC mode since the pyroglutamated variant was less hydrophilic than the unmodified variant. This predictive model could aid in the analysis of complex protein mixtures by adding another layer of confidence in peak identifications as well as decrease the analysis time. Such a strategy would assist in ensuring safety and efficacy of therapeutic drug products that could be prone to glycation and pyroglutamation modifications.

Chapter 4 described an analytical method to perform relative and absolute quantitation of glycated IgGs such as Adalimumab (IgG1), Natalizumab (IgG4), and 'Frankenmab' (custom IgG2). The percentage of relative glycation was determined by adding a known amount of heavy isotope-labeled variant of the target protein (containing ^{13}C and ^{15}N lysine and arginine). Bottom-up HILIC-MS approach was employed after performing trypsin digestion. The ratio of light to heavy peptides was calculated and averaged for tryptic peptides meeting specific criteria: they neither contained nor were adjacent to a glycation site, had peptide intensities >1000 counts, did not co-elute with other species, had m/z values above 500, and did not contain potential deamidation sites

that could consume unmodified peptides. Further, the light-to-heavy ratio of peptides containing or adjacent to a glycation site was calculated. Any decrease in this ratio compared to the averaged value for unmodified peptides indicated the percentage of relative glycation at that site. Absolute quantitation was achieved by multiplying the light-to-heavy ratio of peptides prone to glycation by the absolute amount of the heavy isotope-labeled internal standard used (normalized to 1 µmol). Subtracting this value from 1 µmol provided the absolute quantitation. Moreover, dilution experiments were conducted to evaluate the linearity of this approach. The use of a heavy isotope-labeled internal standard was found to enhance the accuracy and precision of glycation quantitation compared to a commonly used strategy, where the abundance of glycated missed cleavage peptides is compared to their tryptic peptide counterparts. Although this study focused on glycation PTM, this strategy could be adapted to quantify other PTMs, such as deamidation.

Further, Chapter 5 examined several LC-MS sample preparation strategies that are used to detect N-glycans. The selection of a protocol for N-glycan analysis was observed to impact the absolute and relative abundance of N-glycans in protein samples. Specifically, differences in the abundances of bovine fetuin and human serum N-glycans were observed when comparing the use of $NaBH_3CN$ and EMP reducing agents during Procainamide labeling step. Notably, $NaBH_3CN$ led to higher absolute abundances, while EMP resulted in lower values. Additionally, the relative abundance of heavier sialylated N-glycans was elevated when EMP was employed as the reducing agent. This observation might be attributed to the higher temperature (65°C) at which the $NaBH_3CN$ reductive amination step was conducted compared to the EMP protocol (37°C), possibly

causing sialic acid to dissociate from N-glycans and reducing the abundances of heavier sialylated N-glycans in $NaBH_3CN$ protocol. Nevertheless, variations in N-glycan abundances were insignificant when comparing desalting and clean-up strategies. In conclusion, the selection of an LC-MS sample preparation method played a crucial role in N-glycan quantitation. While each method may have its own advantages and disadvantages, it is vital that the chosen approach is used consistently throughout a study to improve the accuracy of N-glycosylation analyses.

Finally, Chapter 6 described an online survey that was conducted to gather comprehensive insights into Shared Resource Laboratories (SRLs) utilizing various types of flow cytometers, including analyzers, sorters, imaging flow cytometers, and mass cytometers. The survey gathered responses from 146 SRL professionals across 14 countries, predominantly from core facility directors and managers representing universities, private institutions, and companies. The findings revealed operational trends within SRLs. Analyzers were commonly operated by both users and staff, especially older analyzers. Sorters were typically staff-operated, although newer sorters saw greater user involvement. Imaging flow cytometers were often utilized by both users and staff, while mass cytometers were exclusively staff-operated due to their mass spectrometry aspect. Maintenance costs varied by instrument type, with analyzers having an average annual cost of $14,922, sorters at $25,328, imaging flow cytometers at $10,271, and mass cytometers at $72,500. Newer instruments incurred higher maintenance expenses, often due to service contract costs tied to instrument prices. A substantial portion of the newest analyzers and sorters were under warranty or service contracts. Further, the study highlighted the significance of routine maintenance in maintaining instrument uptime.

Additionally, funding for flow cytometer purchases in the US was commonly supported by NIH S10 awards, indicating their pivotal role in advancing research in SRLs. Overall, the survey results offered valuable insights for establishing and managing core labs, emphasizing the role of maintenance, user training, and funding sources in sustaining these critical research facilities.

REFERENCES

1) Pan, S., & Chen, R. Pathological Implication of Protein Post-translational Modifications in Cancer. *Mol. Asp. Med.* **2022**, 86, 101097.

2) Karve, T. M., & Cheema, A. K. Small Changes Huge Impact: The Role of Protein Posttranslational Modifications in Cellular Homeostasis and Disease. *J. Amino acids.* **2011**, 2011, 207691.

3) Johnson, H., Eyers, C.E. Analysis of Post-translational Modifications by LC-MS/MS. In: Cutillas, P., Timms, J. (eds) LC-MS/MS in Proteomics. *Methods Mol. Biol.* **2010**, 658.

4) Wu, S.L.; Hühmer, A.F.R.; Hao, Z.; Karger, B.L. On-Line LC−MS Approach Combining Collision-Induced Dissociation (CID), Electron-Transfer Dissociation (ETD), and CID of an Isolated Charge-Reduced Species for the Trace-Level Characterization of Proteins with Post-Translational Modifications. *J. Proteome Res.* **2007**, 6(11), 4230–4244.

5) Alpert, A.J. Hydrophilic-interaction chromatography for the separation of peptides, nucleic acids, and other polar compounds. *J. Chromatogr. A.* **1990**, 499, 177-196.

6) Alpert, A.J., Shukla, M., Shukla, A.K., Zieske, L.R., Yuen, S.W., Ferguson, M.A.J., Mehlert, A., Pauly, M., Orlando, R. Hydrophilic-interaction chromatography of complex carbohydrates. *J. Chromatogr. A.* **1994**, 676(1), 191-202.

7) Monu, Agnihotri, P.; Biswas, S., AGE/Non-AGE Glycation: An Important Event in Rheumatoid Arthritis Pathophysiology. *Inflammation* **2022**, 45, 477–496.

8) Ulrich, P., & Cerami, A. Protein glycation, diabetes, and aging. *Recent Prog. Horm. Res.* **2001**, 56, 1-21.

9) Münch, G., Thome, J., Foley, P., Schinzel, R., & Riederer, P. Advanced glycation endproducts in ageing and Alzheimer's disease. *Brain Res. Rev.* **1997**, 23(1-2), 134-143.

10) Wei, B., Berning, K., Quan, C., & Zhang, Y.T. Glycation of antibodies: Modification, methods, and potential effects on biological functions. *Mabs*,**2017**, 9(4), 586-594.

11) Badgett, M.J., Boyes, B., & Orlando, R. Peptide retention prediction using hydrophilic interaction liquid chromatography coupled to mass spectrometry. *J. Chromatogr. A.* **2018**, 1537, 58-65.

12) Thornalley, P.J., Battah, S., Ahmed, N., Karachalias, N., Agalou, S., Babaei-Jadidi, R., & Dawnay, A. Quantitative screening of advanced glycation endproducts in cellular and extracellular proteins by tandem mass spectrometry. *Biochem. J.* **2003**, 375(3), 581-592.

13) Milkovska-Stamenova, S., Schmidt, R., Frolov, A., & Birkemeyer, C. GC-MS Method for the Quantitation of Carbohydrate Intermediates in Glycation Systems. *J. Agric. Food Chem.* **2015**, 63(25), 5911-5919.

14) Frolov, A., & Hoffmann, R. Identification and relative quantification of specific glycation sites in human serum albumin. *Anal. Bioanal. Chem.* **2010**, 397, 2349-2356.

15) Yeboah, F. K., & Yaylayan, V. A. Analysis of glycated proteins by mass spectrometric techniques: qualitative and quantitative aspects. *Mol. Nutr. Food Res.* **2001**, 45(3), 164-171.

16) Solá, R. J., & Griebenow, K. Effects of glycosylation on the stability of protein pharmaceuticals. *J. Pharm. Sci.* **2009**, 98(4), 1223-1245.

17) Shental-Bechor, D., & Levy, Y. Effect of glycosylation on protein folding: A close look at thermodynamic stabilization. *PNAS* **2008**, 105(24), 8256-8261.

18) Ruhaak, L. R., Huhn, C., Waterreus, W. J., de Boer, A. R., Neusüss, C., Hokke, C. H., Deelder, A. M., & Wuhrer, M. Hydrophilic Interaction Chromatography-Based High-Throughput Sample Preparation Method for N-Glycan Analysis from Total Human Plasma Glycoproteins. *Anal. Chem.* **2008**, 80(15), 6119–6126.

19) Tao, S., Huang, Y., Boyes, B. E., & Orlando, R. Liquid Chromatography-Selected Reaction Monitoring (LC-SRM) Approach for the Separation and Quantitation of Sialylated N-Glycans Linkage Isomers. *Anal. Chem.* **2014**, 86(21), 10584–10590.

20) McKinnon, K. M. Flow cytometry: An overview. *Curr. Protoc. Immunol.* **2018**, 120, 5.1.1.

21) Coskun, O. Separation techniques: Chromatography. *North Clin Istanbul* **2016**, 3(2), 156–60.

22) Hibbert, D. B. Experimental design in chromatography: A tutorial review. *J. Chromatogr. B* **2012**, 910, 2-13.

23) Bhardwaj, S. K.; Dwivedi, K.; Agarwal, D. D. A review: HPLC method development and validation. *Int J Anal Bioanal Chem*. **2015**, 5(4), 76-81.

24) Olsen, B. A.; Castle, B. C.; Myers, D. P. Advances in HPLC technology for the determination of drug impurities. *TrAC, Trends Anal. Chem.* **2006**, 25(8), 796-805.

25) Rusli, H.; Putri, R. M.; Alni, A. Recent Developments of Liquid Chromatography Stationary Phases for Compound Separation: From Proteins to Small Organic Compounds. *Molecules.* **2022**, 27(3), 907.

26) François, I.; Sandra, K.; Sandra, P. Comprehensive liquid chromatography: Fundamental aspects and practical considerations—A review. *Anal. Chim. Acta* **2009**, 641(1), 14-31.

27) Johnson, D.; Boyes, B.; Orlando, R. The Use of Ammonium Formate as a Mobile-Phase Modifier for LC-MS/MS Analysis of Tryptic Digests. J Biomol Tech. 2013 Dec; 24(4): 187–197.

28) Patel, D. C.; Breitbach, Z. S.; Wahab, M. F.; Barhate, C. L.; Armstrong, D. W. Gone in Seconds: Praxis, Performance, and Peculiarities of Ultrafast Chiral Liquid Chromatography with Superficially Porous Particles. *Anal. Chem.* **2015**, 87(18), 9137–9148.

29) Bobály, B.; Veuthey, J.-L.; Guillarme, D.; Fekete, S. New developments and possibilities of wide-pore superficially porous particle technology applied for the liquid chromatographic analysis of therapeutic proteins. *J Pharm Biomed Anal* **2018**, 158, 225-235.

30) Kirkland, J. J.; Truszkowski, F. A.; Dilks Jr., C. H.; Engel, G. S. Superficially porous silica microspheres for fast high-performance liquid chromatography of macromolecules. *J. Chromatogr. A* **2000**, 890(1), 3-13.

31) Van Deemter, J. J.; Zuiderweg, F. J. Longitudinal diffusion and resistance to mass transfer as causes of nonideality in chromatography. *Chem Engng Sci.* **1956**, 5, 271-289.

32) Gritti, F.; Guiochon, G. The van Deemter equation: Assumptions, limits, and adjustment to modern high-performance liquid chromatography. *J. Chromatogr. A* **2013**, 1302, 1-13.

33) Knox, J. H.; Scott, H. P. B and C terms in the Van Deemter equation for liquid chromatography. *J. Chromatogr. A* **1983**, 282, 297-313.

34) Andersen, J. E. T.; Mukami, H. W.; Maina, I. W. Evaluation of the van Deemter equation in terms of open-ended flow to chromatography. *J. Sep. Sci.* **2020**, 43 (16), 3251-3265.

35) Snyder, L. R.; Kirkland, J. J.; Dolan, J. W. Introduction to Modern Liquid Chromatography. 3rd ed. Hoboken, NJ: Wiley-Blackwell; **2009**.

36) Salisbury, J. J. Fused-core particles: A practical alternative to sub-2 micron particles. *J. Chromatogr. Sci.* **2008**, 46, 883-886.

37) Kirkland, J. J.; Schuster, S. A.; Johnson, W. L.; Boyes, B. E. Fused-core particle technology in high-performance liquid chromatography: An overview. *J Pharm Anal.* **2013**, 3(5), 303-312.

38) Schuster, S. A.; Boyes, B. E.; Wagner, B. M.; Kirkland, J. J. Fast high-performance liquid chromatography separations for proteomic applications using fused-core silica particles. *J. Chromatogr. A* **2012**, 1228, 232-241.

39) Knox, J. H.; Scott, H. P. B and C terms in the van Deemter equation for liquid chromatography. *J Chromatogr. A* **1983**, 282, 297-313.

40) Neue, U. D. Theory of peak capacity in gradient elution. *J Chromatogr A.* **2005**, 1079, 153-161.

41) Paliwal, S. K.; de Frutos, M.; Regnier, F. E. Rapid separations of proteins by liquid chromatography. *Methods Enzymol.* **1996**, 270, 133-151.

42) Grün, M.; Kurganov, A. A.; Schacht, S.; Schüth, F.; Unger, K. K. Comparison of an Ordered Mesoporous Aluminosilicate, Silica, Alumina, Titania, and Zirconia in Normal-Phase High-Performance Liquid Chromatography. *J. Chromatogr. A* **1996**, 740 (1), 1–9.

43) Borówko, M.; Ościk-Mendyk, B. Selectivity in Normal-Phase Liquid Chromatography with Binary Mobile Phase. *Adsorption* **2010**, 16 (4–5), 397–403.

44) Ali, I.; Aboul-Enein, H. Y.; Singh, P.; Singh, R.; Sharma, B. Separation of biological proteins by liquid chromatography. *Saudi Pharm J.* **2010**, 18(2), 59-73.

45) Mant, C. T.; Zhou, N. E.; Hodges, R. S. Correlation of protein retention times in reversed-phase chromatography with polypeptide chain length and hydrophobicity. *J Chromatogr A.* **1989**, 476, 363-375.

46) Mitulovic, G.; Mechtler, K. HPLC techniques for proteomics analysis-a short overview of latest developments. *Brief Funct Genomic Proteomic.* **2006**, 5(4), 249-260.

47) Horvath, C.; Molnar, I. Separation of amino acids and peptides on non-polar stationary phases by high-performance liquid chromatography. *J Chromatogr A.* **1977**, 142, 623-640.

48) Dorsey, J. G.; Dill, K. A. The molecular mechanism of retention in reversed-phase liquid chromatography. *Chem Rev.* **1989**, 89, 331-346.

49) Rafferty, J. L.; Zhang, L.; Siepmann, J. I.; Schure, M. R.; Carlo, M. Retention mechanism in reversed-phase liquid chromatography: A molecular perspective. *Anal Chem.* **2007**, 79, 6551-6558.

50) Boersema, P. J.; Mohammed, S.; Heck, A. J. R. Hydrophilic interaction liquid chromatography (HILIC) in proteomics. *Anal. Bioanal. Chem.* **2008**, 151-159.

51) Prathap, B.; Dey, A.; Srinivasa, G. H.; Johnson, P.; Arthanariswaran, P. A review - Importance of RP-HPLC in analytical method development. *Int J Nov Trends Pharm Sci.* **2013**, 3(1), 15-23.

52) Bensaddek, D.; Nicolas, A.; Lamond, A. I. Evaluating the use of HILIC in large-scale, multidimensional proteomics: Horses for courses? *Int J Mass Spectrom.* **2015**, 391,105-114.

53) Buszewski, B.; Noga, S. Hydrophilic interaction liquid chromatography (HILIC) - a powerful separation technique. *Anal Bioanal Chem.* **2012,** 402, 231-247.

54) Heaton, J.; Smith, N. W. Advantages and disadvantages of HILIC; A brief overview. *Chrom Today.* **2012**, 44-47.

55) Jandera, P. Stationary and mobile phases in hydrophilic interaction chromatography: A review. *Analytica Chimica Acta.* **2011**, 692, 1-25.

56) Qiao, L.; Dou, A.; Shi, X.; Li, H.; Shan, Y.; Lu, X.; Xu, G. Development and evaluation of new imidazolium-based zwitterionic stationary phases for hydrophilic interaction chromatography. *J Chromatogr A.* **2013**, 1286, 137-145.

57) Hemström, P.; Irgum, K. Hydrophilic interaction chromatography. *J Sep Sci.* **2006,** 29(12), 1784-1821.

58) McCalley, D. V.; Neue, U. D. Estimation of the extent of the water-rich layer associated with the silica surface in hydrophilic interaction chromatography. *J Chromatogr A.* **2008,** 1192(2), 225-229.

59) Dong, M. W.; Wysocki, J. PERSPECTIVES IN MODERN HPLC. 10.

60) Kruve, A.; Rebane, R.; Kipper, K.; Oldekop, M.-L.; Evard, H.; Herodes, K.; Ravio, P.; Leito, I. Tutorial review on validation of liquid chromatography–mass spectrometry methods: Part I. *Anal. Chim. Acta* **2015**, 870, 29-44.

61) Makarov, A.; Scigelova, M. Coupling liquid chromatography to Orbitrap mass spectrometry. *J. Chromatogr. A*, **2010**, 1217(25), 3938-3945.

62) Browne, C. A.; Bennett, H. P. J.; Solomon, S. The isolation of peptides by high-performance liquid chromatography using predicted elution positions. *Anal Biochem.* **1982**, 124, 201-208.

63) Guo, D.; Mant, C. T.; Taneja, A. K.; Parker, J. M. R.; Rodgers, R. S. Prediction of peptide retention times in reversed-phase high-performance liquid chromatography I.

Determination of retention coefficients of amino acid residues of model synthetic peptides. *J Chromatogr A.* **1986,** 359, 499-518.

64) Krokhin, O. V.; Spicer, V. Predicting peptide retention times for proteomics. *Curr Protoc Bioinformatics.* **2010,** 1-15.

65) Le Maux, S.; Nongonierma, A. B.; Fitzgerald, R. J. Improved short peptide identification using HILIC-MS/MS: Retention time prediction model based on the impact of amino acid position in the peptide sequence. *Food Chem.* **2015,** 173, 847-854.

66) Meek, J. L. Prediction of peptide retention times in high-pressure liquid chromatography on the basis of amino acid composition. *Proc Natl Acad Sci USA.* **1980,** 77(3), 1632-1636.

67) O'Hare, M. J.; Nice, E. C. Hydrophobic high-performance liquid chromatography of hormonal polypeptides and proteins on alkylsilane bonded silica. *J Chromatogr A.* **1979,** 171, 209-226.

68) Palmblad, M.; Ramström, M.; Markides, K. E.; Håkansson, P.; Bergquist, J. Prediction of chromatographic retention and protein identification in liquid chromatography/mass spectrometry. *Anal Chem.* **2002,** 74(22), 5826-5830.

69) Badgett, M. J.; Boyes, B.; Orlando, R. Peptide retention prediction using hydrophilic interaction liquid chromatography coupled to mass spectrometry. J. Chromatogr. A 2018, 1537, 58-65.

70) Badgett, M. J.; Boyes, B.; Orlando, R. Predicting the Retention Behavior of Specific O-Linked Glycopeptides. *J Biomol Tech.* **2017**, 28(3), 122–126.

71) Badgett, M. J.; Mize, E.; Fletcher, T.; Boyes, B.; Orlando, R. Predicting the HILIC Retention Behavior of the N-Linked Glycopeptides Produced by Trypsin Digestion of Immunoglobulin Gs (IgGs). *J Biomol Tech.* **2018**, 29(4), 98–104.

72) Badgett, M. J.; Boyes, B.; Orlando, R. The Separation and Quantitation of Peptides with and without Oxidation of Methionine and Deamidation of Asparagine Using Hydrophilic Interaction Liquid Chromatography with Mass Spectrometry (HILIC-MS). *J. Am. Soc. Mass Spectrom.* **2017**, 28, 5, 818–826.

73) Gross J. H., Mass Spectrometry A Textbook. 2nd ed. Heidelberg: Springer-Verlag; **2011**, 561-620.

74) Banerjee, S.; Mazumdar, S. Electrospray ionization mass spectrometry: A technique to access the information beyond the molecular weight of the analyte. *Int J Anal Chem.* **2012**, 2012, 1-40.

75) Domon, B.; Aebersold, R. Mass Spectrometry and Protein Analysis. *Science.* **2006**, 312(5771), 212-217.

76) Glish, G. L.; Vachet, R. W. The basics of mass spectrometry in the twenty-first century. *Nat. Rev. Drug Discov.* **2003**, 2, 140–150.

77) Mann, M.; Hendrickson, R. C.; Pandey, A. Analysis of Proteins and Proteomes by Mass Spectrometry. *Annu. Rev. Biochem.* **2001**, 70, 437-473.

78) Chowdhury, S. K.; Katta, V.; Chait, B. T. Electrospray ionization mass spectrometric peptide mapping: a rapid, sensitive technique for protein structure analysis. *Biochem Biophys Res Commun.* **1990**, 167(2), 686-692.

79) Aebersold, R.; Mann, M. Mass spectrometry-based proteomics. *Nature*. **2003**, 422(6928), 198-207.

80) Meissner, F.; Geddes-McAlister, J.; Mann, M.; Bantscheff, M. The emerging role of mass spectrometry-based proteomics in drug discovery. *Nat. Rev. Drug Discov.* **2022**, 21, 637–654.

81) Savaryn, J. P.; Toby, T. K.; Kelleher, N. L. A researcher's guide to mass spectrometry-based proteomics. *Proteomics* **2016**, 16(18), 2435-2443.

82) Dole, M.; Mack, L. L.; Hines, R. L., et al. Molecular Beams of Macroions. *J Chem Phys.* **1968**, 49(5), 2240-2249.

83) Kebarle, P.; Verkerk, U. H. Electrospray: From ions in solution to ions in the gas phase, what we know now. *Mass Spectrom Rev.* **2009**, 28, 898-917.

84) Wilm, M. Principles of electrospray ionization. *Mol Cell Proteomics.* **2011**, 10(7), 1-8.

85) Iribarne, J. V.; Thomson, B. A. On the evaporation of small ions from charged droplets. *J Chem Phys.* **1976**, 64(6), 2287-2294.

86) Nguyen, S.; Fenn, J. B. Gas-phase ions of solute species from charged droplets of solutions. *Proc Natl Acad Sci USA*. **2007**, 104(4), 1111-1117.

87) Singhal, N.; Kumar, M.; Kanaujia, P. K.; Virdi, J. S. MALDI-TOF mass spectrometry: An emerging technology for microbial identification and diagnosis. *Front Microbiol.* **2015**, 6, 1-16.

88) Darie-Ion, L.; Whitham, D.; Jayathirtha, M.; Rai, Y.; Neagu, A.-N.; Darie, C. C.; Petre, B. A. Applications of MALDI-MS/MS-Based Proteomics in Biomedical Research. *Molecules* **2022**, 27(19), 6196.

89) Haag, A. M. Mass Analyzers and Mass Spectrometers. In: Mirzaei, H., Carrasco, M. (eds) Modern Proteomics – Sample Preparation, Analysis and Practical Applications. Advances in Experimental Medicine and Biology, **2016**, 919.

90) Dawson, P. Quadrupole mass analysers: Performance, design and some recent applications. *Mass Spectrom Rev*. **1986**, 5, 1-37.

91) Dawson, P. H. Quadrupole Mass Spectrometry and Its Applications. 1st ed. Amsterdam, Netherlands: *Elsevier B.V.*, **1976**.

92) Johnson, J. V.; Yost, R. A.; Kelley, P. E.; Bradford, D. C. Tandem-in-space and tandem-in-time mass spectrometry: triple quadrupoles and quadrupole ion traps. *Anal Chem.* **1990**, 62(20), 2162-2172.

93) Vidova, V.; Spacil, Z. A review on mass spectrometry-based quantitative proteomics: Targeted and data independent acquisition. *Analytica Chimica Acta.* **2017***,* 964, 7-23.

94) March, R. E. Quadrupole ion trap mass spectrometry: a view at the turn of the century. *Int J Mass Spectrom.* **2000**, 200, 285-312.

95) March, R. E. Quadrupole ion traps. *Mass Spectrom Rev.* **2009**, 28(6), 961-989.

96) Mamyrin, B. A. Time-of-flight mass spectrometry (concepts, achievements, and prospects). *Int. J. Mass Spectrom.* **2001**, 206(3), 251-266.

97) Cotter, R. J. Time-of-Flight Mass Spectrometry for the Structural Analysis of Biological Molecules. *Anal. Chem.* **1992**, 64, 21.

98) Boesl, U. Time-of-flight mass spectrometry: Introduction to the basics. *Mass Spectrom. Rev.* **2017**, 36(1), 86-109.

99) Kaufmann, R.; Chaurand, P.; Kirsch, D.; Spengler, B. Post-source Decay and Delayed Extraction in Matrix-assisted Laser Desorption/Ionization-Reflectron Time-of-Flight Mass Spectrometry. Are There Trade-offs? *RCM* **1996**, 10(10), 1199-1208.

100) Haney, L. L.; Riederer, D. E. Delayed extraction for improved resolution of ion/surface collision products by time-of-flight mass spectrometry. *Anal. Chim. Acta.* **1999**, 397(1-3), 225-233.

101) Doroshenko, V. M.; Cotter, R. J. Ideal velocity focusing in a reflectron time-of-flight mass spectrometer. *JASMS* **1999**, 10(10), 992-999.

102) Marshall AG, Hendrickson CL. Fourier transform ion cyclotron resonance detection: Principles and experimental configurations. *Int. J. Mass Spectrom.* **2002**, 215, 59-75.

103) Nikolaev EN, Kostyukevich YI, Vladimirov GN. Fourier transform ion cyclotron resonance (FT ICR) mass spectrometry: Theory and simulations. *Mass Spectrom. Rev.* **2016**, 35, 219-258.

104) Schmid DG, Grosche P, Bandel H, Jung G. FTICR-mass spectrometry for high-resolution analysis in combinatorial chemistry. *Biotechnol. Bioeng.* **2000**, 71(2), 149-161.

105) Eliuk S, Makarov A. Evolution of orbitrap mass spectrometry instrumentation. *Annu. Rev. Anal. Chem.* **2015**, 8(1), 61-80.

106) Perry RH, Cooks G, Noll RJ. Orbitrap mass spectrometry: Instrumentation, ion motion, and applications. *Mass Spectrom. Rev.* **2008**, 27, 661-699.

107) Molina, H.; Matthiesen, R.; Kandasamy, K.; Pandey, A. Comprehensive Comparison of Collision Induced Dissociation and Electron Transfer Dissociation. *Anal. Chem.* **2008**, 80(13), 4825–4835.

108) Paizs, B.; Suhai, S. Fragmentation Pathways of Protonated Peptides. *Mass Spectrom. Rev.* **2005**, 24(4), 508–548.

109) Zubarev, R. A. Electron-Capture Dissociation Tandem Mass Spectrometry. *COBIOT* **2004**, 15(1), 12–16.

110) Dietz, L. A. Basic Properties of Electron Multiplier Ion Detection and Pulse Counting. *Methods in Mass Spectrometry. Rev. Sci. Instrum* **1965**, 36(12), 1763–1770.

111) Liu, R.; Li, Q.; Smith, L. M. Detection of Large Ions in Time-of-Flight Mass Spectrometry: Effects of Ion Mass and Acceleration Voltage on Microchannel Plate Detector Response. *J. Am. Soc. Mass Spectrom.* **2014**, 25 (8), 1374–1383.

112) Richter, S.; Goldberg, S. A.; Mason, P. B.; Traina, A. J.; Schwieters, J. B. Linearity Tests for Secondary Electron Multipliers Used in Isotope Ratio Mass Spectrometry. *Int. J. Mass Spectrom*. **2001**, 206 (1–2), 105–127.

113) Witze, E. S.; Old, W. M.; Resing, K. A.; Ahn, N. G. Mapping protein post-translational modifications with mass spectrometry. *Nat. Methods.*, **2007**, 4, 798–806.

114) Macek, B.; Forchhammer, K.; Hardouin, J.; Weber-Ban, E.; Grangeasse, C.; Mijakovic, I. Protein post-translational modifications in bacteria. *Nat. Rev. Microbiol*, **2019**, 17, 651–664.

115) Ramazi, S.; Zahiri, J. Post-translational modifications in proteins: resources, tools and prediction methods. *Database* **2021**, 2021.

116) Schroeder Jr., H.W.; Cavacini, L. Structure and function of immunoglobulins. *J. Allergy Clin. Immunol.* **2010**, 125(2), S41-S52.

117) Karsten, C.M.; Köhl, J. The immunoglobulin, IgG Fc receptor and complement triangle in autoimmune diseases. *Immunobiol.* **2012**, 217(11), 1067-1079.

118) Baliakas, P. et al. Clinical effect of stereotyped B-cell receptor immunoglobulins in chronic lymphocytic leukaemia: a retrospective multicentre study. *Lancet Haematol.* **2014**, 1(2), E74-E84.

119) Muhammed, Y. The Best IgG Subclass for the Development of Therapeutic Monoclonal Antibody Drugs and their Commercial Production: A Review. *Immunome Research*, **2020**, 16(1), 1-12.

120) Ząbczyńska, M.; Polak, K.; Kozłowska, K.; Sokołowski, G.; Pocheć, E. The Contribution of IgG Glycosylation to Antibody-Dependent Cell-Mediated Cytotoxicity (ADCC) and Complement-Dependent Cytotoxicity (CDC) in Hashimoto's Thyroiditis: An in Vitro Model of Thyroid Autoimmunity. *Biomolecules* **2020**, 10(2), 171.

121) Johnson, D.E. Biotherapeutics: Challenges and Opportunities for Predictive Toxicology of Monoclonal Antibodies. *Int J Mol Sci.* **2018**, 19(11), 3685.

122) Dimitrov, D.S. Therapeutic Proteins. *Methods Mol Biol.* **2012**, 899, 1–26.

123) Walsh, G. Post-translational modifications of protein biopharmaceuticals. *Drug Discov. Today* **2010**, 15(17–18), 773-780.

124) Wei, B., Berning, K., Quan, C., Zhang, Y. T. Glycation of antibodies: Modification, methods and potential effects on biological functions. *MABS.* **2017**, 9(4), 586–594.

125) Yehuda, S., Padler-Karavani, V. Glycosylated Biotherapeutics: Immunological Effects of N-Glycolylneuraminic Acid. *Front Immunol.* **2020**, 11, 21.

126) Liu, Y. D., Goetze, A. M., Bass, R. B., & Flynn, G. C. N-terminal Glutamate to Pyroglutamate Conversion in Vivo for Human IgG2 Antibodies. *J Biol Chem.* **2011**, 286(13), 11211–11217.

127) Ligier, S.; Fortin, P. R.; Newkirk, M. M., A new antibody in rheumatoid arthritis targeting glycated IgG: IgM anti-IgG-AGE. *Br J Rheumatol* **1998**; 37(12), 1307-14.

128) Brownlee, M., Advanced protein glycosylation in diabetes and aging. *Annu Rev Med* **1995**; 46, 223-34.

129) Ahmed, S. et al., Nonenzymatic glycosylation of isolated human immunoglobulin-G by D-ribose. *Cell Biochem. Funct.* **2022**, 40(5), 526-534.

130) Soboleva, A.; Vikhnina, M.; Grishina, T.; Frolov, A, Probing Protein Glycation by Chromatography and Mass Spectrometry: Analysis of Glycation Adducts. *Int. J. Mol. Sci.* **2017**, 18(12), 2557.

131) Li, W. et. al., State-of-the-Art and Emerging Technologies for Therapeutic Monoclonal Antibody Characterization Volume 2. Biopharmaceutical Characterization: The NISTmAb Case Study., **2015**, 119-183.

132) Hart, G. W. Glycosylation. COCEBI 1992, 4(6), 1017-1023.

133) Chang, D., Zaia, J. Methods to improve quantitative glycoprotein coverage from bottom-up LC-MS data. *Mass Spectrom. Rev.* **2022**, 41(6), 922-937.

134) Zhou S, Dong X, Veillon L, Huang Y, Mechref Y. LC-MS/MS analysis of permethylated N-glycans facilitating isomeric characterization. *Anal. Bioanal. Chem.* **2017**, 409, 453–466.

135) Lauber MA et al., Rapid Preparation of Released N-Glycans for HILIC Analysis Using a Labeling Reagent that Facilitates Sensitive Fluorescence and ESI-MS Detection. *Anal. Chem.* **2015**, 87, 10, 5401–5409.

136) Beyer, B.; Schuster, M.; Jungbauer, A.; Lingg, N., Microheterogeneity of Recombinant Antibodies: Analytics and Functional Impact. *Biotechnol. J.* **2018**, 13, 1700476.

137) Schlenzig, D. et al., Pyroglutamate Formation Influences Solubility and Amyloidogenicity of Amyloid Peptides. *Biochemistry* **2009**, 48, 29, 7072–7078.

138) Zhen, J.; Kim, J.; Zhou, Y.; Gaidamauskas, E.; Subramanian, S.; Feng, P., Antibody characterization using novel ERLIC-MS/MS-based peptide mapping. *MABS* **2018**, 10(7), 951-959.

139) "Biopharmaceutical Market" Prescient & Strategic Intelligence, Sep. **2022**, https://www.psmarketresearch.com/market-analysis/biopharmaceuticals-market.

140) Jenkins, N., Modifications of therapeutic proteins: challenges and prospects. *Cytotechnology* **2007**; 53(1-3), 121-125.

141) Kaltashov, I. A.; Bobst, C. E.; Abzalimov, R. R., Wang, G.; Baykal, B.; Wang S., Advances and challenges in analytical characterization of biotechnology products: mass spectrometry-based approaches to study properties and behavior of protein therapeutics. *Biotechnol Adv.* **2012**; 30(1), 210–222.

142) Maillard, L. C., Action of amino acids on sugars. Formation of melanoidins in a methodical way. *Compt. Rend* **1912**, 154, 66-68.

143) Popova, E.; Mironova, R. S.; Odjakova, M., Non-Enzymatic Glycosylation and Deglycating Enzymes. *Biotechnol. Biotechnol. Equip.* **2010**, 24 (3), 1928-1935.

144) Palimeri, S.; Palioura, E.; Diamanti-Kandarakis, E., Current perspectives on the health risks associated with the consumption of advanced glycation end products: Recommendations for dietary management. *Diabetes Metab Syndr Obes* **2015**, 415 (8), 26.

145) Videira, P. Q.; Castro-Caldas, M., Linking Glycation and Glycosylation With Inflammation and Mitochondrial Dysfunction in Parkinson's Disease. *Front. Neurosci.* **2018**, 12, 381.

146) Quan, C.; Alcala, E.; Petkovska, I.; Matthews, D.; Canova-Davis, E.; Taticek, R.; Ma, S., A study in glycation of a therapeutic recombinant humanized monoclonal antibody: Where it is, how it got there, and how it affects charge-based behavior. *Anal Biochem* **2008**; 373(2), 179-91.

147) Banks, D. D.; Hambly, D. M.; Scavezze, J. L.; Siska, C. C.; Stackhouse, N. L.; Gadgil, H. S., The effect of sucrose hydrolysis on the stability of protein therapeutics during accelerated formulation studies. *J Pharm Sci* **2009**, 98(12), 4501-10.

148) Miller, A. K.; Hambly, D. M.; Kerwin, B. A.; Treuheit, M. J.; Gadgil, H. S., Characterization of site-specific glycation during process development of a human therapeutic monoclonal antibody. *J Pharm Sci* **2011**, 100 (7), 2543-50.

149) Rabbani, N.; Ashour, A.; Thornalley, P. J., Mass spectrometric determination of early and advanced glycation in biology. *Glycoconj J* **2016**, 33, 553–568.

150) Zhang, B.; Yang, Y.; Yuk, I.; Pai, R.; McKay, P.; Eigenbrot, C.; Dennis, M.; Katta, V.; Francissen, K. C., Unveiling a glycation hot spot in a recombinant humanized monoclonal antibody. *Anal Chem* **2008**, 80(7), 2379-90.

151) Goetze, A. M.; Liu, Y. D.; Arroll, T.; Chu, L.; Flynn, G. C., Rates and impact of human antibody glycation *in vivo*. *Glycobiology* **2012**, 22(2), 221-34.

152) Brady, L. J.; Martinez, T.; Balland, A., Characterization of nonenzymatic glycation on a monoclonal antibody. *Anal Chem* **2007**, 79(24), 9403-13.

153) Lapolla, A.; Fedele, D.; Reitano, R.; Arico, N. C.; Seraglia, R.; Traldi, P.; Marotta, E.; Tonani, R., Enzymatic digestion and mass spectrometry in the study of advanced glycation end products/peptides. *J Am Soc Mass Spectrom* **2004**, 15(4), 496-509.

154) Duivelshof, B. L.; Fekete, S.; Guillarme, D.; D'Atri, V., A generic workflow for the characterization of therapeutic monoclonal antibodies—application to daratumumab. *Anal. Bioanal. Chem.* **2019**, 411, 4615–4627.

155) Vrdoljak, A.; Trescec, A.; Benko, B.; Hecimovic, D.; Simic, M., In vitro glycation of human immunoglobulin G. *Clin Chim Acta* **2004**, 345(1–2), 105-11.

156) Yim, M. B.; Yim, H.; Lee, C.; Kang, S.; Chock, P., Protein Glycation. *Ann. N. Y. Acad. Sci.***2001**, 928(1), 1-385.

157) Kikuchi, S.; Shinpo, K.; Takeuchi, M.; Yamagishi, S.; Makita, Z.; Sasaki, N.; Tashiro, K., Glycation—a sweet tempter for neuronal death. *Brain Res. Rev.* **2003**, 41(2), 306-323.

158) Horvat, S.; Jakas, A. Peptide and amino acid glycation: new insights into the Maillard reaction. *J. Pept. Sci.* **2003**, 10(3), 119-137.

159) Harris, R. J.; Shire, S. J.; Winter, Commercial manufacturing scale formulation and analytical characterization of therapeutic recombinant antibodies. *C. Drug Dev. Res.* **2004**, 61(3), 137−154.

160) Goldberg, T.; Cai, W.; Peppa, M.; Dardaine, V.; Baliga, B. S.; Uribarri, J.; Vlassara, H. Advanced glycoxidation end products in commonly consumed foods. *J. Am. Diet. Assoc.* **2004**, 104, 1287– 1291.

161) Zhang, G.; Huang, G.; Xiao, L.; Mitchell, A. E. Determination of Advanced Glycation End products by LC-MS/MS in Raw and Roasted Almonds (Prunus dulcis). *J. Agric. Food Chem.* **2011**, 59, 22, 12037–12046.

162) Yaacoub, R.; Saliba, R.; Nsouli, B.; Khalaf, G.; Birlouez-Aragon, I. Formation of lipid oxidation and isomerization products during processing of nuts and sesame seeds. *J. Agric. Food Chem.* **2008**, 56, 7082–7090.

163) Zhang, J.; Zhang, T.; Jiang, L.; Hewitt, D.; Huang, Y.; Kao, Y.; Katta, V., Rapid Identification of Low Level Glycation Sites in Recombinant Antibodies by Isotopic Labeling with $^{13}C_6$-Reducing Sugars. *Anal. Chem.* **2012**, 84, 2313−2320.

164) Zhang, M.; Xu, W.; Deng, Y., A New Strategy for Early Diagnosis of Type 2 Diabetes by Standard-Free, Label-Free LC-MS/MS Quantification of Glycated Peptides. *Diabetes* **2013**, 62(11), 3936–3942.

165) Liu, H.; Ponniah, G.; Neill, A.; Patel, R.; Andrien, B., Identification and comparative quantitation of glycation by stable isotope labeling and LC–MS. *J. Chromatogr. B*. **2014**, 958, 90-95.

166) Shin, A.; Connolly, S.; Little, R.; Kabytaev, K., Quantitation of glycated albumin by isotope dilution mass spectrometry. *Clin. Chim. Acta* **2021**, 521, 215-222.

167) Mo, J.; Jin, R.; Yan, Q.; Sokolowska, I.; Lewis, M. J.; Hu, P., Quantitative analysis of glycation and its impact on antigen binding. *MABS* **2018**, 10(3), 406–415.

168) Zhou, F.; Xu, W.; Hong, M.; Pan, Z.; Sinko, P. J.; Ma, J.; You, G., The intrinsic and extrinsic effects of N-linked glycans on glycoproteostasis. *Nat. Chem. Biol.* **2014**; 10:902–910.

169) Zhou, F.; Xu, W.; Hong, M.; Pan, Z.; Sinko, P. J.; Ma, J.; You, G., The Role of N-Linked Glycosylation in Protein Folding, Membrane Targeting, and Substrate Binding of Human Organic Anion Transporter hOAT4. *Mol Pharmacol* **2004**; 67:868–876.

170) Wang, Y.; Lee, H.; Hsu, J. L.; Yu, D.; Hung, M., The impact of PD-L1 N-linked glycosylation on cancer therapy and clinical diagnosis. *J. Biomed. Sci.* **2020**; 27:77.

171) Buck, T. M.; Eledge, J.; Skach, W. R., Evidence for stabilization of aquaporin-2 folding mutants by N-linked glycosylation in endoplasmic reticulum. *Am. J. Physiol. Cell Physiol.* **2004**; 287:C1292-C1299.

172) Imperiali, B.; O'Connor, S. E., Effect of N-linked glycosylation on glycopeptide and glycoprotein structure. *Curr Opin Chem Biol.* **1999**; 3:643–649.

173) Helle, F.; Vieyres, G.; Elkrief, L.; Popescu, C.; Wychowski, C.; Descamps, V.; Castelain, S.; Roingeard, P.; Duverlie, G.; Dubuisson, J., Role of N-Linked Glycans in the Functions of Hepatitis C Virus Envelope Proteins Incorporated into Infectious Virions. *J. Virol.* **2010**; 84:22.

174) Matsuda, K.; Zheng, J.; Du, G.; Klöcker, N.; Madison, L. D.; Dallos, P., N-linked glycosylation sites of the motor protein prestin: effects on membrane targeting and electrophysiological function. *J. Neurochem.* **2004**; 89:928–938.

175) Dawood, A. A.; Altobje, M. A., Inhibition of N-linked Glycosylation by Tunicamycin May Contribute to The Treatment of SARS-CoV-2. *Microb. Pathog.* **2020**; 149:104586.

176) Mitra, N.; Sinha, S.; Ramya, T. N. C.; Surolia, A., N-linked oligosaccharides as outfitters for glycoprotein folding, form, and function. *Trends Biochem. Sci.* **2006**; 31:3.

177) Duivelshof, B. L. et al., Quantitative N-Glycan Profiling of Therapeutic Monoclonal Antibodies Performed by Middle-Up Level HILIC-HRMS Analysis. *Pharmaceutics* **2021**, 13(11), 1744.

178) Fridriksson, E. K.; Beavil, A.; Holowka, D.; Gould, H. J.; Baird, B.; McLafferty, F. W., Heterogeneous Glycosylation of Immunoglobulin E Constructs Characterized by Top-Down High-Resolution 2-D Mass Spectrometry. *Biochemistry* **2000**, 39(12), 3369–3376.

179) Tran, B. Q. et al., Comprehensive glycosylation profiling of IgG and IgG-fusion proteins by top-down MS with multiple fragmentation techniques. *J Proteomics.* **2016**, 134, 93-101.

180) Chang, D.; Zaia, J., Methods to improve quantitative glycoprotein coverage from bottom-up LC-MS data. *Mass Spectrom. Rev.* **2022**, 41, 6, 922-937.

181) Giorgetti, J.; Beck, A.; Leize-Wagner, E.; François, Y., Combination of intact, middle-up and bottom-up levels to characterize 7 therapeutic monoclonal antibodies by capillary electrophoresis – Mass spectrometry. *J Pharm Biomed Anal.* **2020**, 182, 113107.

182) Camperi, J.; Guillarme, D.; Stella, C., Targeted Bottom-up Characterization of Recombinant Monoclonal Antibodies by Multidimensional LC/MS. *Anal. Chem.* **2020**, 92, 19, 13420–13426.

183) Shiratoria, K. et al., Selective reaction monitoring approach using structure-defined synthetic glycopeptides for validating glycopeptide biomarkers pre-determined by bottom-up glycoproteomics. *RSC Adv.,* **2022**, 12, 21385-21393.

184) Jones, A., N-Glycan Analysis of Biotherapeutic Proteins. *BioPharm Int.* **2017**, 30 (6), 20–25.

185) Khatri, K., Confident Assignment of Site-Specific Glycosylation in Complex Glycoproteins in a Single Step. *J. Proteome Res.* **2014**, 13, 10, 4347–4355.

186) Huang, B.; Yang, C.; Liu, C.; Liu, C., Stationary phases for the enrichment of glycoproteins and glycopeptides. *Electrophor.* **2014**, 35(15), 2091-2107.

187) Zhou, S.; Dong, X.; Veillon, L.; Huang, Y.; Mechref, Y., LC-MS/MS analysis of permethylated N-glycans facilitating isomeric characterization. *Anal. Bioanal. Chem.* **2017**, 409, 453–466.

188) Lauber, M. A. et al., Rapid Preparation of Released N-Glycans for HILIC Analysis Using a Labeling Reagent that Facilitates Sensitive Fluorescence and ESI-MS Detection. *Anal. Chem.* **2015**, 87, 10, 5401–5409.

189) Reider, B.; Szigeti, M.; Guttman, A., Evaporative fluorophore labeling of carbohydrates via reductive amination. *Talanta* **2018**, 185, 365-369.

190) Ruhaak, L. R.; Steenvoorden, E.; Koeleman, C. A. M.; Deelder, A. M.; Wuhrer, M.; 2-Picoline-borane: A non-toxic reducing agent for oligosaccharide labeling by reductive amination. *Proteomics* **2010**, 10(12), 2330-2336.

191) Burkhardt, E. R.; Coleridge, B. M.; Reductive amination with 5-ethyl-2-methylpyridine borane. *Tetrahedron Lett.* **2008**, 49(35), 5152-5155.

192) Schedin-Weiss, S. et al., Glycan biomarkers for Alzheimer disease correlate with T-tau and P-tau in cerebrospinal fluid in subjective cognitive impairment. *FEBS J.* **2020**, 287(15), 3221-3234.

193) Sauvageau, J. et al., Simplifying glycan monitoring of complex antigens such as the SARS-CoV-2 spike to accelerate vaccine development. *Commun. Chem.* **2023**, 6, 189.

194) Alpert, A. J., Hydrophilic-interaction chromatography for the separation of peptides, nucleic acids and other polar compounds. *J. Chromatogr. A.* **1990**, 499, 177-196.

195) Veillon, L.; Huang, Y.; Peng, W.; Dong, X.; Cho, B. G.; Mechref, Y., Characterization of isomeric glycan structures by LC-MS/MS. *Electrophor.* **2017**, 38(17), 2100-2114.

196) Badgett, M. J.; Boyes, B.; Orlando, R., The Separation and Quantitation of Peptides with and without Oxidation of Methionine and Deamidation of Asparagine Using Hydrophilic Interaction Liquid Chromatography with Mass Spectrometry (HILIC-MS). *J. Am. Soc. Mass Spectrom.* **2017**, 28, 5, 818–826.

197) Badgett, M. J.; Mize, E.; Fletcher, T.; Boyes, B.; Orlando, R., Predicting the HILIC Retention Behavior of the N-Linked Glycopeptides Produced by Trypsin Digestion of Immunoglobulin Gs (IgGs). *J Biomol Tech.* **2018**, 29(4), 98–104.

198) Planinc, A.; Bones, J.; Dejaegher, B.; Antwerpen, P. V.; Delporte, C., Glycan characterization of biopharmaceuticals: Updates and perspectives. *Analytica Chimica Acta* **2016**, 921, 13-27.

199) Yang, S.; Zhang, L.; Thomas, S.; Hu, Y.; Li, S.; Cipollo, J.; Zhang, H., Modification of Sialic Acids on Solid Phase: Accurate Characterization of Protein Sialylation. *Anal. Chem.* **2017**, 89, 12, 6330–6335.

200) Adan, A.; Alizada, G.; Kiraz, Y.; Baran, Y.; Nalbant, A., Flow Cytometry: Basic Principles and Applications. *Crit Rev Biotechnol.* **2017**;37(2):163-17.

201) Tanner, S. D.; Bandura, D. R.; Ornatsky, O.; Baranov, V. I.; Nitz, M.; Winnik, M. A.; Flow Cytometer with Mass Spectrometer Detection for Massively Multiplexed Single-Cell Biomarker Assay. *Pure Appl Chem.* **2008**;80(12):2627-2641.

202) Hulett, H. R.; Bonner, W. A.; Barrett, J.; Herzenberg, L. A., Cell sorting: automated separation of mammalian cells as a function of intracellular fluorescence. *Science*. **1969**;166(3906):747-749.

203) Büscher, M., Flow Cytometry Instrumentation - An Overview. *Curr Protoc Cytom.* **2019**;87(1):52.

204) Jayasinghe, S. N., Reimagining Flow Cytometric Cell Sorting. *Adv Biosyst.* **2020**;4(8):2000019.

205) Shapiro, H. M.; Telford, W. G., Lasers for Flow Cytometry: Current and Future Trends. *Curr Protoc Cytom.* **2018**;83:1-9.

206) Herzenberg, L. A.; Tung, J.; Moore, W. A.; Parks, D. R., Interpreting flow cytometry data: a guide for the perplexed. *Nat Immunol.* **2006**;7(7):681-5.

207) Herzenberg, L. A.; Parks, D.; Sahaf, B.; Perez, O.; Roederer, M., The history and future of the fluorescence activated cell sorter and flow cytometry: a view from Stanford. *Clin Chem.* **2002**;48(10):1819-27.

208) De Rosa, S. C.; Herzenberg, L. A.; Roederer, M., 11-color, 13-parameter flow cytometry: identification of human naive T cells by phenotype, function, and T-cell receptor diversity. *Nat Med.* **2001**;7(2):245-8.

209) Tirouvanziam, R.; Davidson, C. J.; Lipsick, J. S.; Herzenberg, L. A., Fluorescence-activated cell sorting (FACS) of Drosophila hemocytes reveals significant functional similarities to mammalian leukocytes. *Proc Natl Acad Sci U S A.* **2004**;101(9):2912-7.

210) Nolan, G.P.; Fiering, S.; Nicolas, J. F.; Herzenberg, L. A., Fluorescence-activated cell analysis and sorting of viable mammalian cells based on beta-D-galactosidase activity after transduction of Escherichia coli lacZ. *Proc Natl Acad Sci U S A.* **1988**;85(8):2603-7.

211) Herzenberg, L. A., Genetics, FACS, immunology, and redox: a tale of two lives intertwined. *Annu Rev Immunol*. **2004**;22:1-31.

212) Parks, D. R.; Hardy, R. R.; Herzenberg, L. A., Dual immunofluorescence - exploring new horizons in cell analysis and sorting. *Immunol Today.* **1983**;4(5):145-50.

213) Kerr, W. G.; Nolan, G. P.; Herzenberg, L. A., In situ detection of transcriptionally active chromatin and genetic regulatory elements in individual viable mammalian cells. *Immunol Suppl.* **1989**;2:74-8;79.

214) Herzenberg, L. A, Hsu, C.; Alberti, S.; Kavathas, P., Transfection and cloning of genes for membrane antigens using the FACS. *Med Oncol Tumor Pharmacother.* **1984**;1(4):219-24.

215) Horan, P. K.; Wheeless, L. L. Jr., Quantitative Single Cell Analysis and Sorting: Rapid analysis and sorting of cells is emerging as an important new technology in research and medicine. *Science*. **1977**;198(4313):149-157.

216) Fulwyler, M. J., Electronic Separation of Biological Cells by Volume. *Science*. **1965**;150(3698):910-911.

217) Bandura, D. R.; Baranov, V. I.; Ornatsky, O. I.; Antonov, A.; Kinach, R.; Lou, X. et al., Mass Cytometry: Technique for Real-Time Single Cell Multitarget Immunoassay Based on Inductively Coupled Plasma Time-of-Flight Mass Spectrometry. *Anal Chem.* **2009**;81:6813–6822.

218) Ornatsky, O.; Bandura, D.; Baranov, V.; Nitz, M.; Winnik, M. A.; Tanner, S., Highly Multiparametric Analysis by Mass Cytometry. *J Immunol Methods.* **2010**;361:1–20.

219) Spitzer, M. H.; Nolan, G. P., Mass Cytometry: Single Cells, Many Features. *Cell.* **2016**;165(4):780-791.

220) Rees, P.; Summers, H. D.; Filby, A.; Carpenter, A. E.; Doan, M., Imaging Flow Cytometry. *Nature Reviews*. **2022**;2:86.

221) Dashkova, V.; Malashenkova, D.; Poulton, N.; Vorobjeva, I.; Barteneva, N. S., Imaging Flow Cytometry for Phytoplankton Analysis. *Methods.* **2017**;112:188-200.

222) Barteneva, N. S.; Fasler-Kan, E.; Vorobjev, I. A., Imaging Flow Cytometry: Coping with Heterogeneity in Biological Systems. *J. Histochem. Cytochem.* **2012**;60(10):723-733.

223) Bonilla, D. L.; Reinin, G.; Chua, E., Full Spectrum Flow Cytometry as a Powerful Technology for Cancer Immunotherapy Research. *Front Mol Biosci.* **2020**;7:612801.

224) Sanders, C. K.; Mourant, J. R., Advantages of Full Spectrum Flow Cytometry. *J. Biomed. Opt*. **2013**;18(3):037004.

225) Collier, J. L., Flow Cytometry and the Single Cell in Phycology. *J. Phycol.* **2000**;36:628-644.

226) Warth, S.; Kunkel, D., Setting Up Mass Cytometry in a Shared Resource Lab Environment. *Methods Mol Biol.* **2019**;1989:3-11.

227) Monti, F.; Rosetti, M.; Masperi, P.; Tommasini, N.; Dorizzi, R. M., Shared resource laboratories: impact of new design criteria to consolidate flow cytometry diagnostic service. *Int. J. Lab. Hematol*. **2012**;34:533-540.

228) Barsky, L. W.; Black, M.; Cochran, M. et al., International Society for Advancement of Cytometry (ISAC) flow cytometry shared resource laboratory (SRL) best practices. *Cytometry A.* **2016**;89(11):1017-1030.

229) S10 Instrumentation Programs: Awards. National Institutes of Health: Office of Research Infrastructure Programs. Accessed August 16, **2023**. https://orip.nih.gov/construction-and-instruments/s10-instrumentation-programs/